

University of Massachusetts Medical School

eScholarship@UMMS

---

GSBS Dissertations and Theses

Graduate School of Biomedical Sciences

---

1997-06-01

## Molecular Basis of the Mechanism and Regulation of Receptor-GTP Binding Protein Interactions: A Thesis

Marianne Wessling-Resnick

*University of Massachusetts Medical School*

Let us know how access to this document benefits you.

Follow this and additional works at: [https://escholarship.umassmed.edu/gsbs\\_diss](https://escholarship.umassmed.edu/gsbs_diss)



Part of the [Amino Acids, Peptides, and Proteins Commons](#), [Biological Factors Commons](#), [Enzymes and Coenzymes Commons](#), and the [Molecular Biology Commons](#)

---

### Repository Citation

Wessling-Resnick M. (1997). Molecular Basis of the Mechanism and Regulation of Receptor-GTP Binding Protein Interactions: A Thesis. GSBS Dissertations and Theses. <https://doi.org/10.13028/f3j6-1t57>.

Retrieved from [https://escholarship.umassmed.edu/gsbs\\_diss/100](https://escholarship.umassmed.edu/gsbs_diss/100)

This material is brought to you by eScholarship@UMMS. It has been accepted for inclusion in GSBS Dissertations and Theses by an authorized administrator of eScholarship@UMMS. For more information, please contact [Lisa.Palmer@umassmed.edu](mailto:Lisa.Palmer@umassmed.edu).

MOLECULAR BASIS OF THE MECHANISM AND REGULATION  
OF RECEPTOR-GTP BINDING PROTEIN INTERACTIONS

A Thesis Presented

By

Marianne Wessling-Resnick

Submitted to the faculty of the  
University of Massachusetts Medical School in partial  
fulfillment of the requirements for the degree of

DOCTOR OF PHILOSOPHY IN MEDICAL SCIENCES

June

1987

Biochemistry

MOLECULAR BASIS OF THE MECHANISM AND REGULATION  
OF RECEPTOR-GTP BINDING PROTEIN INTERACTIONS

A Thesis

By

Marianne Wessling-Resnick

Approved as to style and content by:

---

Dr. Anthony Carruthers, Chairman of Committee

---

Dr. Michael P. Czech, Member

---

Dr. Roger Craig, Member

---

Dr. Craig C. Malbon, Member

---

Dr. Reid Gilmore, Member

---

Dr. Thomas B. Miller, Jr., Dean  
of Graduate Studies

Department of Biochemistry

June

1987

## ABSTRACT

The photon receptor, rhodopsin, and the GTP-binding regulatory protein, transducin, belong to a family of G protein-coupled receptors. The activation process through which guanine nucleotide exchange of the G protein is accomplished was investigated utilizing these components of the visual transduction system. Rhodopsin, modelled as an enzyme in its interaction with substrates, transducin and guanine nucleotides, was characterized to catalyze the G protein's activation by a double-displacement mechanism. Remarkable allosteric behavior was observed in these kinetic studies. Equilibrium binding studies were performed to investigate the molecular basis of the positive cooperative behavior between transducin and rhodopsin. These experiments show that the origins of the allosterism must arise from oligomeric assemblies between receptor and G protein. The determined Hill coefficient,  $n_H = 2$ , suggests that at least two transducin molecules are involved, and the  $B_{max}$  parameter also indicates that multimeric assemblies of rhodopsin may participate in the positive cooperative interactions. Physical studies of transducin in solution were performed and do not indicate the existence of a dimeric structure, in contrast to the kinetic and binding experiments which analyze interactions at the membrane surface. Since the latter environment represents the native surroundings in vivo, aspects of the allosteric behavior must be considered for a complete understanding of the signal transduction mechanism. The reported findings are interpreted in the context of homologies between other G protein-coupled receptor systems in order to develop a model for the molecular basis of the mechanism and regulation of this mode of signal transduction.

## ACKNOWLEDGEMENTS

I would like to express my gratitude for the support and encouragement given by my thesis advisor, Dr. Gary L. Johnson, as well as other members of his laboratory, particularly Daniel J. Kelleher, with whom I have had many stimulating discussions about this work. I also thank Denise Bassett for her patience and expertise in typing this manuscript. Finally, all of this could not have been accomplished without the continued support, encouragement and devotion of my husband, Paul Resnick, who continues to motivate all of my achievements.

## TABLE OF CONTENTS

|                            |  |      |
|----------------------------|--|------|
| ABSTRACT . . . . .         |  | iii  |
| ACKNOWLEDGEMENTS . . . . . |  | iv   |
| LIST OF TABLES . . . . .   |  | vii  |
| LIST OF FIGURES . . . . .  |  | viii |
| ABBREVIATIONS . . . . .    |  | ix   |
| CHAPTER I                  | INTRODUCTION: LITERATURE REVIEW . . . . .  | 1    |
|                            | Homologies Between Receptor-GTP Binding Proteins . . . . .   | 1    |
|                            | Visual Transduction . . . . .  | 5    |
|                            | Mechanism of Rhodopsin's Activation of Transducin . . . . .  | 8    |
| CHAPTER II                 | METHODS AND MATERIALS . . . . .  | 11   |
|                            | Preparation of Transducin and Rhodopsin . . . . .  | 11   |
|                            | Kinetic Measurements . . . . .   | 13   |
|                            | Equilibrium Binding Assay . . . . .  | 16   |
|                            | Physical Measurements . . . . .  | 17   |
|                            | Materials . . . . .  | 18   |
| CHAPTER III                | ALLOSTERIC BEHAVIOR IN TRANSDUCIN ACTIVATION<br>MEDIATED BY RHODOPSIN: INITIAL RATE ANALYSIS OF<br>GUANINE NUCLEOTIDE EXCHANGE . . . . .               | 19   |
|                            | Results and Discussion . . . . .   | 19   |
|                            | Conclusions . . . . .  | 34   |
| CHAPTER IV                 | MOLECULAR ORIGINS OF ALLOSTERIC BEHAVIOR:<br>EQUILIBRIUM BINDING STUDIES BETWEEN RHODOPSIN<br>TRANSDUCIN . . . . .                                     | 36   |
|                            | Results and Discussion . . . . .   | 36   |
|                            | Conclusions . . . . .  | 45   |
| CHAPTER V                  | KINETIC AND HYDRODYNAMIC PROPERTIES OF TRANSDUCIN:<br>COMPARISON OF PHYSICAL AND STRUCTURAL PARAMETERS OF<br>GTP-BINDING REGULATORY PROTEINS . . . . . | 46   |
|                            | Results and Discussion . . . . .   | 46   |
|                            | Conclusions . . . . .  | 62   |
| CHAPTER VI                 | DISCUSSION: FUTURE DIRECTIONS . . . . .  | 65   |
|                            | Receptors as Enzymes . . . . .   | 67   |
|                            | A General Class of Ligand-Exchange Enzymes . . . . .   | 68   |
|                            | Allosteric Behavior . . . . .  | 70   |
|                            | Oligomeric Associations . . . . .  | 72   |
|                            | Mg <sup>2+</sup> Effects and Transducin Structure . . . . .  | 75   |

|  |     |
|--|-----|
| Thermodynamic Considerations of Molecular Interactions . . . . . | 79  |
| Structural Model for Rhodopsin . . . . .                         | 83  |
| Summary . . . . .  | 89  |
| APPENDIX I . . . . .   | 91  |
| APPENDIX II . . . . .  | 96  |
| APPENDIX III . . . . .   | 99  |
| REFERENCES . . . . .   | 101 |

LIST OF TABLES

|           |   |    |
|-----------|---|----|
| TABLE I   | Summary of Sedimentation Velocity Studies . . . . .   | 52 |
| TABLE II  | Comparison of Guanine Nucleotide Binding Characteristics<br>Between Members of the G Protein Family . . . . . | 55 |
| TABLE III | Comparison of Hydrodynamic Parameters Reported for<br>Purified G Proteins . . . . .                           | 64 |
| TABLE IV  | Sequence Homologies Between GTP-Binding Regulatory<br>Proteins . . . . .                                      | 78 |



## LIST OF FIGURES

|           |   |    |
|-----------|---|----|
| FIGURE 1  | Linear relationship between rhodopsin concentration and rate of guanine nucleotide exchange reaction . . . . .          | 20 |
| FIGURE 2  | Selwyn's plot of reaction progress as a function of the product of rhodopsin concentration multiplied by time . . . . . | 21 |
| FIGURE 3  | Timecourse of guanine nucleotide exchange of transducin .   | 24 |
| FIGURE 4  | Kinetics of $T\alpha$ subunit activation . . . . .  | 26 |
| FIGURE 5  | Allosterism observed in substrate-velocity plot . . . . .   | 27 |
| FIGURE 6  | Lineweaver-Burke plots for the rhodopsin catalyzed guanine nucleotide exchange reaction . . . . .                       | 29 |
| FIGURE 7  | Linear transformation of double reciprocal plots with respect to transducin . . . . .                                   | 30 |
| FIGURE 8  | Mechanistic pathways of allosteric behavior . . . . .   | 32 |
| FIGURE 9  | Binding interactions between transducin and rhodopsin . .   | 38 |
| FIGURE 10 | Light-dependent binding of transducin to rhodopsin . . .  | 40 |
| FIGURE 11 | Light-dependent binding of transducin to purified, reconstituted rhodopsin . . . . .                                    | 42 |
| FIGURE 12 | Timecourse of V8 protease digest of rhodopsin . . . . .   | 44 |
| FIGURE 13 | Timecourse of GTP $\gamma$ S binding . . . . .  | 47 |
| FIGURE 14 | Effect of Mg <sup>+2</sup> on the timecourse of GTP $\gamma$ S binding . . . . .  | 49 |
| FIGURE 15 | Equilibrium binding of GTP $\gamma$ S to transducin . . . . .   | 53 |
| FIGURE 16 | Plots of $\ln v_0$ <u>versus</u> $\ln$ [transducin] as a function of [GTP $\gamma$ S] . . . . .                         | 56 |
| FIGURE 17 | Plots of $\ln v_0$ <u>versus</u> $\ln$ [GTP $\gamma$ S] as a function of [transducin] . . . . .                         | 57 |
| FIGURE 18 | Sucrose density gradient ultracentrifugation of transducin  | 60 |
| FIGURE 19 | Determination of the Stokes radius for transducin . . . . .   | 61 |
| FIGURE 20 | Energy profiles for a dissociative type mechanism . . . . .   | 81 |
| FIGURE 21 | Structural model for rhodopsin . . . . .  | 84 |

## ABBREVIATIONS

|                 |   |
|-----------------|---|
| DTT             | dithiothreitol  |
| G Protein       | regulatory GTP-binding protein                                      |
| G <sub>i</sub>  | the inhibitory GTP-binding protein of the adenylate cyclase system  |
| G <sub>o</sub>  | the regulatory GTP-binding protein found in brain                   |
| G <sub>s</sub>  | the stimulatory GTP-binding protein of the adenylate cyclase system |
| G <sub>T</sub>  | the regulatory GTP-binding protein of the rod outer segment         |
| GTPγS           | guanosine 5'-(3-O-thio) triphosphate                                |
| HEPES           | 4-(2-hydroxyethyl)-1-piperazineethane sulfonic acid                 |
| Rho             | active form of rhodopsin  |
| Rho'            | inactive form of rhodopsin  |
| ROS             | rod outer segment   |
| SDS-PAGE        | sodium dodecyl sulfate polyacrylamide gel electrophoresis           |
| T <sub>α</sub>  | the α subunit of transducin   |
| T <sub>βγ</sub> | the β·γ subunit complex of transducin                               |
| UROS            | urea-stripped rod outer segments                                    |

## CHAPTER I

## INTRODUCTION: LITERATURE REVIEW

A family of GTP-binding proteins, called G proteins, has been shown to provide a signal transduction mechanism for many cell surface receptors. These receptors act catalytically to mediate the guanine nucleotide exchange of G proteins: this process is referred to as activation and results in the displacement of bound GDP for GTP. The concomitant dissociation of the G protein's  $\alpha$  subunit, with GTP bound, from the  $\beta\gamma$  subunit complex initiates the signal to elicit the appropriate cellular response. One example of such a signal transduction system is the photon receptor, rhodopsin, and its G protein, transducin. This G protein-coupled receptor system has been chosen in order to investigate the molecular events involved in the activation process. The following points provide a framework in which the study takes context.

Homologies Between Receptor-GTP Binding Protein Systems

Signal transduction for a variety of hormone receptors involves GTP-binding proteins, which mediate changes in cell function, metabolism, and growth (1). Several proteins comprise a family of GTP-binding regulatory elements (G proteins). Perhaps the best known example of this type of transduction mechanism is the adenylate cyclase system, which in many cell types is under regulatory control exerted through the stimulatory  $G_s$  protein and the inhibitory  $G_i$  protein. Transducin ( $G_T$ ) is also a member of this family, regulating the activity of the rod cell cGMP phosphodiesterase. A fourth GTP-binding protein,  $G_o$ , has

been identified in brain; however, no known function has been correlated with its activity. Accumulating evidence suggests the possible existence of other G proteins as well, with different regulatory functions. GTP-binding proteins have been implicated to function in  $\text{Ca}^{2+}$  and arachidonate mobilization by stimulating phospholipase C ( $G_{p1c}$ ) or phospholipase  $A_2$  ( $G_{p1a}$ ) (3-8). Another G protein,  $G_K$ , is thought to be an activator of  $K^+$  channels (9). Finally, other effector systems under regulatory control of G proteins may also include both the positive and negative regulation of voltage-gated  $\text{Ca}^{2+}$  channels and possible negative regulation of phospholipase C (10).

A broad range of cell surface receptors couple to the effector systems listed above via the regulatory G proteins. These include receptors for adrenergic and muscarinic agents, as well as peptide hormones such as ACTH, LH, FSH, and GRF. The list of hormones which interact with G protein-coupled receptors also includes glucagon, secretin, and vasopressin. Chemotactic factors (FMLP), thrombin, bombesin, histamine, and prostaglandins are among the other ligands which exert effects through this signal transduction mechanism. Receptors for environmental factors such as light, olfactory and taste signals also are coupled to G proteins. This survey of G protein-coupled receptors is far from complete (10), but serves to underscore the variety of stimuli which utilize this mode of signal transduction.

The structural homologies observed between G proteins have advanced our understanding of the relationships between the GTP-binding regulatory elements. These proteins are heterotrimers composed of  $\alpha$ ,  $\beta$ , and  $\gamma$  subunits. The  $\alpha$  subunits range in size from 39 to 52 kD and contain the

site for guanine nucleotide binding, as well as the GTPase activity associated with their function. The fact that the  $\alpha$  subunits serve as substrates for ADP-ribosylation by either cholera or pertussis toxins has greatly aided in elucidating the physiological role of G proteins (11,12). Recently, the nucleotide sequences of cDNA's for six distinct  $\alpha$  subunits have been published: transducin (rod) (13-15), transducin (cone) (16),  $G_S$  (17-21),  $G_i-1$  (19,20),  $G_i-2$  (21) and  $G_O$  (19). The strong conservation observed in primary sequence serves to emphasize the relationship between members of the G protein family, whereas structural differences may hold the key to understanding their functional roles.

The  $\beta\gamma$  subunits of G proteins are isolated as a non-covalent complex which is dissociated only under denaturing conditions. The  $\beta$  subunits of  $G_S$  and  $G_i$  have been found to be identical in molecular weight (35 kD), amino acid composition, and peptide maps (22). Not surprisingly, they are functionally equivalent, serving to aid in the activation of either  $G_{S\alpha}$  or  $G_{i\alpha}$ . Identical cDNAs coding for the  $\beta$  subunit of transducin (23,24) and  $G_S/G_i$  (25) have been isolated. Another form of  $\beta$  (36 kD) has also been identified and shown to be immunologically distinct from the 35 kD species (26). The  $\gamma$  subunit does exhibit some heterogeneity between different G proteins. Peptide maps of  $\gamma$  subunits of  $G_S$  and  $G_i$  are identical, but differ remarkably from maps of transducin's  $\gamma$  subunit (27). Immunological evidence also indicates  $G_T\gamma$  is distinct from  $G_S/G_i\gamma$  (28). The  $\gamma$  subunit of transducin has been cloned and its primary sequence suggests that the peptide is fairly hydrophilic (29-31). This is consistent with the fact that transducin may be isolated as a soluble protein, in contrast to other G proteins which require solubilization by detergent. Thus, the

prediction has been made that the  $\gamma$  subunits of  $G_s/G_i$  are hydrophobic in nature, and in the complex with the  $\beta$  subunit, provide a membrane anchor for the  $\alpha$  subunit of G proteins.

Gilman and collaborators (1,32,33) have advanced the hypothesis that the  $\beta\gamma$  subunit complex may play a regulatory role by allowing communication between G proteins which share these subunits in common. Thus,  $\beta\gamma$  released from  $G_i$  upon receptor activation can functionally serve to inhibit adenylate cyclase by re-associating with free  $G_{s\alpha}$  subunits. By limiting the amount of free  $\alpha$  subunit, the common  $\beta\gamma$  subunits would allow "cross-talk" between different receptors which must simultaneously respond through this signal transduction mechanism.

All of the current evidence supports an emerging picture in which G proteins provide a complex communication network that is coordinately regulated and through which a given extracellular stimulus may exert pleotropic effects. The relationships between the family of G protein-coupled regulatory systems is strengthened by studies showing the interchangeability of G proteins between different receptor systems. Rhodopsin has been found to be capable of activating  $G_i$  as well as  $G_T$  (34-37). The  $\beta$ -adrenergic receptor can activate not only  $G_s$  but also  $G_i$  (38). These observations suggest that in addition to the conservation in G protein structure, receptors which mediate signal transduction via this mechanism must also share a high degree of conservation in tertiary structure. Indeed, striking homology has been observed in the primary sequences of rhodopsin (39-41), the  $\beta$ -adrenergic receptor (42-44) and the muscarinic receptor (45), particularly in those regions predicted to compose membrane bilayer domains. Immunological evidence also suggests

structural conservation between domains of rhodopsin and the  $\beta$ -adrenergic receptor (46). Therefore, molecular studies on the interactions between rhodopsin and transducin can provide insight into structural and functional relationships among the class of hormone receptors known to exert their effects through GTP-binding proteins.

### Visual Transduction

The integral membrane protein, rhodopsin, is the primary protein constituent present in the outer segment discs of rod cells. The photoisomerization of its chromophore, 11-cis-retinal leads to the hyperpolarization of the rod cell plasma membrane by a signal transduction mechanism which appears to involve cGMP and  $Ca^{++}$ . Photolyzed rhodopsin catalytically activates the GTP-binding protein, transducin, which in turn activates a cGMP phosphodiesterase (PDE) (47). The responsiveness of the photoreceptor to light becomes reduced after photoexcitation, a process which is known as light adaptation (48). The mechanism of this regulatory phenomenon has been proposed to be exerted via the phosphorylation of rhodopsin (49-53). Although a complete picture of visual transduction has yet to emerge, the following observations must be integrated into a coherent model, and they are outlined to provide guidelines in which to relate molecular studies to cellular physiology.

The modulation of cGMP levels has been implicated in the phototransduction mechanism: in patch clamp studies, exposure of the cytoplasmic surface of isolated membrane patches to low levels of cGMP opens ion channels (54) and this event appears to be regulated by the cooperative binding of two molecules of cGMP to the channel protein (55). It is proposed that the channels are maintained in an open state in the

dark by high levels of cGMP, and that light activates the rapid hydrolysis of cGMP, which causes the channels to close. Cytoplasmic levels of  $\text{Ca}^{++}$  are also increased in response to light, and it has been observed that increased levels of  $\text{Ca}^{++}$  decrease the light sensitivity of rod cells (48,56,57). The latter observation suggests that  $\text{Ca}^{++}$  may mediate light adaptation, and it has been shown for the Limulus photoreceptor that inositol triphosphate ( $\text{InsP}_3$ ) may also be involved in this desensitization. Increased levels of  $\text{InsP}_3$  are detected upon photoexcitation, and when injected into photoreceptors,  $\text{InsP}_3$  has been shown to reduce responsiveness to subsequent flashes of light (58). The proposed general role of  $\text{InsP}_3$  as a calcium-mobilizing intracellular second messenger suggests that it acts to release internal stores of  $\text{Ca}^{++}$  (59). Although there are clear differences in visual transduction between vertebrate rod cells and invertebrate photoreceptors, it is interesting to note that generation of  $\text{InsP}_3$  is a result of hydrolysis of phosphatidylinositol 4,5-bisphosphate with the concomitant release of diacylglycerol (DAG). This hydrolysis is mediated by activation of phospholipase C, an enzyme which in other cell types has been identified to be controlled by GTP-binding proteins (3,4).

In mammalian rod cells, rhodopsin is phosphorylated upon exposure to light by rhodopsin kinase, a regulatory mechanism which has been implicated to be involved in light adaptation (49). Rhodopsin kinase itself does not require photoactivation; rather it appears that rhodopsin undergoes a light-induced conformational change which allows phosphorylation to occur. In vitro measurements of PDE activity reveal that addition of ATP and rhodopsin kinase diminish the light-stimulated



activity of PDE mediated by rhodopsin's activation of transducin (52). Recent evidence has also demonstrated the presence of a  $\text{Ca}^{++}$ /phospholipid-dependent protein kinase in rod cells (60,61). Commonly referred to as protein kinase C, the enzyme's activity is stimulated by the presence of DAG and its  $\text{Ca}^{++}$ -dependent translocation to the membrane surface results in phosphorylation of rhodopsin. This phenomenon provides a speculative role for the increased  $\text{Ca}^{++}$  levels involved in the adaptation process. Protein kinase C has been found to phosphorylate rhodopsin in the dark, as well as after bleaching. Hence, phosphorylation by protein kinase C may provide a regulatory mechanism independent of light activation.

The structural and topographical information known for the rod cell's visual pigment has been reviewed by several investigators (63-64). The current model for the disposition of rhodopsin's 348 amino acid length predicts that the integral membrane protein has seven transmembrane domains with approximately half of the protein's mass embedded in the lipid environment. The carboxy-terminal tail, which contains the serine and threonine residues phosphorylated by rhodopsin kinase and protein kinase C, is exposed to the cytoplasm along with three hydrophilic loop regions which connect the hydrophobic membrane-spanning domains. The cytoplasmic face of rhodopsin represents about one-quarter of the protein's mass with the remaining mass occluded in the lumen of the rod cell outer disc. The latter portion of rhodopsin represents three more hydrophilic connecting loop regions as well as the amino-terminal tail which contains two short asparagine-linked oligosaccharide chains. The seven membrane-spanning domains are thought to have an  $\alpha$ -helical conformation and to be arranged in a horse-shoe configuration in relation to one

another, similar to the folding pattern observed for bacteriorhodopsin. A unique lysine is present at the predicted midpoint of the most C-terminal helix. This residue exists as a protonated Schiff base with 11-cis-retinal. Thus, the inside surfaces of the membrane-spanning domains must neutralize this charge and provide a binding pocket for the chromophore. Given this structural framework, little information is known about functional aspects which contribute to rhodopsin's role in visual transduction.

#### Mechanism of Rhodopsin's Activation of Transducin

Rhodopsin's ability to mediate GDP-GTP exchange of transducin upon photoexcitation has been characterized by observations based on binding interactions (65-71). In the dark, transducin binds GDP with high affinity. Photon capture by rhodopsin induces formation of a rhodopsin·transducin·GDP complex in such a way that the affinity for GDP is lowered, and exchange for GTP occurs. The binding of GTP to the rhodopsin·transducin complex results in the dissociation of transducin·GTP and a concomitant increase in transducin's apparent affinity for GTP. The specificity for GTP in this exchange induces dissociation of transducin's subunits,  $\alpha$ ·GTP and  $\beta\gamma$ . Phosphodiesterase activation occurs via the interaction between  $\alpha$ ·GTP and an inhibitory subunit of PDE (72). The  $\alpha$  subunit exhibits a slow GTPase activity, and upon hydrolysis,  $\alpha$ ·GDP binds with  $\beta\gamma$  to form holo-transducin. Subsequently, the inhibitory subunit can reassociate with PDE to prevent its activity. One bleached rhodopsin is estimated to activate  $10^2$  GTP-binding proteins, which interact to stimulate  $10^3$  PDEs: this cascade results in an amplification of  $10^5$ . The advantages of this transduction system lie not only in its

amplification: the exchange of GTP for GDP may occur very rapidly, much more so than, for example, a covalent modification, and due to the hydrolysis of GTP, the system has been set to turn off in a temporal manner which reflects the amount of bleaching which has occurred.

Characterization of the molecular interactions between rhodopsin and transducin has been limited to the model discussed above. Several key questions remain, however, concerning the molecular mechanism through which the receptor interacts with the G protein. These questions are not only pertinent to our knowledge of the physiology and regulation of visual transduction, but also are vital to understanding the structural and functional relationships between other G protein-coupled receptor systems. The advantages of addressing these issues utilizing components of the visual signal transduction mechanism are clear: rhodopsin is highly abundant in rod outer disc membranes which serve as a source to purify large quantities of the receptor; transducin, unlike other G proteins, is a soluble protein which may also be isolated in milligram quantities from retina; rapid methods of purification are available for both receptor and G protein; and sequence information is available not only for rhodopsin (39-41), but also for each of transducin's subunits (13-15,23,24,29-31). Thus, it is possible to begin to define structure-function relationships at the molecular level in hopes of providing insight into the conserved homologies between G protein-coupled receptor transduction systems. The approach employed here is to model the receptor, rhodopsin, as an enzyme which catalytically interacts with substrates, transducin and guanine nucleotides. Therefore, the kinetic methods which have provided a fundamental basis in mechanistic studies of soluble enzymes are utilized

in order to define molecular events involved in the activation process. The use of this method provides a conceptual basis for understanding structural interactions and the regulation of the signal transduction mechanism associated with the family of G protein-coupled receptors.

## CHAPTER II

## METHODS AND MATERIALS

Preparation of Transducin and Rhodopsin

Transducin and stripped membranes containing rhodopsin were prepared from rod outer segments (ROS) isolated from frozen, dark-adapted bovine retinas following protocols adapted from Fung *et al.* (65,70). Thawed retinas were placed in ice-cold 20 mM Tris, pH 7.4, 1 mM CaCl<sub>2</sub>, 45% (w/w) sucrose and passed several times through a syringe; ROS disrupted in this manner were collected by flotation, washed in buffer without sucrose, and pooled before being layered over a step gradient of 25% and 35% (w/w) sucrose in 20 mM Tris, pH 7.4, 1 mM CaCl<sub>2</sub>. ROS were collected from the 25%/35% interface after centrifugation at 100,000 x g for 30 minutes at 4°C, and were subjected to a series of extensive washes. The first series of four isotonic washes were carried out in a buffer of 10 mM Tris, pH 7.4, 100 mM NaCl, 5 mM MgCl<sub>2</sub>, 1 mM DTT, 0.1 mM EDTA; the ROS were then washed four times in a hypotonic buffer of 10 mM Tris, pH 7.4, 1 mM DTT, 0.1 mM EDTA. These centrifugation steps were performed at 100,000 x g for 15 minutes at 4°C.

All of the preparative methods were performed with illumination in order to obtain transducin, which was extracted from the washed ROS by incubation for 15 minutes in 10 mM Tris, pH 7.4, 1 mM DTT, 0.1 mM EDTA, in the presence of 40 μM GTP, followed by centrifugation at 100,000 x g for 15 minutes at 4°C. The supernatant, containing transducin, was collected and subjected to dialysis against 10 mM Tris, pH 7.4, 100 mM NaCl, 5 mM MgCl<sub>2</sub>, 1 mM DTT, 0.1 mM EDTA, and concentrated 25-fold by vacuum

dialysis. This procedure yielded preparations of transducin which were at least 90% pure, as judged by Coomassie staining on SDS-polyacrylamide gels routinely run to assess the quality of the product (see, for example, Figure 13). Equimolar amounts of transducin's subunits were present, as verified by their comigration in sucrose gradient centrifugation analysis (Figure 18). Typically, transducin was immediately employed in the kinetic assays; if stored, the preparation was made 50% in glycerol and kept at  $-20^{\circ}\text{C}$ . Transducin's  $\alpha$  subunit was further purified and separated from the  $\beta\gamma$  subunit complex by chromatography over Blue Sepharose (73,74). Purified  $\alpha$  subunit was concentrated, dialyzed and manipulated as described for holotransducin. In some experiments, holo-transducin was further purified by chromatography over hexyl-agarose as described by Fung *et al.* (65).

Stripped membranes containing rhodopsin were prepared under dim red light following the steps outlined above. After the isotonic and hypotonic washes, the ROS were further extracted with urea, according to methods described by Yamazaki *et al.* (73). ROS were suspended in 20 mM Tris, pH 7.4, 1 mM EDTA, 2 mM  $\text{MgCl}_2$ , 0.5 mM DTT, and a solution of 5 M urea, 50 mM HEPES, pH 8.0, 5 mM EDTA, 0.5 mM DTT was added such that the final concentration of urea was 4.7 M. This suspension was kept on ice and intermittently passed through a syringe with an attached 21 G needle for a period of 60 minutes, after which time 20 mM HEPES, pH 8.0, 2 mM EDTA, 0.5 mM DTT was added to dilute the urea 5-fold. This mixture was centrifuged at  $100,000 \times g$  for 30 minutes at  $4^{\circ}\text{C}$ ; the pelleted membranes were then washed once with 20 mM HEPES, pH 8.0, 2 mM EDTA, 0.5 mM DTT and three times with 20 mM Tris, pH 7.4, 1 mM EDTA, 0.5 mM DTT, and stored at

-70°C in the latter buffer. This preparation yields a spectral ratio  $A_{280}/A_{498}$  of 1.9, comparable to values of 1.7-1.8 obtained by other purification methods. Rhodopsin concentration was determined from its absorbance at 498nm, using a molar extinction coefficient of 42,700 M<sup>-1</sup> cm<sup>-1</sup> (75). Rhodopsin was further purified by solubilization in octyl glucoside and subsequent chromatography over concanavalin A-Sepharose (76); reconstitution into vesicles containing egg phosphatidylcholine and phosphatidylethanolamine was accomplished by dialysis (77). Control experiments indicated that less than 1% of the rhodopsin population was photolyzed prior to exposure to room light.

#### Kinetic Measurements

[<sup>35</sup>S]-GTPγS, a non-hydrolyzable GTP analog, was employed to monitor guanine nucleotide exchange of transducin catalyzed by photo-activated rhodopsin. Purity of the radiolabelled compound was evaluated by thin layer chromatography on PEI-cellulose, with 0.5M K<sub>2</sub>HPO<sub>4</sub> as developing buffer. Initial rate measurements were obtained by a filtration assay which takes advantage of the fact that transducin will bind to nitrocellulose filters. A 300 μl reaction mixture typically contained 5.4 nM rhodopsin, with appropriate concentrations of transducin and [<sup>35</sup>S]-GTPγS, 1.5-2x10<sup>5</sup> cpm/pmol, in 10 mM Tris, pH 7.4, 100 mM NaCl, 5 mM MgCl<sub>2</sub>, 1 mM DTT, 0.1 mM EDTA. Components of the reaction mixture were kept at 4°C just prior to use. All measurements were made at ambient temperature. Rhodopsin was photolyzed under room light, mixed with [<sup>35</sup>S]-GTPγS, and incubated 1 minute. The exchange reaction was initiated by the rapid addition of transducin, and 50 μl aliquots were withdrawn at timed intervals (5-60 seconds), filtered through nitrocellulose filters

(Schleicher and Schuell, BA85) and immediately washed with two 3.5 ml aliquots of ice-cold buffer (10 mM Tris, pH 7.4, 100 mM NaCl, 5 mM MgCl<sub>2</sub>, 0.1 mM EDTA). The filters were dissolved in scintillation fluid, and the amount of [<sup>35</sup>S]-GTPγS associated with the filters was measured in a Beckman LSC.

Preliminary results indicated that 80% of transducin present in the reaction mixture bound to the nitrocellulose. Accordingly, all calculations incorporated this correction factor. Initial rates of the exchange reaction were determined from the slopes of plots of [<sup>35</sup>S]-GTPγS bound versus time representing that portion of the progress curve which was linear (see, for example, Figure 3). In control experiments, the amount of [<sup>35</sup>S]-GTPγS bound by transducin in the absence of rhodopsin was measured, and the calculated rate was utilized to correct for a final initial velocity,  $v_0$ , corresponding to the rhodopsin-catalyzed reaction. In the absence of transducin, it was determined that less than 0.01% of the bound cpm could be attributed to the rhodopsin preparation or background [<sup>35</sup>S]-GTPγS associated with the filter. The measured initial rates were proportional to rhodopsin concentration under all experimental conditions, and were obtained within a time period in which no more than 10% of the maximum extent of reaction occurred (see Figures 1 and 3).

Initial velocities as a function of variable transducin concentration were determined at several fixed levels of [<sup>35</sup>S]-GTPγS concentration. Graphically, reciprocal values of velocity were plotted against the reciprocals of substrate concentrations to generate Lineweaver-Burke plots. Any occasional points which deviated greatly were discarded. The



data were fit to equation [1] using a non-linear least squares method

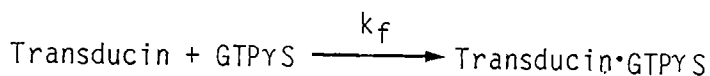
$$v_0 = V_{\max}^{\text{app}} [S] / K_m^{\text{app}} + [S] \quad [1]$$

assuming equal variance for the velocities; calculations were made using an adaptation of a BMDP program. In the case of sigmoidal curves, the data were fit to the approximated equation [2] discussed in Appendix I and in reference 78.

$$v_0 = V_{\max}^{\text{app}} [S]^2 / K_m^{\text{app}} + [S]^2 \quad [2]$$

The values of  $K_m^{\text{app}}$  and  $V_{\max}^{\text{app}}$  were provided with standard errors of their estimates.

Initial rates were also determined as described above for the following non-catalyzed reaction (in the absence of rhodopsin):



The rate equation for this reaction may be written in terms of initial velocity,  $v_0$ ,

$$v_0 = \frac{d [\text{Transducin}\cdot\text{GTP}\gamma\text{S}]}{dt} = k_f [\text{Transducin}]^q [\text{GTP}\gamma\text{S}]^r$$

where  $q + r = n$ ,  $n$  representing reaction order, and  $k_f$  indicating the rate constant for the reaction. In linear form:

$$\ln v_0 = \ln k_f + q \ln [\text{Transducin}] + r \ln [\text{GTP}\gamma\text{S}]$$

Accordingly, the parameters  $k_f$ ,  $q$  and  $r$  were calculated from the slopes and intercepts determined for plots of  $\ln v_0$  versus  $\ln [\text{Transducin}]$  or  $\ln$

[GTP $\gamma$ S], with respect to constant concentration of the appropriate reaction component (see, for example, Figures 16 and 17).

#### Equilibrium Binding Assay

A centrifugation technique was developed to monitor the binding of transducin to rhodopsin. Transducin (0.005-0.5  $\mu$ M) and rhodopsin (0.05-0.15  $\mu$ M) were suspended to 1 ml in a buffer containing 10 mM Tris, pH 7.4, 100 mM NaCl, 5 mM MgCl<sub>2</sub>, 1 mM DTT, 0.1 mM EDTA. Triplicate samples were incubated in the presence or absence of light for 30 minutes and then centrifuged for 15 min at 10,000 x g at 4°C. Aliquots (100  $\mu$ l) of the supernatants were taken, and the remaining volume was carefully removed by aspiration. The pellets, containing transducin bound to rhodopsin, were immediately resuspended in 200  $\mu$ l of buffer and samples which had been maintained in the dark were subjected to photolysis at this time. To the supernatant aliquots, photolyzed rhodopsin was added such that the amount was equivalent to that isolated in the pellets. A 50  $\mu$ l aliquot of [<sup>35</sup>S]-GTP $\gamma$ S (3.5 x 10<sup>3</sup> cpm/pmol) was added to all samples with a final concentration of 1  $\mu$ M. After a 60 minute incubation, 200  $\mu$ l aliquots were filtered through nitrocellulose filters and washed twice with 3 ml aliquots of ice-cold buffer. The amount of [<sup>35</sup>S]-GTP $\gamma$ S associated with the filter, which reflects the amount of transducin present, was measured by scintillation counting in a Beckman LSC. Corrections for background were made using values obtained for control samples measured in the absence of transducin. All measurements were performed at ambient temperature.

The use of the GTP $\gamma$ S binding assay to measure transducin activity associated with the pellets or supernatants relies on the fact that the G

protein binds guanine nucleotides with a 1:1 stoichiometry. The GTP $\gamma$ S binding reaction was complete within 60 minutes at saturating concentrations of rhodopsin and GTP $\gamma$ S employed. The amount of transducin determined to be present in the pellet was calculated as that amount bound; values determined for the supernatant aliquots were adjusted for the total assay volume and calculated as free transducin. Determinations for the triplicate samples were routinely within 3% of one another, and the average of these values was employed for Scatchard analysis. The data presented are representative of at least 3 independent experiments performed in this manner. Measurements of the total transducin concentrations employed in the binding assay were also accomplished by measuring the amount of [ $^{35}$ S]-GTP $\gamma$ S incorporated in the presence of rhodopsin, and these values were within 5% compared to the total amount of free and bound transducin determined for each point.

#### Physical Measurements

Sucrose density gradient centrifugation experiments were accomplished with a 4.5 ml linear 5-20% gradient in 10 mM Tris, pH 7.4, 100 mM NaCl, 5 mM MgCl $_2$ , 1 mM DTT, 0.1 mM EDTA. Samples containing protein of interest along with marker proteins (catalase,  $S_{20,w} = 11.3S$ ; BSA,  $S_{20,w} = 4.31S$  cytochrome C,  $S_{20,w} = 1.71S$ ) were overlaid and subjected to centrifugation at 40,000 rpm for 13 hours in a Beckman Ti 50.1 rotor. Following fractionation into 250  $\mu$ l aliquots, samples were analyzed by SDS-PAGE and by densitometry of the resultant Coomassie-staining pattern. Gel filtration over Sephacryl S-300 (Pharmacia) was accomplished using a 1.5 x 80 cm column with a flow rate of 1 ml/min. The buffer employed in these studies contained 10 mM Tris, pH 7.4, 100 mM NaCl, 5 mM MgCl $_2$ , 1 mM

DTT, 0.1 mM EDTA. Void volume was measured by monitoring the migration of Blue Dextran, total volume was obtained using [ $^3\text{H}$ ]- $\text{H}_2\text{O}$ . The column was calibrated using the following standards with their respective Stokes radii: chymotrypsinogen, 20.9 Å, BSA, 35.5 Å, catalase, 52.2 Å, and  $\beta$ -galactosidase, 69.1 Å. One ml fractions were collected and protein content was assayed by the method of Bradford (79) as well as by SDS-PAGE. GTPyS binding in the presence of rhodopsin was measured by the filtration assay described above in order to monitor the elution of transducin and its  $\alpha$  subunit (Figure 19). SDS-PAGE was performed by methods described by Laemmli (80). Immunoblotting experiments were performed by electrophoresing protein from SDS-PAGE gels to nitrocellulose at 380 mA for 20 minutes. The blot was incubated with a 1:100 dilution of antibodies in Tween-PBS, washed, and [ $^{125}\text{I}$ ]-protein A was added; immunoreactivity was detected by autoradiography.

#### Materials

Transducin and rhodopsin were obtained using frozen, dark-adapted bovine retinas purchased from J. Lawson and Co., Lincoln, NB. [ $^{35}\text{S}$ ]-GTPyS was from New England Nuclear, and GTPyS was obtained from Boehringer-Mannheim. All other materials were reagent grade and purchased from Sigma.

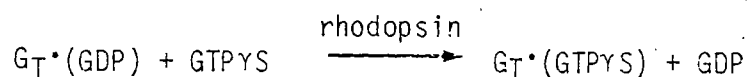
## CHAPTER III

## ALLOSTERIC BEHAVIOR IN TRANSDUCIN ACTIVATION MEDIATED BY RHODOPSIN:

## INITIAL RATE ANALYSIS OF GUANINE NUCLEOTIDE EXCHANGE

Results and Discussion

Initial rate analysis provides a powerful tool in order to investigate the mechanics of catalyzed reactions. This method may be utilized to study catalytic interactions between photolyzed rhodopsin and its substrates, transducin and guanine nucleotides. The validity of this kinetic approach relies on the capacity to measure initial rates of the reaction, thereby allowing an interpretation of the data based on steady-state assumptions. A functional means to ensure initial velocity measurements is to employ experimental conditions such that measured rates are proportional to enzyme concentration. Figure 1 presents the linear relationship between initial velocity and rhodopsin concentration, determined in the catalyzed reaction between transducin,  $G_T$ , and [ $^{35}S$ ]-GTP $\gamma$ S:



The non-hydrolyzable GTP analog, GTP $\gamma$ S, was employed to study the guanine nucleotide exchange reaction in order to avoid possible interference arising from the slow GTPase activity intrinsic to  $T\alpha$ . The rate of production of  $G_T \cdot (\text{GTP}\gamma\text{S})$  was monitored by rapid filtration through nitrocellulose filters which bind transducin. Experimental details of the exchange reaction assay are described in Chapter II, and discussed below. Typically, a rhodopsin concentration of 5.4 nM was employed in the initial

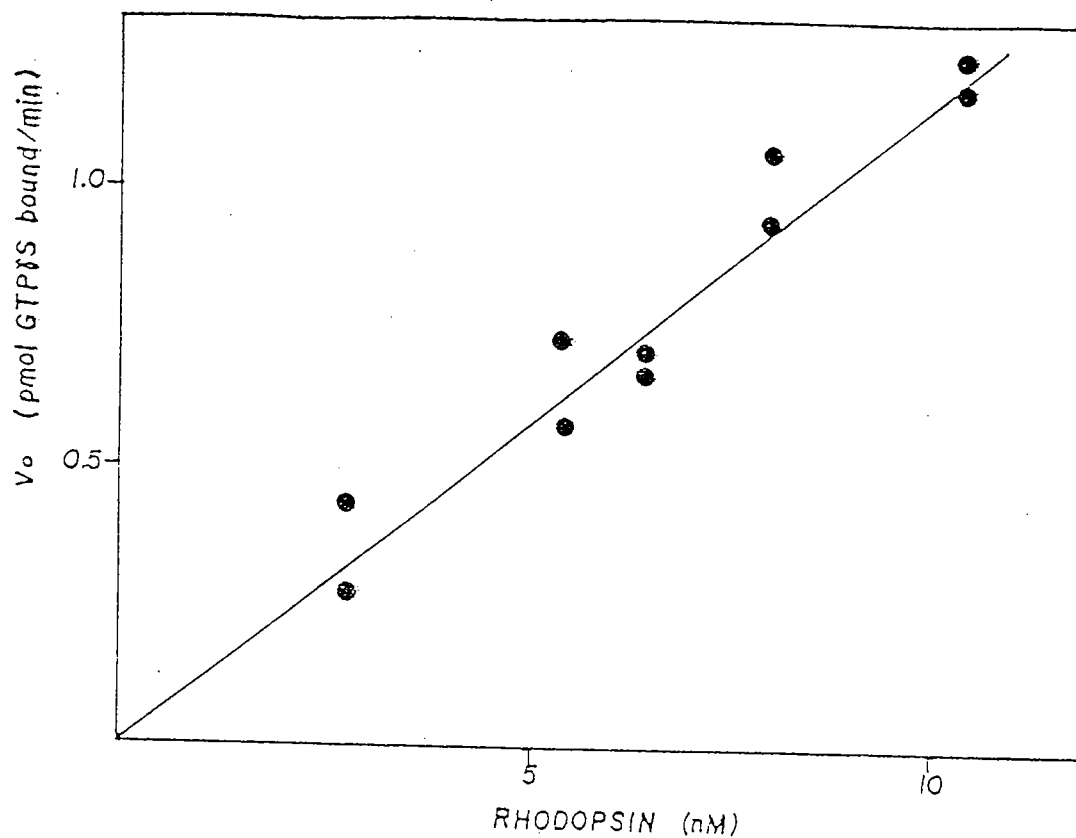


FIGURE 1 Linear relationship between rhodopsin concentration and rate of guanine nucleotide exchange reaction. Initial velocities,  $v_0$ , were determined from the slopes of progress curves measured for the reaction catalyzed by rhodopsin (2.7-10.7 nM) with 0.10  $\mu\text{M}$  [ $^{35}\text{S}$ ]-GTP $\gamma$ S and 0.25  $\mu\text{M}$  transducin. The initial velocities were corrected for the rate of reaction measured in the absence of rhodopsin. Shown is the plot of  $v_0$ , pmol [ $^{35}\text{S}$ ]-GTP $\gamma$ S bound/min, as a function of rhodopsin concentration (nM).

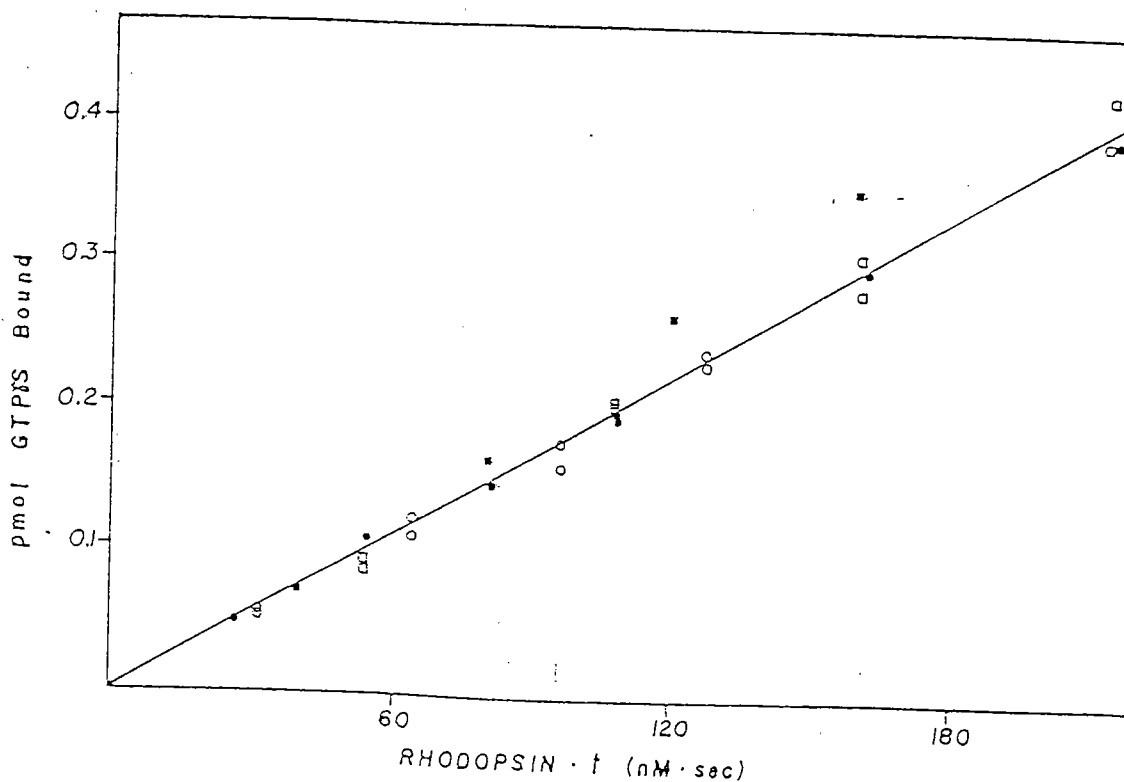


FIGURE 2 Selwyn's plot of reaction progress as a function of the product of rhodopsin concentration multiplied by time. The amount of  $[^{35}\text{S}]\text{-GTP}\gamma\text{S}$  exchanged on transducin was determined by filtration through nitrocellulose filters; 50  $\mu\text{l}$  aliquots were withdrawn from a 300  $\mu\text{l}$  reaction assay, rapidly filtered and immediately washed twice with buffer. Assay mixtures contained a 0.25  $\mu\text{M}$  transducin, 0.1  $\mu\text{M}$   $[^{35}\text{S}]\text{-GTP}\gamma\text{S}$ , and rhodopsin concentrations as follows: 5.4 nM (o), 6.4 nM (●), 8 nM (■), and 10.7 nM (□). The measured amount of radioactivity associated with the filters is proportional to the amount of  $[^{35}\text{S}]\text{-GTP}\gamma\text{S}$  bound to transducin. The product of rhodopsin concentration (nM) multiplied by the reaction time (seconds) is plotted versus the amount of  $[^{35}\text{S}]\text{-GTP}\gamma\text{S}$  (pmol) determined for that time point.

rate assays, within the linear range indicated by the result presented in Figure 1 which confirms that initial velocities were measured under steady-state conditions. A second concern was the possibility of inactivation of rhodopsin complicating the measurement of reaction rates. A simple test of this situation is provided by Selwyn's plot, shown in Figure 2. This method is based on the reasoning that for any catalyzed reaction, product formation is a function of enzyme concentration and time; therefore, for any given extent of reaction, the value of enzyme concentration multiplied by time must be a constant. As Figure 2 shows, this relationship was verified by the linear correlation between the extent of reaction, pmol [ $^{35}\text{S}$ ]-GTPYS bound, and [rhodopsin] x time, at concentrations between 5.4-10.7 nM rhodopsin during time periods used in the study. If time-dependent inactivation of rhodopsin were to conflict with this measurement, distinct progress curves would be distinguished for different concentrations of rhodopsin. The results of this experiment eliminate the possibility that photoinactivation interferes with the kinetic measurements. Finally, the isomerization of rhodopsin's chromophore 11-cis retinal to all-trans initiates the bleaching of the photopigment producing a series of spectral changes, eventually transforming rhodopsin to the metarhodopsin II form. In order to ensure a homogeneous population of rhodopsin molecules, the reaction components were photolyzed a full minute prior to initiation of guanine nucleotide exchange. Pre-incubation in the light for up to 30 minutes did not qualitatively alter results. Thus, possible aberrations which might occur at early time points due to the phototransition seem unlikely.

In order to fully investigate the catalytic mechanism of transducin



activation mediated by rhodopsin, it is necessary to explore the relationships between initial velocities measured at different substrate concentrations,  $[G_T]$  and  $[GTP\gamma S]$ . Figure 3 shows a series of timecourse measurements of guanine nucleotide exchange in reaction mixtures which contained varying transducin concentrations and  $0.167 \mu M$   $[^{35}S]$ -GTP $\gamma$ S, in the presence or absence of  $5.4 \text{ nM}$  rhodopsin. As depicted, linear portions of reaction progress curves were measured under the experimental conditions used throughout this investigation. Initial rates were obtained as the slopes of the generated lines; the rate of exchange measured in the absence of rhodopsin was deducted from that determined in its presence in order to obtain a value for the catalyzed reaction. Serial determinations in this manner allow analysis of the relationship between velocity and substrate concentration. The lower right panel of Figure 3 presents the Michaelis-Menten curve of the initial velocities,  $V_0$ , determined in this experiment, as a function of transducin concentration. The substrate-velocity relationship revealed an unexpected finding - the sigmoidal nature of this curve is indicative of positive cooperative allosteric behavior. Analysis of the rate of the guanine nucleotide exchange reaction for transducin in the absence of rhodopsin showed no evidence of sigmoidal behavior (Chapter IV). This latter result implies that the cooperative effect resides in the interactions between rhodopsin and transducin rather than between GTP $\gamma$ S and transducin.

Since transducin is a heterotrimer of  $\alpha\beta\gamma$  subunits, it is possible that the observed allosterism could involve molecular events between  $T\alpha$  and rhodopsin,  $T\beta\gamma$  and rhodopsin, or  $T\alpha$ - $T\beta\gamma$  and rhodopsin. In order to discriminate between these possibilities, purified  $T\alpha$  was separated from

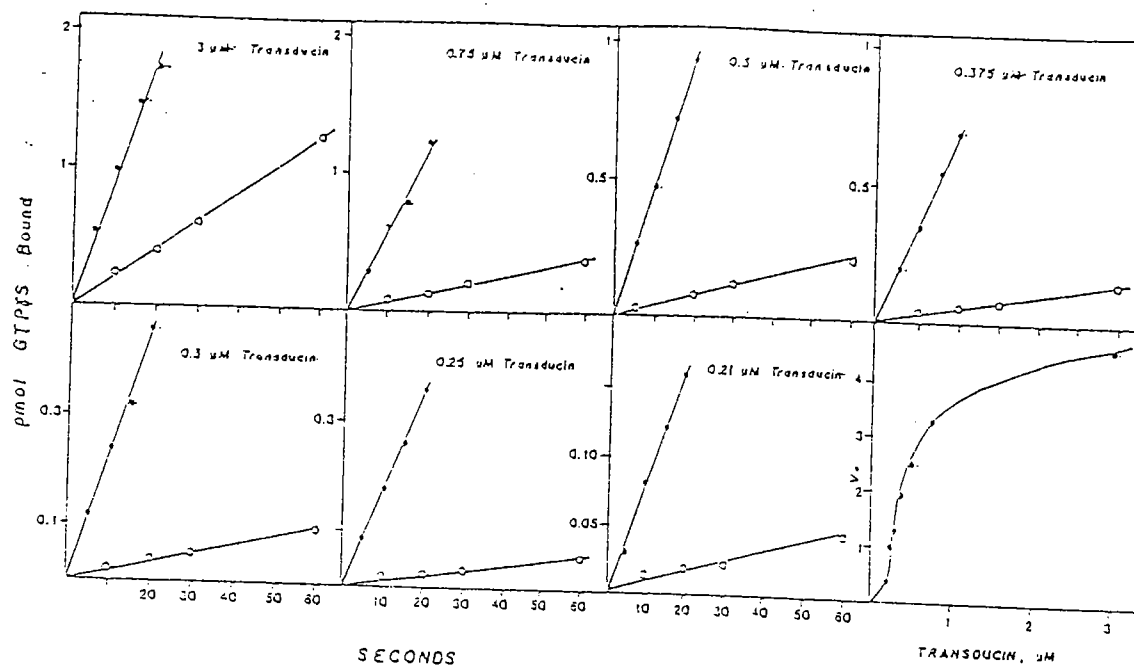


FIGURE 3 Timecourse of guanine nucleotide exchange of transducin. A 300  $\mu$ l assay mixture was prepared by incubating 5.4 nM rhodopsin and 0.167  $\mu$ M [ $^{35}$ S]-GTP $\gamma$ S in the light for 1 minute, and initiating the exchange reaction by the addition of the appropriate amount of transducin (as indicated in the figure panels). At times shown, a 50  $\mu$ l sample was withdrawn, rapidly filtered through nitrocellulose filters, and immediately washed with ice-cold buffer. The amount of radioactivity counted is proportional to the amount of [ $^{35}$ S]-GTP $\gamma$ S exchanged on transducin and is plotted as a function of time. The reaction time course was monitored in the presence (●) and absence (○) of rhodopsin, and initial rates were determined from the slopes of these lines. The exchange reaction rate in the absence of rhodopsin was deducted from that measured in its presence in order to obtain the initial velocity for the catalyzed exchange. As shown, the linear portion of the reaction time course was studied. Lower right panel: Michaelis-Menten curve for the initial velocities of the rhodopsin mediated guanine nucleotide exchange determined as a function of transducin concentration. This plot shows the relationship between  $v_0$ , pmol [ $^{35}$ S]-GTP $\gamma$ S bound/min, and transducin,  $\mu$ M, determined for the data shown.

T $\beta\gamma$  by column chromatography and employed in similar kinetic assays, the results of which are presented in Figure 4. It should be noted that the initial rates measured in experiments with free T $\alpha$  were markedly decreased when compared to those obtained at similar concentrations of holo-transducin. This can be expected since T $\beta\gamma$  has been shown to enhance the interaction of T $\alpha$  with rhodopsin (71). The Eadie-Hofstee plot shows the downward curvature expected of a system displaying positive cooperative behavior. The fact that cooperativity is observed in the absence of T $\beta\gamma$  indicates that the basis for this phenomenon must arise from interactions between transducin's  $\alpha$  subunit and the photoreceptor. The dashed line in Figure 4 represents the curvature expected from a positive cooperative interaction with  $n_{app} = 2$ , whereas the dotted line indicates the straight line observed in the absence of cooperative behavior. This allosteric response is corroborated by the Hill plot of data from a separate experiment with holotransducin, shown in Figure 5. The plot of  $\log (v_0/V_{max}-v_0)$  versus  $\log [\text{transducin}]$  displays a positive slope of  $n_H = 2.2$ . The Hill coefficient determined for a series of similar experiments was found to be  $1.97 \pm 0.22$  ( $n = 16$ ). Analysis of kinetic data obtained using purified T $\alpha$  yielded a value of  $n_H = 1.95 \pm 0.44$  ( $n = 4$ ).

To complete the kinetic investigation, initial velocities as a function of transducin concentration were measured at several fixed levels of [ $^{35}\text{S}$ ]-GTP $\gamma\text{S}$  concentration. Figure 6 shows the results from one such experiment, presented in double reciprocal form. The Lineweaver-Burke plots with respect to reciprocal transducin concentration (panel B) show the curvature expected in a system displaying positive cooperative

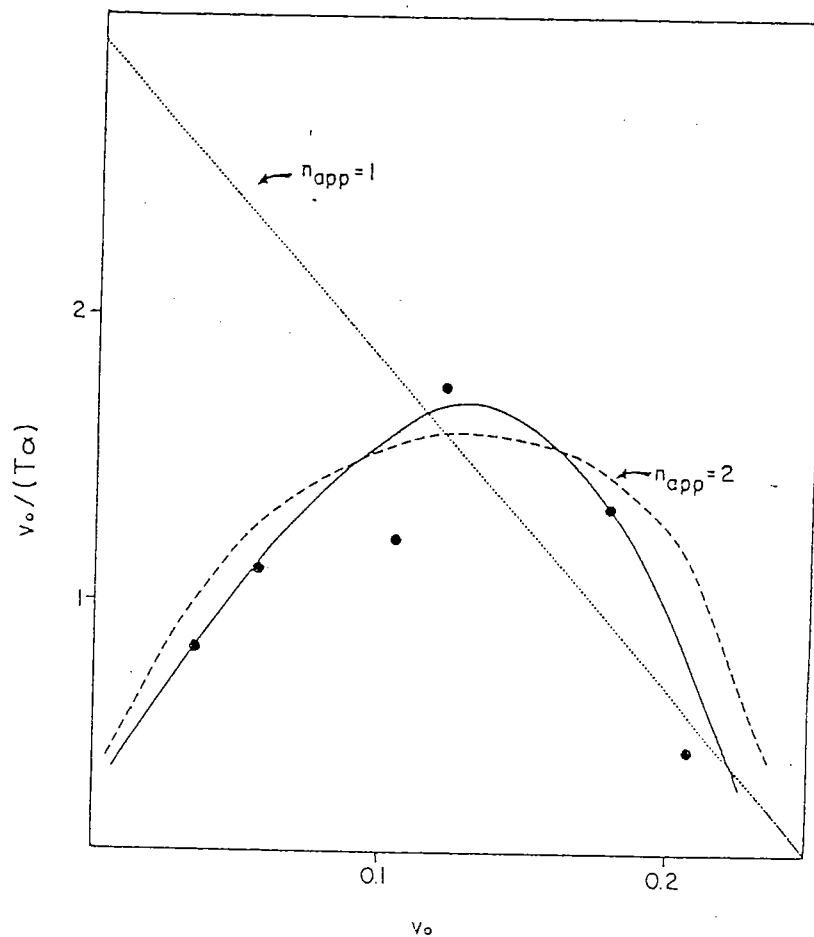


FIGURE 4 Kinetics of  $T_{\alpha}$  subunit activation. Purified  $\alpha$  subunit from transducin was employed in kinetic assays as described for Figure 3. Initial rates were determined at concentrations of  $T_{\alpha}$  from 0.048-0.592  $\mu\text{M}$  and  $[\text{GTP}\gamma\text{S}]$  of 0.15  $\mu\text{M}$ . Shown is the Eadie-Hofstee plot of  $v_o/[\text{T}\alpha]$  versus  $v_o$  (filled circles). The dashed line represents the normalized curve expected from a system having a Hill coefficient of 2. The dotted line depicts the normalized straight line which is obtained in the absence of allosteric behavior.

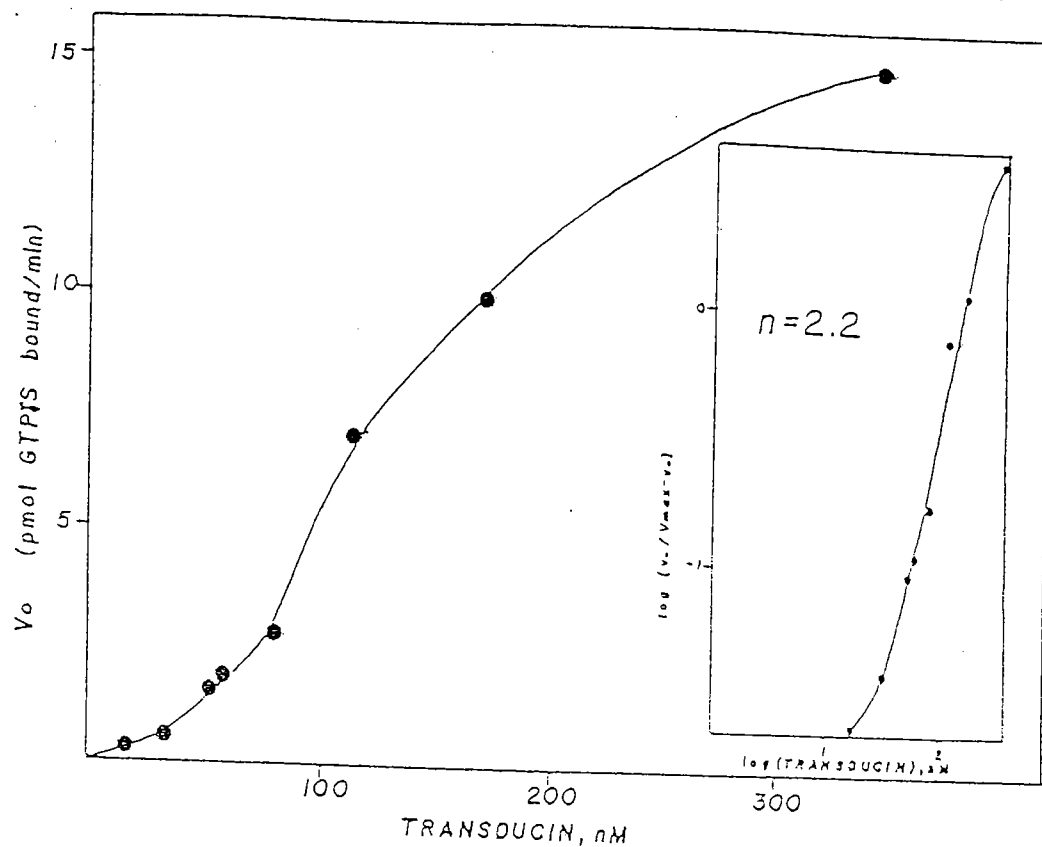


FIGURE 5 Allosterism observed in substrate-velocity plot. Initial velocities,  $v_o$ , were determined for the rhodopsin-catalyzed reaction between  $0.5 \mu\text{M}$  [ $^{35}\text{S}$ ]-GTP $\gamma$ S and transducin at concentrations as indicated in the figure. Measurements were performed as described for Figure 3, and similarly, the Michaelis-Menten curve generated by the plot of  $v_o$  as a function of transducin concentration is sigmoidal in character. A value of  $V_{max}^{app} = 18.34 \pm 0.86$  pmol GTP $\gamma$ S bound/min was obtained for the experimental data using non-linear regression analysis as described in Chapter II. Inset shows Hill plot of data.  $\log [v_o / (V_{max} - v_o)]$  is plotted as a function of  $\log [\text{Transducin}]$  in order to analyze data according to the Hill equation. As shown, a positive slope corresponding to  $n_H = 2.2$  was determined.

behavior. In the absence of allosteric behavior, these plots would be expected to be linear. Indeed, Lineweaver-Burke plots with respect to reciprocal  $[^{35}\text{S}]\text{-GTP}\gamma\text{S}$  concentration do generate a series of parallel lines (panel A). The Michaelis-Menten plots of  $[^{35}\text{S}]\text{-GTP}\gamma\text{S}$  concentration versus initial velocity were always found to be of a normal hyperbolic form. Data from these experiments were analyzed as detailed in the Methods section. Secondary plots of the slopes of the double reciprocal lines,  $(K_m^{\text{app}}/V_{\text{max}}^{\text{app}})$ , were found to be independent of the square of transducin concentration,  $[\text{G}_\text{T}]^2$ , and GTP $\gamma$ S concentration. Secondary plots of the intercepts,  $(1/V_{\text{max}}^{\text{app}})$ , were found to be linear with respect to  $[\text{G}_\text{T}]^2$  or  $[\text{GTP}\gamma\text{S}]$ , accordingly. The data were found to be in agreement with the following initial rate equation, derived from principles of steady-state kinetics and discussed in Appendix I.

$$\frac{1}{v_0} = \frac{1}{V_{\text{max}}} \left[ \frac{K_m}{[\text{G}_\text{T}]^2} + \frac{K_m}{[\text{GTP}\gamma\text{S}]} + 1 \right]$$

The approximated initial velocity equation predicts that plots of reciprocal velocity as a function of the reciprocal of the square of transducin concentration would generate a series of parallel lines. Figure 7 shows that this latter prediction is met; the linear transformations are presented using data from panel B in Figure 6. From the intercepts and slopes of the secondary plots determinations of the kinetic parameters may be made. Values of  $K_m^{\text{G}_\text{T}} = 0.1\text{-}1.5 \times 10^{-6} \text{ M}^2$ ,  $K_m^{\text{GTP}\gamma\text{S}} = 0.1\text{-}1.7 \times 10^{-6} \text{ M}$ , and  $V_{\text{max}} = 0.9\text{-}6.0 \times 10^{-8} \text{ M/min}$  were obtained from data analysis of three individual experiments performed in this fashion. All of the experimental data were found to agree quite well with the approximated initial rate equation. However, in order to obtain highly

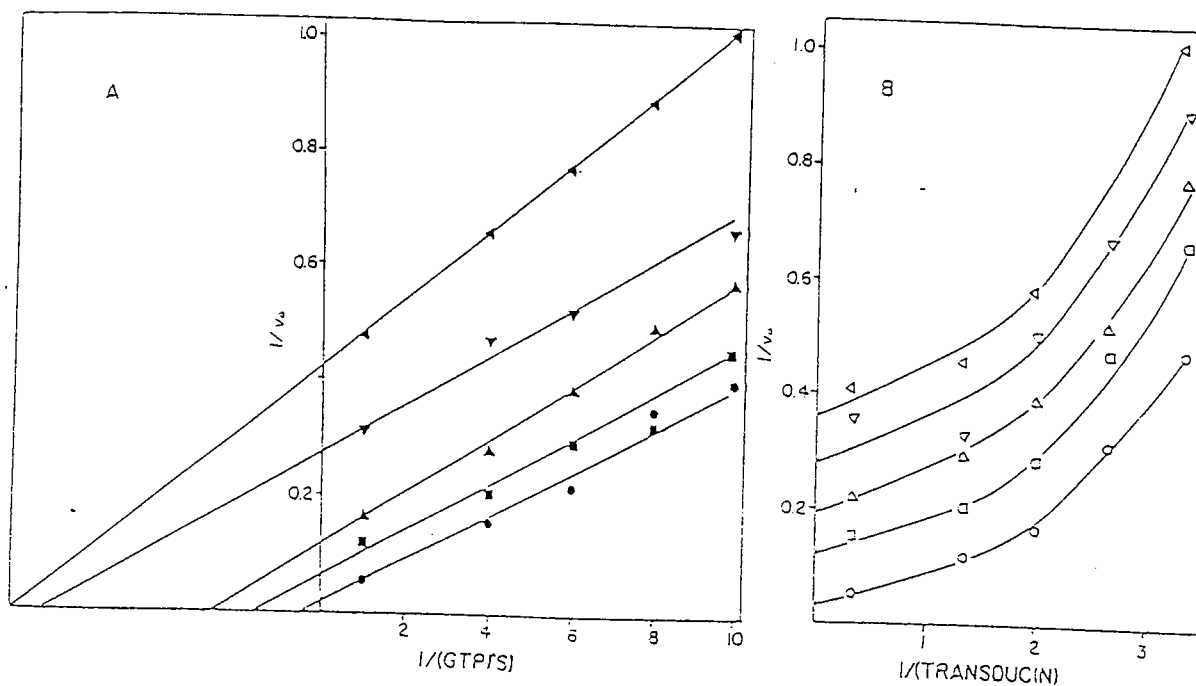


FIGURE 6 Lineweaver-Burke plots for the rhodopsin catalyzed guanine nucleotide exchange reaction. Initial velocities were determined at varying concentrations of transducin at several fixed levels of [ $^{35}\text{S}$ ]-GTPYS. Shown is representative data from one of three experiments in which initial rates were obtained. Panel A: Double reciprocal plots of  $v_0^{-1}$  as a function of  $[\text{GTPYS}]^{-1}$ , with transducin concentrations of 3  $\mu\text{M}$  ( $\circ$ ), 0.75  $\mu\text{M}$  ( $\blacksquare$ ), 0.5  $\mu\text{M}$  ( $\blacktriangle$ ), 0.375  $\mu\text{M}$  ( $\blacktriangledown$ ), and 0.3  $\mu\text{M}$  ( $\blacktriangleleft$ ). A series of parallel lines are observed, providing evidence of a double displacement catalytic mechanism for rhodopsin. Panel B: Double reciprocal plots of  $v_0^{-1}$  as a function of  $[\text{transducin}]^{-1}$ , at concentrations of GTPYS of 1  $\mu\text{M}$  ( $\circ$ ), 0.25  $\mu\text{M}$  ( $\square$ ), 0.167  $\mu\text{M}$  ( $\Delta$ ), 0.125  $\mu\text{M}$  ( $\nabla$ ), and 0.1  $\mu\text{M}$  ( $\triangleleft$ ). The curvilinearity depicted in these plots is indicative of positive cooperative behavior. Units are:  $v_0^{-1}$  in terms of (pmol GTPYS bound/min) $^{-1}$  and substrate concentrations as ( $\mu\text{M}$ ) $^{-1}$ .

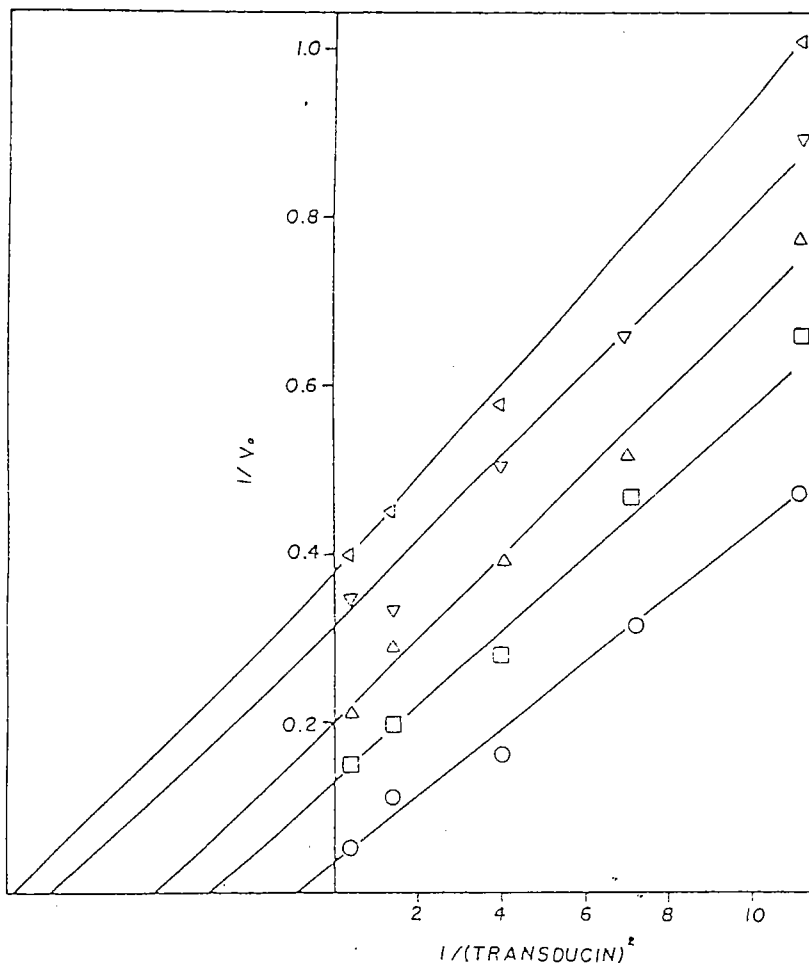


FIGURE 7 Linear transformation of double reciprocal plots with respect to transducin. Shown is the experimental data from Figure 6, Panel B, plotted as the inverse square of transducin concentration ( $\mu\text{M}$ )-2. A series of parallel lines is generated, supporting the rate equation as discussed in the text.



accurate values of the kinetic parameters given above, it is necessary to include experimental data from rate assays containing concentrations of substrates an order of magnitude higher than  $K_m$ . This is the single limitation of the kinetic studies, imposed by the constraints of obtaining a large enough quantity of transducin within realistic means. It should be emphasized, however, that this limitation by no means invalidates the information obtained in support of the rate equation, it only indicates that there will be some degree of error in the quantitation of its kinetic parameters.

Formally, catalyzed reactions fall into two categories: the double-displacement type (also known as substituted enzyme or ping-pong mechanisms) or the single-displacement type (also referred to as ternary complex or sequential mechanisms). These findings demonstrate that rhodopsin catalyzes guanine nucleotide exchange by a double displacement mechanism and exhibits allosterism with respect to the GTP-binding protein. If it is considered that the allosteric behavior arises from positive cooperative interactions, the data describe the following model which is presented in Figure 8A and detailed in Appendix I. Although the diagram depicts two binding sites for transducin on rhodopsin, equivalent schemes could be formulated based on dimerization of transducin and/or rhodopsin. Here it is considered that transducin interacts with rhodopsin in a manner which is sensitive to the presence of a second molecule of transducin (as witnessed in the curvilinearity of the double reciprocal plots of Panel B in Figure 6 and supported by the linear transformations as the square of transducin concentration plotted in Figure 7). As indicated by Plowman (81), models of this type can be obtained if one of

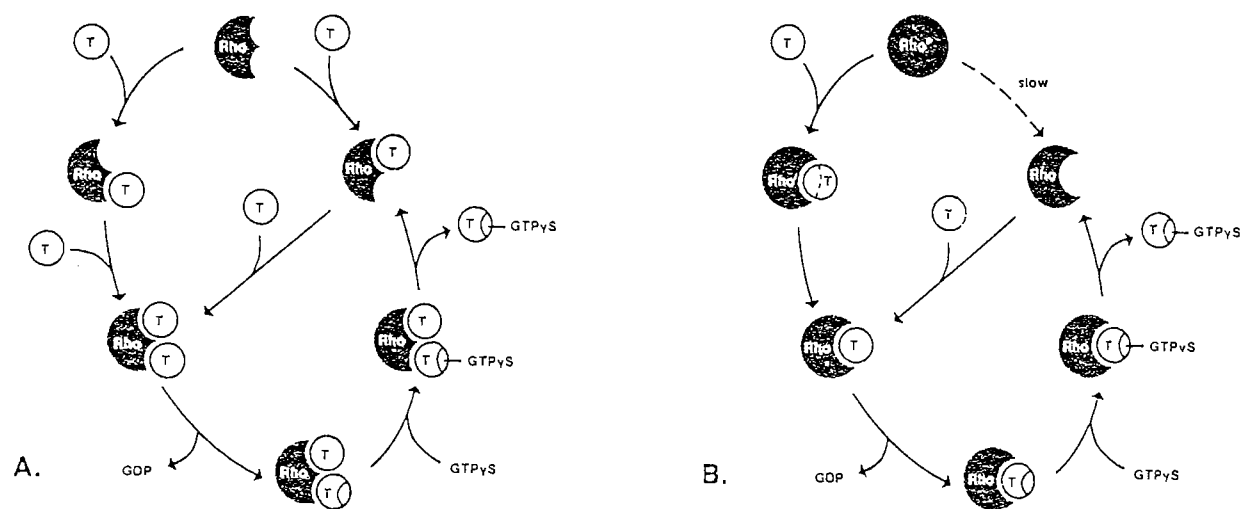


FIGURE 8 Mechanistic pathways of allosteric behavior. A: Diagram indicating positive cooperative interactions between multiple binding sites on rhodopsin. The double displacement catalytic mechanism is shown by the release of GDP prior to the binding of GTPγS. B: Hysteresis is modelled in this scheme as arising from the conversion of inactive Rho' to Rho: although a slow step, this process is enhanced by the presence of transducin which induces the necessary conformational alteration. Note that a double-displacement pathway is also described for guanine nucleotide exchange.

the sites is essentially a regulatory rather than catalytic site. The fact that the allosterism is observed with the  $\alpha$  subunit of transducin (Figure 4) suggest that the cooperativity is localized to interactions between rhodopsin and  $T\alpha$ . This interaction promotes the displacement of the bound guanine nucleotide (GDP) (2,3), generating a "substituted enzyme complex" between rhodopsin and transducin, now devoid of guanine nucleotide. The formation of the latter complex is predicted by the nature of the parallel double reciprocal lines in Figs. 6 and 7. Convergent lines would otherwise indicate the presence of a "ternary complex" which might be thought of in this case to represent a complex between rhodopsin, transducin, and both guanine nucleotides. The GTP analog, GTP $\gamma$ S, associates with the rhodopsin-transducin "substituted enzyme" complex, and causes activated transducin, with GTP $\gamma$ S bound, to exit the reaction complex. The character of the rate equation and double reciprocal plots requires that the first guanine nucleotide (GDP) exit from the reaction complex prior to the addition of GTP $\gamma$ S, defining a double-displacement mechanism for the catalytic interactions between rhodopsin, transducin, and guanine nucleotides. Although a double-displacement type mechanism has been generally assumed, this is the first direct demonstration of this reaction mechanism.

An alternative model may be developed to explain the observed allosterism, depicted in Figure 8B. As shown, the exchange reaction proceeds through a double-displacement mechanism, which is required by the character of the double reciprocal plots. However, the possibility that rhodopsin is a hysteretic enzyme must be considered (see discussion of Scheme III in Appendix I). In this model, transducin binds to an inactive

form of rhodopsin,  $Rho'$ , promoting the conversion to the active form,  $Rho$ , which participates in the exchange reaction. The results suggest that  $T\alpha$  would be intimately involved in this molecular event. The conversion of  $Rho' \rightarrow Rho$  is otherwise a slow process representing hysteretic activity. Since this isomerization is dependent on transducin concentration, it is possible that sigmoidal behavior could be described by incorporating hysteresis into models describing the kinetics of the exchange process. Neet (82) and Ainsworth (83) have discussed this aspect of allosteric behavior to some length, which presents a distinct alternative to models which involve cooperative interactions between multiple binding sites. A key point in order to distinguish this possibility is that hysteretic cooperativity can be witnessed only in kinetic studies; measurements from equilibrium binding techniques would not reveal this behavior. Instead, oligomeric associations arising from cooperative interactions would be observed (this is demonstrated by the discussion in Appendix I). In order to further explore the molecular basis for the allosteric behavior, a direct equilibrium binding assay was developed, the results of which are presented in Chapter IV.

#### Conclusions

1. Interactions between rhodopsin and its substrates, transducin and GTPyS, may be investigated by employing initial rate analysis.
2. The initial rate studies describe a double-displacement catalytic mechanism for rhodopsin.
3. Michaelis-Menten curves show allosteric behavior with respect to transducin, with a Hill coefficient of 2 found for the positive cooperativity.

4. Similar allosterism is witnessed in kinetic studies with  $T_{\alpha}$ , suggesting that this phenomenon arises from interactions between the G protein's  $\alpha$  subunit and rhodopsin.
5. An approximated initial rate equation is derived which models the kinetic data well.
6. Values determined for the kinetic parameters are:  $V_{\max} = 0.9 - 6.0 \times 10^{-8} \text{ M/min}$ ,  $K_m^{GT} = 0.1 - 1.5 \times 10^{-6} \text{ M}^2$ , and  $K_m^{GTPYS} = 0.1 \times 10^{-6} \text{ M}$ .

## CHAPTER IV

MOLECULAR ORIGINS OF ALLOSTERIC BEHAVIOR: EQUILIBRIUM BINDING  
STUDIES BETWEEN RHODOPSIN AND TRANSDUCINResults and Discussion

The allosterism observed in the initial rate studies of transducin activation by rhodopsin raised questions concerning the molecular basis of this phenomenon. As discussed in Chapter III, the kinetic methods employed cannot discriminate between positive cooperative behavior induced by oligomeric associations or allosterism produced by hysteresis in the activity of rhodopsin. However, the interactions between substrate and enzyme at equilibrium can be used to differentiate between the two models. Since hysteresis is purely a kinetic phenomenon, cooperativity would not be observed in binding curves if this mechanism accounts for the allosteric behavior, as discussed in Appendix I. Therefore, a centrifugation method was developed to measure the equilibrium binding of transducin to rhodopsin. The basic premise is to separate transducin bound to the integral membrane protein rhodopsin by sedimentation, and to assay the amount of transducin found in the pellet and that remaining in the supernatant by measuring guanine nucleotide binding activity. Sedimentation techniques have been previously employed to study the light-dependent binding of proteins to rhodopsin, however, results from these studies have relied on Coomassie-stained profiles from SDS-PAGE (84-86) or the determination of bound radiolabelled transducin at a single concentration (71). The technique described here permits the accurate quantitation of functional bound transducin over a range of concentrations

such that binding curves may be constructed and analyzed for the parameters involved in interactions between rhodopsin and transducin. This is the first direct assay which has been developed to monitor the interactions between receptors and G proteins. The usefulness of this method is demonstrated by the results, which reveal positive cooperative behavior in the molecular interactions between receptor and G protein.

Figure 9 shows the binding curve produced by incubating UROS, which contains rhodopsin, in the presence of light with increasing amounts of transducin. The amount of  $^{35}\text{S}$ -GTPYS binding activity isolated in the pellet after centrifugation of the mixture was assayed as described in Chapter II and provides a measurement of functional bound transducin. As a control, equivalent amounts of UROS were treated with hydroxylamine in order to remove the photon receptor's chromophore, 11-cis-retinal, producing the protein opsin (75). The data in Figure 9 demonstrate the specific binding of transducin to rhodopsin, as compared to results obtained with opsin-containing UROS. Since opsin is unable to activate the G protein, it would appear that loss of the chromophore removes rhodopsin's capacity to interact with transducin. This is supported by the results presented in Figure 9, which suggest that transducin weakly associates with opsin-containing UROS membranes in a non-specific manner as would be expected for an extrinsic membrane protein.

In order to confirm that the centrifugation technique coupled to the GTPYS binding assay provides a quantitative description of binding interactions between rhodopsin and transducin, the amount of protein isolated in the pellets was analyzed by SDS-PAGE. Panel A of Figure 9 presents the Coomassie-staining profile produced by UROS pellets

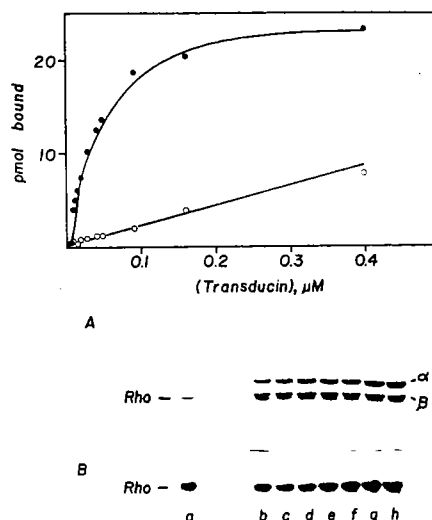


FIGURE 9 Binding interactions between transducin and rhodopsin. One ml assay mixtures containing 86 nM rhodopsin in UROS and 5-500 nM transducin were incubated in the presence of light for 30 minutes and subjected to centrifugation. The isolated pellets were resuspended in buffer containing [ $^{35}\text{S}$ ]-GTPYS and, after a 60 minute incubation period, aliquots were removed, filtered onto nitrocellulose filters, and washed. The amount of radioactivity bound to the filter was measured and is proportional to the amount of transducin bound in the pellet (●). As a control, equivalent amounts of UROS were treated with hydroxylamine to remove the 11-*cis*-retinal chromophore of rhodopsin (○), and treated exactly as described above with the exception that native UROS was added to the pellets in order to catalyze the GTPYS binding reaction. Panel A shows the Coomassie profile from SDS-PAGE of pellets obtained in a similar assay with 114 nM rhodopsin. Panel B is an autoradiograph of identical samples which were electrophoresed by SDS-PAGE, transferred to nitrocellulose, and blotted using anti-rhodopsin antibodies. Lanes represent: a, control showing amount of rhodopsin added prior to centrifugation and b-h, material isolated in the pellets from samples initially containing 35, 50, 65, 80, 100, 250 and 500 nM transducin, respectively.



sedimented after incubation in the light with increasing amounts of added transducin. It is observed that the amount of transducin associated with the UROS increases in a proportional manner as suggested by the centrifugation binding assay. Panel B of Figure 9 shows an immunoblot of identical samples using anti-rhodopsin antibodies (46). This result confirms that amounts of rhodopsin found in the pellets are equivalent to the total amount added, providing evidence that the UROS may be quantitatively isolated by centrifugation.

Preliminary control experiments indicated that the binding of transducin to UROS in the light was extremely rapid. No detectable difference in GTP $\gamma$ S binding activity could be discerned in the pellets at times of incubation between 5 and 60 minutes. These results confirmed that the measurements obtained represent true equilibrium binding. These data are also in agreement with measurements which suggest that binding interactions between transducin and rhodopsin are very fast (69,86).

The centrifugation procedure was also used to detect light-dependent binding of transducin to rhodopsin. Figure 10, panel A compares the binding curves obtained from identical samples incubated either in the presence or absence of light. A dramatic increase in the amount of bound transducin is observed in the presence of photolyzed rhodopsin compared to the dark control samples. However, there is a small but significant increase in transducin binding to UROS in the dark when compared to binding to opsin-containing UROS (Figure 9). This finding is in agreement with other studies which have suggested that transducin is unable or only weakly interacts with rhodopsin in the absence of light (71,84-86). The results also verify that the centrifugation assay provides a reliable and specific

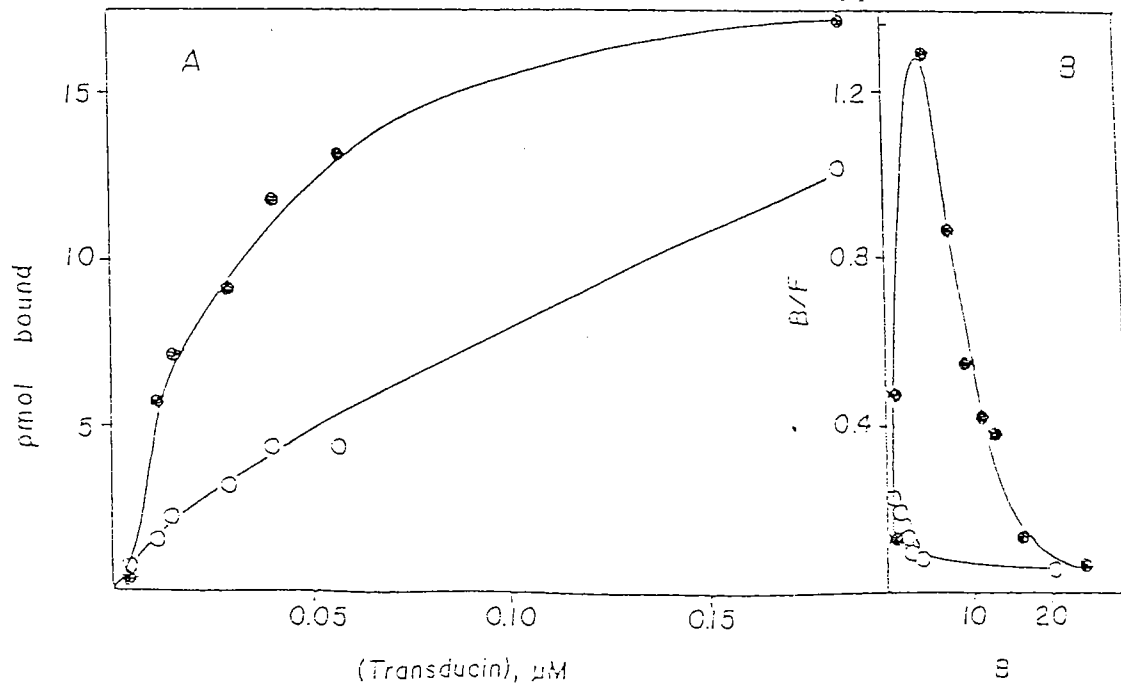


FIGURE 10 Light-dependent binding of transducin to rhodopsin. Assay mixtures containing 59 nM UROS and 5-200 nM transducin were incubated in the presence (●) or absence (○) of light and manipulated as described for Figure 9. Panel A shows the binding curves generated in this experiment. Panel B presents the Scatchard plots of this data produced by measuring the amount of transducin remaining in the supernatants as well as that bound in the pellets, providing values for Bound/Free (B/F) versus Bound (B, pmol).

measurement of binding interactions between transducin and rhodopsin.

The transducin binding curves shown in Figures 9 and 10 display sigmoidicity which is characteristic of an allosteric response. Panel B of Figure 10 presents Scatchard plots for transducin binding in the presence and absence of light. Such plots were constructed by measuring the amount of unbound (or free) transducin remaining in the supernatant after centrifugation, as well as that amount bound to rhodopsin. The downward curvature displayed for light-dependent transducin binding is a clear indication that positive cooperative interactions occur between the G protein and rhodopsin. These observations were further confirmed by studying the binding interactions between transducin and rhodopsin which had been purified and reconstituted into lipid vesicles. The Scatchard plots for data obtained in the presence and absence of light in the reconstituted system are shown in Figure 11. The characteristics of light-dependent binding observed for the liposome-reconstituted system were identical to results obtained from studies employing UROS.

The observation of allosteric behavior in binding interactions between transducin and rhodopsin correlates with the positive cooperativity witnessed in kinetic studies of the activation process (Chapter III). Furthermore, the equilibrium binding results demonstrate that the molecular basis for the allosteric behavior must arise from interactions between multiple transducins acting in a positive cooperative manner with rhodopsin. The initial rate studies could not discern the molecular origins of this phenomenon. As discussed in Chapter III, it is possible that the allosterism could be a result of hysteresis in rhodopsin's activity. This behavior would be detected kinetically, but

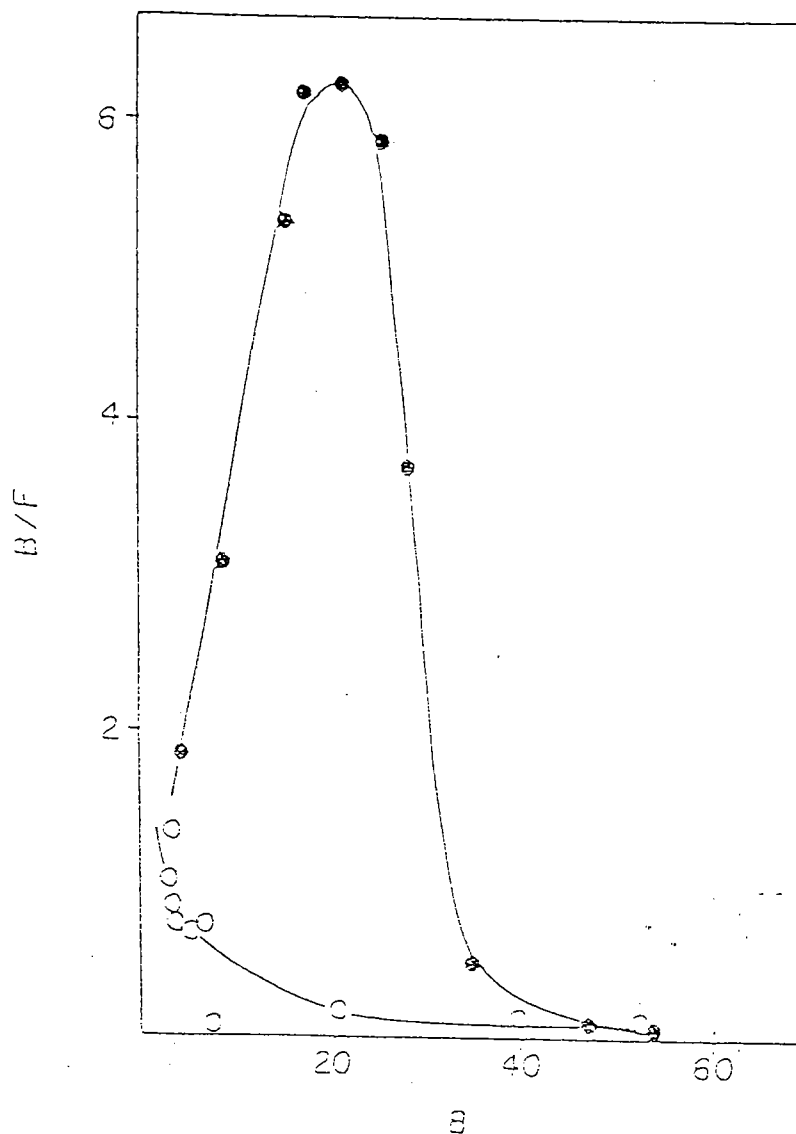


FIGURE 11 Light-dependent binding of transducin to purified reconstituted rhodopsin. The centrifugation binding assay was employed to monitor interactions between transducin (5-700 nM) and rhodopsin (114 nM) which had been purified and reconstituted into lipid vesicles. Shown are the Scatchard plots of data obtained in the presence (●) and absence (○) of light (Bound/Free versus Bound, pmol).

would not be observed in equilibrium binding studies. Thus, the binding data serve to clarify the role of allosteric behavior in the G protein's activation process and preclude alternative explanations.

Binding data was analyzed by methods detailed in Appendix II. A Hill coefficient,  $n_H = 1.92 \pm 0.16$  ( $n = 6$ ), was determined and found to be in excellent agreement with the value determined for allosteric behavior revealed by initial rate analysis of the guanine nucleotide exchange reaction. This result emphasizes the correlation between these studies and indicates that at least two transducins are involved in the positive cooperative response. A  $K_d^{app}$  (for combined sites) was found to be  $0.05 \mu\text{M}$ , a value which, interestingly, is close to the range of  $K_m^{GT}$  values determined from kinetic analysis of the activation process (7). Similar values were obtained in studies of both UROS and reconstituted rhodopsin, indicating that these parameters reflect the native properties of the receptor.

The final parameter obtained from analysis of the binding data,  $B_{max}$ , was routinely found to represent only about 25% of the total amount of rhodopsin employed in the assay. Since no increase in binding was observed over a 60 minute period (see above), this result could not arise from incomplete bleaching of rhodopsin at early time points. In order to assess transducin's accessibility to rhodopsin, the ability of V8 protease to specifically cleave rhodopsin at its cytoplasmic face (87) was measured in both UROS and liposome-reconstituted preparations. Figure 12 shows that about 70% of the rhodopsin in these preparations was accessible to V8, similar to results of protease protection experiments previously described (88). Thus, the discrepancies found in the  $B_{max}$  determinations

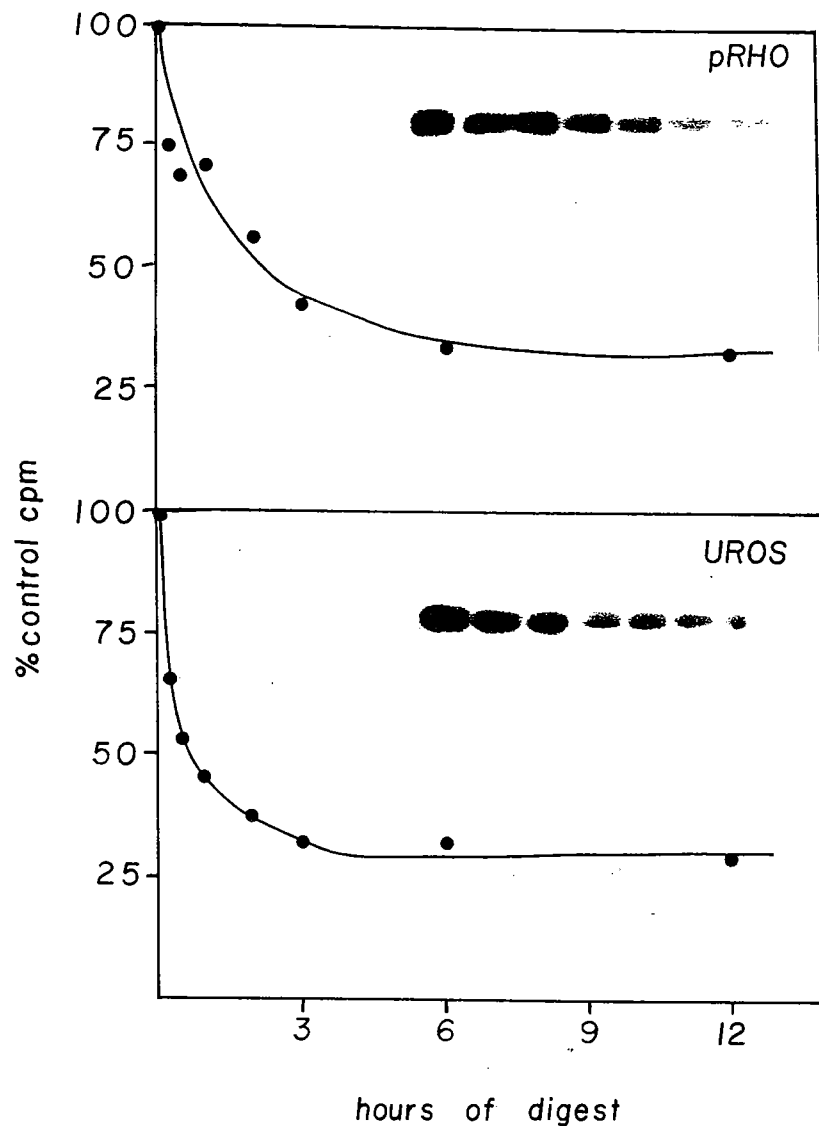


FIGURE 12 Timecourse of V8 protease digest of rhodopsin. A 1 ml reaction mixture containing 80  $\mu$ g rhodopsin and 16  $\mu$ g *S. aureus* V8 protease was incubated at ambient temperature. At times shown, 100  $\mu$ l aliquots were removed, and the proteolytic digest was quenched by mixing with 100  $\mu$ l of ice-cold 10% TCA. Samples for SDS-PAGE were pelleted by 15 minute centrifugation in a microfuge. Protein was transferred to nitrocellulose and immunoblotted with F6 anti-rhodopsin antibodies (46). Bands recognized by autoradiography (insets) were excised and counted. Shown are the digest timecourses for rhodopsin contained in UROS (bottom) as well as reconstituted into phospholipid vesicles (top panel).

are not related to the orientation of rhodopsin in the membrane bilayer. Therefore, the results strongly suggest that oligomeric forms of rhodopsin may be involved in interactions with transducin, and that two or more receptors may contribute to form multiple high affinity binding sites for the G protein. The data also indicate at least two transducins are involved in the cooperative activation process. Physical studies directed toward investigating possible oligomeric forms of the G protein are described in Chapter V.

### Conclusions

1. Equilibrium binding studies also demonstrate positive cooperative interactions between rhodopsin and transducin.
2. The binding results are identical for rhodopsin contained in UROS, or purified and reconstituted into lipid vesicles.
3. A Hill coefficient of 2 was found to describe the allosteric interaction between the G protein and receptor.
4. A  $K_d$  for combined sites of  $0.05 \mu\text{M}$  is determined.
5. Protease protection experiments show that only 30% of the rhodopsin population is occluded from binding transducin in either system studied.
6. The later result, coupled with the fact that determined  $B_{\text{max}}$  values represent only 25% of the total rhodopsin population, strongly suggest that oligomeric complexes of the G protein and receptor form the molecular basis for the allosteric behavior.

## CHAPTER V

KINETIC AND HYDRODYNAMIC PROPERTIES OF TRANSDUCIN: COMPARISON OF  
PHYSICAL AND STRUCTURAL PARAMETERS OF GTP-BINDING REGULATORY PROTEINSResults and Discussion

To further explore the nature of the allosteric behavior described in Chapters III and IV, attention was focussed on the native physiochemical properties of transducin. For example, the binding and exchange of guanine nucleotides by purified transducin independent of rhodopsin have not been characterized in detail and might perhaps reveal insight into oligomeric forms predicted by the allosteric behavior. Since strong homology is observed between members of the G protein family, it is of further interest to compare the properties of transducin to physical characteristics which have been reported for other GTP-binding proteins.

Figure 13 presents a comparison of the timecourse of GTPYS binding by transducin in the absence and presence of rhodopsin. As demonstrated in this figure, transducin binds GTPYS in a time-dependent manner in the absence of the rhodopsin, albeit at a much slower rate. Also shown in Figure 13 is the difference between these two curves which indicates rhodopsin-stimulated binding. In order to verify that the GTPYS exchange observed in the absence of rhodopsin is due to the native capacity of the G protein to undergo this reaction and is not due to the presence of contaminating rhodopsin, immunoblots were performed on the transducin preparation using anti-rhodopsin antibodies (see inset). Overexposure of the autoradiograph for longer times (48 hours) did not show any indication of the presence of rhodopsin in transducin preparations. Immunoblots



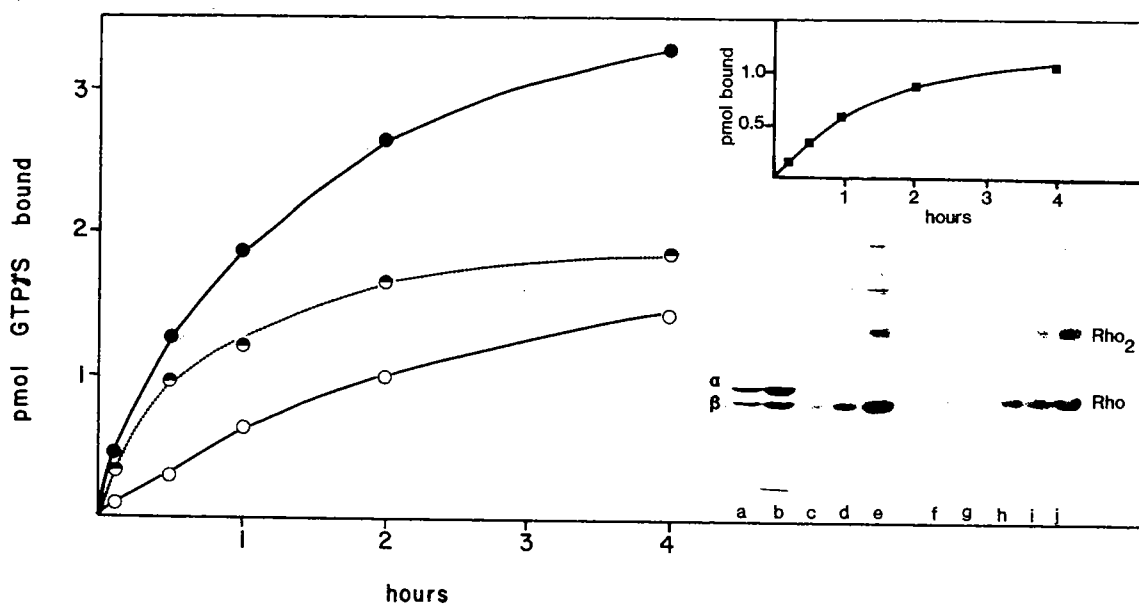


FIGURE 13 Time course of GTP $\gamma$ S binding. A 1 ml assay mixture was prepared containing 0.5  $\mu$ M GTP $\gamma$ S, 0.05  $\mu$ M transducin, in the absence (o) or presence (●) of 5.4 nM rhodopsin. The binding reaction was initiated by the addition of GTP $\gamma$ S, and at the times indicated, 100  $\mu$ l aliquots were withdrawn, filtered and washed as described in Chapter II. The amount of GTP $\gamma$ S bound in the absence of rhodopsin was deducted from that determined in its presence to yield the amount bound to transducin due to interaction with the photoreceptor (●). Also shown is the timecourse of GTP $\gamma$ S binding of hexyl-agarose purified transducin (■), measured in the absence of rhodopsin under similar experimental conditions. Inset shows SDS-PAGE and immunoblot of preparations used in this study. Lanes a-e demonstrate the Coomassie staining pattern of transducin, 5  $\mu$ g (a) and 25  $\mu$ g (b), and UROS (urea-stripped rod outer segment membranes), 2  $\mu$ g (c), 10  $\mu$ g (d), and 20  $\mu$ g (e). Indicated in the figure are rhodopsin, rhodopsin dimer, and the  $\alpha$  and  $\beta$  subunits of transducin. Equivalent lanes were transferred to nitrocellulose, incubated with antibodies prepared against rhodopsin, and  $^{125}$ I-protein A was added. Immunoreactivity was detected by autoradiography as shown by lanes f-j, which correspond directly to lanes a-e.

performed using antibodies raised against synthetic peptides corresponding to specific rhodopsin sequences (46) also failed to detect contaminating rhodopsin. The limits of detection by immunoblotting indicate that contaminating rhodopsin would be present at less than 0.1% of the transducin concentration. Furthermore, the inset of Figure 13 demonstrates the non-catalyzed GTP $\gamma$ S binding activity of hexyl-agarose purified transducin, representing the native capacity of transducin to exchange guanine nucleotides. Finally, analysis of the kinetics of this reaction is consistent with the fact that the binding of GTP $\gamma$ S to transducin represents a non-catalyzed exchange reaction (see Figures 16 and 17 below).

The observation that transducin undergoes receptor-independent exchange is analogous to what has been reported for the GTP-binding proteins of the hormone-sensitive adenylate cyclase system. It has been observed that the receptor-independent exchange of guanine nucleotides by these other G proteins exhibits a marked dependency on Mg $^{2+}$ ; that is, the rate of guanine nucleotide binding by G $_s$  and G $_i$  is stimulated by the presence of Mg $^{2+}$ . Since dissociation of the  $\alpha$  subunits from the  $\beta\gamma$  subunits of the G protein occurs concomitant with binding, Gilman and collaborators have postulated that the action of Mg $^{2+}$  is to promote the release of the  $\alpha$  subunit which subsequently has an enhanced capacity to bind GTP $\gamma$ S (1,32,33). Taking this idea into consideration, the properties of guanine nucleotide exchange by transducin were assessed by measuring initial rates of GTP $\gamma$ S binding as a function of [Mg $^{2+}$ ]. Figure 14 shows that in contrast to what has been characterized for other G proteins, the rate of guanine nucleotide binding displayed little or no dependency on

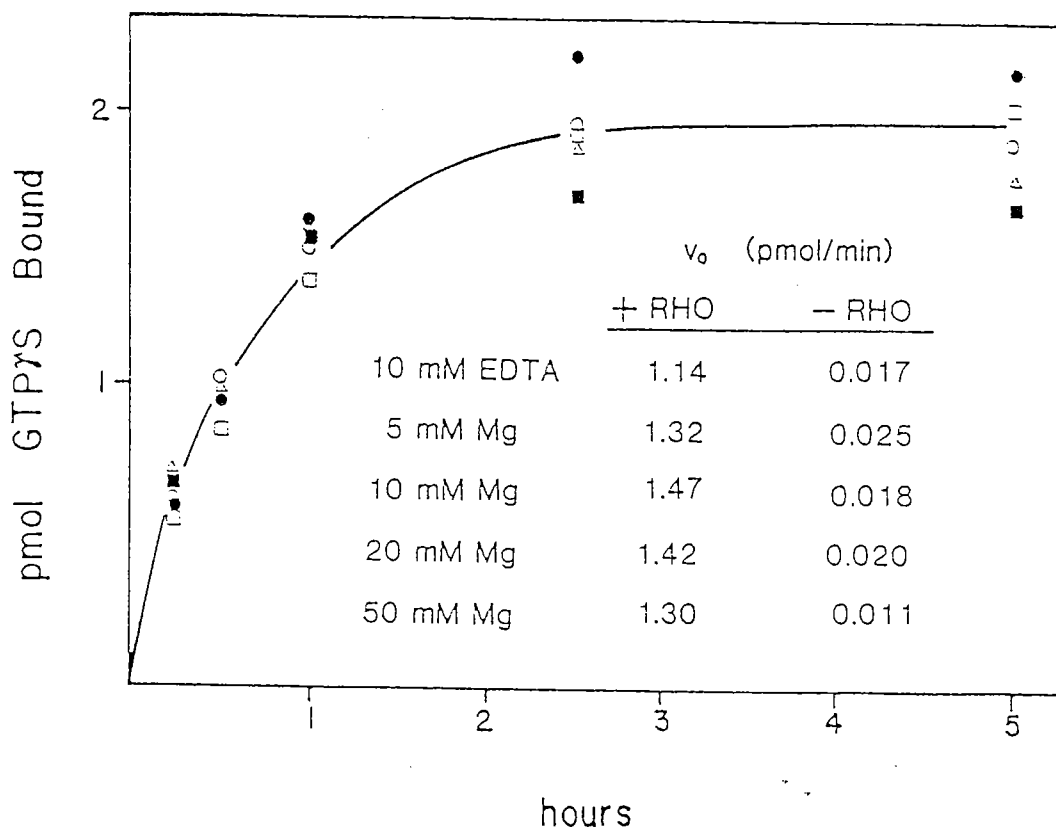


FIGURE 14 Effect of  $Mg^{2+}$  on the time course of GTP $\gamma$ S binding. The time course of rhodopsin-catalyzed binding to transducin was determined essentially as described for Figure 13, with the exception that measurements were accomplished with the following concentrations of  $Mg^{2+}$ : 1 mM ( $\bullet$ ), 5 mM ( $\circ$ ), 10 mM ( $\square$ ), 20 mM ( $\otimes$ ) and 50 mM ( $\Delta$ ). Inset presents data from a separate experiment in which initial rates ( $v_0$ ) of GTP $\gamma$ S exchange were measured in the presence or absence of 25 nM rhodopsin as indicated, under the experimental conditions shown.

$Mg^{2+}$  either in the presence or absence of rhodopsin (Figure 14, inset). Measurements obtained in the presence of excess EDTA indicate that  $Mg^{2+}$  is not required for binding. Furthermore, the timecourse of GTP $\gamma$ S binding in the presence of rhodopsin appears unaltered at concentrations between 1 and 50 mM  $Mg^{2+}$  as demonstrated by the results shown in Figure 14. No effect was observed on the extent of GTP $\gamma$ S binding at these concentrations. It is interesting to note that agonist-promoted guanine nucleotide exchange of  $G_s$ , when reconstituted with the  $\beta$ -adrenergic receptor in a lipid bilayer, is also independent of  $[Mg^{2+}]$  (89).

Yamanaka et al. (90) have found that  $Mg^{2+}$  is required for the GTPase activity of transducin; presumably this is due to the participation of the divalent cation in the mechanism of GTP hydrolysis. In contrast to the results shown here, these authors find that excess EDTA blocked rhodopsin-catalyzed binding of GTP to transducin and promoted the release of bound GDP. It is possible that the difference in these results reflects an alteration in the requirements for GTP $\gamma$ S binding. However, Yamanaka et al. (90) do not directly address the question of whether the stimulatory effect of  $Mg^{2+}$  (2-20 mM) witnessed with other G proteins is also observed with GTP. The results presented here show that this effect is absent for transducin with respect to the binding of GTP $\gamma$ S.

As discussed earlier, it had been postulated that  $Mg^{2+}$  promotes the dissociation of the subunits of other G proteins, with a concomitant increase in the binding of guanine nucleotides to the released  $\alpha$  subunit. Since the kinetics of GTP $\gamma$ S binding by transducin did not display any sensitivity to the presence of  $Mg^{2+}$ , the question arose whether or not the dissociation of  $\alpha$  and  $\beta\gamma$  subunits occurred. Table I summarizes these

results. Sucrose density gradient experiments performed in the presence of 20 mM  $Mg^{2+}$  showed no alteration in the sedimentation behavior of transducin as compared to that observed in the presence of 5 mM  $Mg^{2+}$ : transducin displays a shift in sedimentation only when GTPYS is present. These results indicate that  $Mg^{2+}$  alone does not affect the state of transducin subunit association. Indirect evidence presented by Kuhn (85) and Deterre et al. (91) in relation to  $Mg^{2+}$  effects on the properties of transducin are also consistent with this conclusion. Furthermore, kinetic measurements performed with purified  $T_{\alpha}$  indicate a decreased ability to bind guanine nucleotides in the absence of  $T_{\beta\gamma}$ . Thus, it appears that although transducin can undergo guanine nucleotide exchange independent of receptor, structural characteristics allowing for the stimulatory effect of  $Mg^{2+}$  observed for other G proteins are absent. Finally, binding of GTPYS and dissociation of transducin's subunits appear to be independent of the presence of divalent cation.

Equilibrium binding measurements were obtained in the presence and absence of rhodopsin as shown in Figure 15. Similar curves for the binding of GTPYS to transducin were obtained for both conditions, demonstrating that rhodopsin does not influence the affinity of transducin for guanine nucleotides. These results emphasize the catalytic role of rhodopsin during the guanine nucleotide exchange reaction. Values for the dissociation constant,  $K_d$ , of 0.05-0.10  $\mu M$  were obtained in three independent experiments. Table II compiles similar data reported for other members of the G protein family as shown in part A. It is obvious from this comparison that the regulatory GTP-binding proteins all demonstrate similar affinities for GTPYS. The relative rank of affinities

TABLE I Summary of Sedimentation Velocity Studies

|  |       | <u>S<sub>20,w</sub></u> |
|--|-------|-------------------------|
| 5 mM MgCl <sub>2</sub>                 |       |                         |
|  | αβγ * | 4.23 ± 0.25             |
|  | α *   | 3.42 ± 0.37             |
|  | βγ *  | 4.04 ± 0.20             |
| 20 mM MgCl <sub>2</sub>                |       |                         |
|  | αβγ   | 4.23 ± 0.32             |
| 20 mM MgCl <sub>2</sub> + 100 μM GTPγS |       |                         |
|  | α     | 3.45 ± 0.07             |
|  | βγ    | 3.90 ± 0.14             |
| 10 mM EDTA + 100 μM GTPγS              |       |                         |
|  | α     | 3.23 ± 0.04             |
|  | βγ    | 4.15 ± 0.07             |

Measurements of S<sub>20,w</sub> were obtained from 5-20 % (w/w) linear sucrose gradients in a buffer of 10 mM Tris, pH 7.4, 100 mM NaCl, 1 mM DTT, 0.1 mM EDTA and additions as indicated. Transducin was equilibrated in the appropriate buffers for 24 hours at 4°C. \*Values determined for individual subunits, isolated and separated by chromatography over Blue Sepharose. All other measurements were performed with holotransducin.

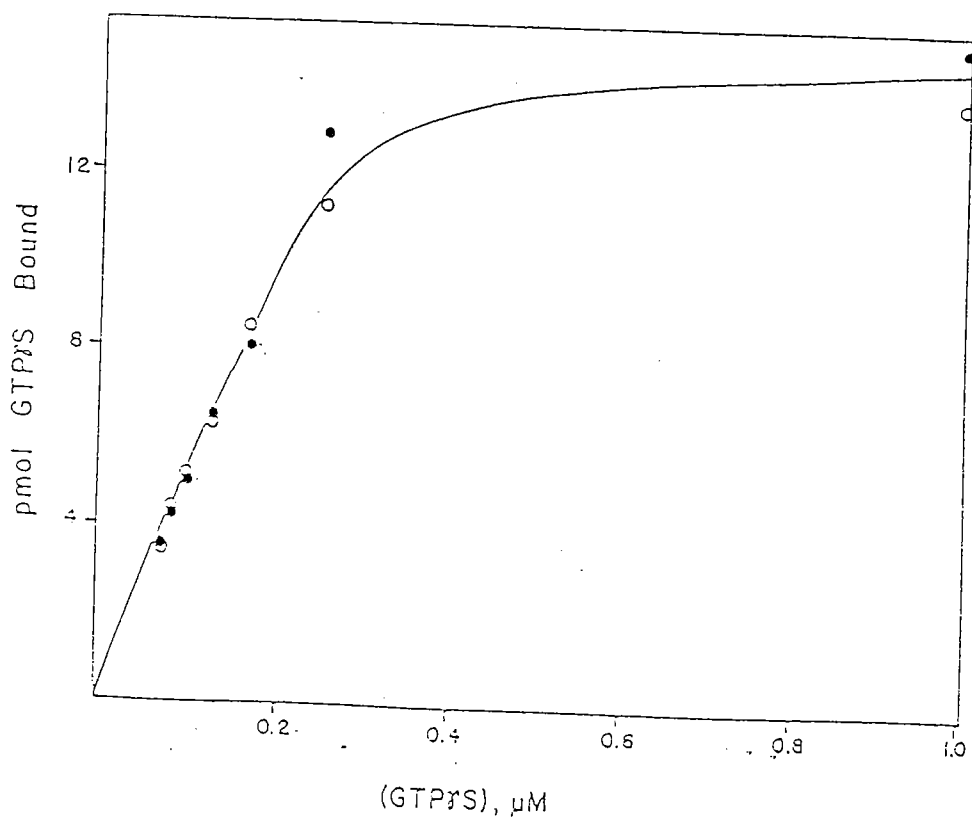


FIGURE 15 Equilibrium binding of GTP $\gamma$ S to transducin. A 300  $\mu$ l assay mixture contained 0.375  $\mu$ M transducin, in the presence ( $\bullet$ ) or absence ( $\circ$ ) of 5.4 nM rhodopsin, with the indicated concentrations of GTP $\gamma$ S. The amount of GTP $\gamma$ S bound to transducin in 50  $\mu$ l aliquot was measured by filtration after an incubation period of 6-8 hours, which had been previously shown to be sufficient time for equilibrium to be achieved.

for guanine nucleotides which have been determined for G proteins are listed in part B of Table II. The similarities demonstrated by this comparison underscore the relationship between transducin and other members of this protein family.

Initial rates of GTPYS binding were measured at several fixed concentrations of transducin in order to investigate the kinetics of the guanine nucleotide exchange reaction. Figure 16 shows the linear plots of  $\ln v_0$  versus  $\ln [\text{transducin}]$  obtained at different levels of GTPYS, as indicated in the figure panels. This data serves to characterize the non-catalyzed exchange reaction as described in Appendix III. The lower right hand panel demonstrates the linear relationship between the intercepts of these plots and  $\ln [\text{GTPYS}]$ . Conversely, Figure 17 presents the same results, with  $\ln v_0$  shown as a function of  $\ln [\text{GTPYS}]$  at several concentrations of transducin. The inset of Figure 4 is the plot of the intercepts of these lines versus  $\ln [\text{transducin}]$ . From the latter relationship, and that shown in the lower right hand panel of Figure 16, an evaluation of  $k_f$ , the forward rate constant for binding, and  $n$ , the reaction order, may be made (for details please refer to Chapter II). Values of  $k_f$  between  $1.7\text{-}2.7 \times 10^7 \text{ M}^{-1} \text{ sec}^{-1}$  were determined in three separate experiments, and the results of these experiments indicate a reaction order of 2; that is, a 1:1 stoichiometry is observed for the binding of GTPYS to transducin.

Several relevant conclusions may be drawn from characteristics of the relationship presented between  $v_0$  and transducin. The investigations of the enzymatic behavior in the rhodopsin-catalyzed guanine nucleotide exchange reaction revealed allosteric behavior with respect to transducin.



TABLE II Comparison of Guanine Nucleotide Binding Characteristics Between Members of the G Protein Family

| A. Determined Values of $K_d$ , the Dissociation Constant, for GTP S Binding |   |  |
|--|---|--|
|  | <u><math>K_d</math> (<math>\mu</math>M)</u>   | <u>References</u>  |
| Transducin, G <sub>T</sub>   | 0.05-0.10                                     | present study  |
|  | 0.05  | Kelleher <u>et al.</u> (92)                              |
| G <sub>s</sub>   | 0.7   | Northup <u>et al.</u> (93)                               |
|  | 0.005-0.010                                   | Asano <u>et al.</u> (89)                                 |
|  | 0.10  | Brandt <u>and</u> Ross (94)                              |
| G <sub>i</sub>   | 0.012   | Bokoch <u>et al.</u> (95)                                |
|  | 0.032   | Huff <u>and</u> Neer (96)                                |
| G <sub>o</sub>   | 0.027   | Huff <u>et al.</u> (97)                                  |
|  | 0.030   | Huff <u>and</u> Neer (96)                                |
| B. Relative Affinities for Guanine Nucleotides Reported for G Proteins       |   |  |
|  | <u>Relative Rank of Affinity</u>              | <u>References</u>  |
| Transducin, G <sub>T</sub>   | GTPYS > GTP >> GppNHp > GDP > GMP             | Kelleher <u>et al.</u> (92); Yamanaka <u>et al.</u> (98) |
| G <sub>s</sub>   | GTPYS > GTP > GDP > Gpp (NH)p                 | Northup <u>et al.</u> (93)                               |
| G <sub>i</sub>   | GTPYS $\geq$ GTP $\geq$ Gpp (NH)p = GDP > GMP | Bokoch <u>et al.</u> (93); Sunyer <u>et al.</u> (99)     |
| G <sub>o</sub>   | GTPYS > GTP > GDP >> GMP                      | Sternweis <u>and</u> Robishaw (100)                      |

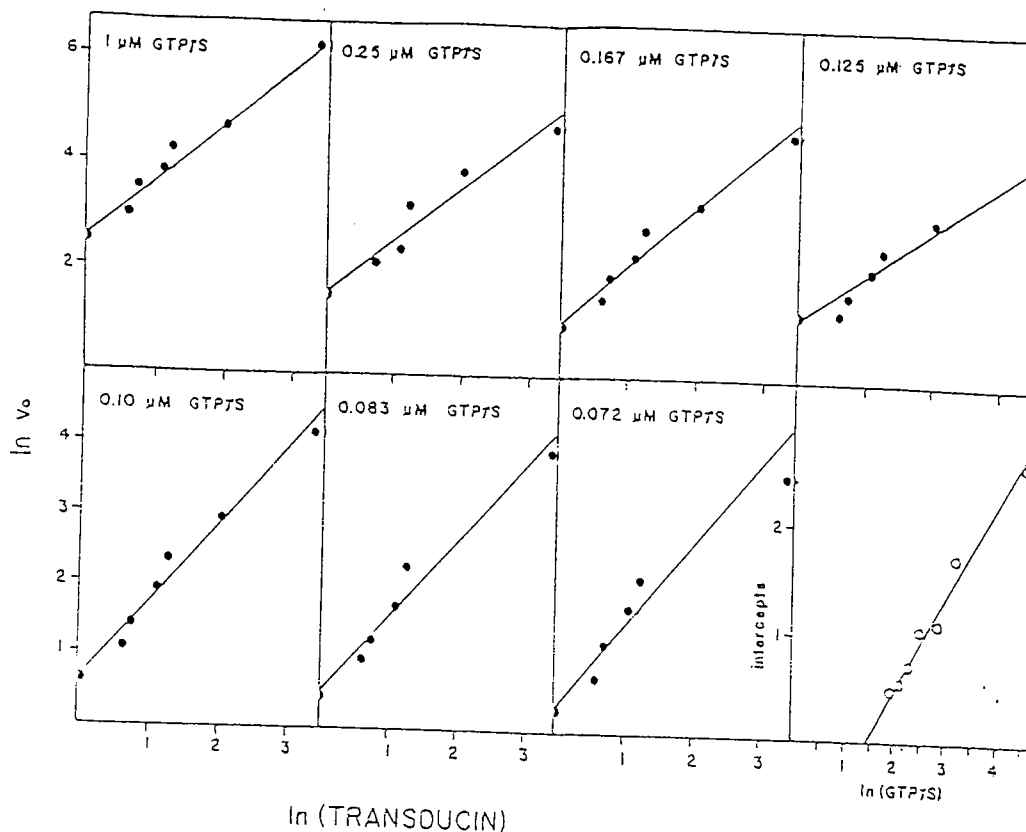


FIGURE 16 Plots of  $\ln v_0$  versus  $\ln$  [transducin] as a function of [GTP $\gamma$ S]. Initial rates ( $v_0$ ) of GTP $\gamma$ S binding to transducin in the absence of rhodopsin were measured using the filtration assay detailed in Chapter II. A 300  $\mu$ l reaction mixture contained the indicated concentrations of transducin, in the presence of different [GTP $\gamma$ S]. At 10, 20, 30 and 60 second timepoints, 50  $\mu$ l aliquots were withdrawn, filtered, washed with ice-cold buffer, and the amount of GTP $\gamma$ S bound was determined. Initial rates were obtained from the slopes of timecourse plots from this data. Shown are the plots of  $\ln v_0$  ( $10^{-2}$  pmol/min) versus  $\ln$  [transducin] ( $10^{-2}$   $\mu$ M) determined with levels of GTP $\gamma$ S as displayed; the lower right hand panel presents the plot of the intercepts of these lines as a function of  $\ln$  [GTP $\gamma$ S] ( $10^{-2}$   $\mu$ M). The linear relationship shown correlates well with the mathematical description of the guanine nucleotide exchange reaction as described in Appendix III.

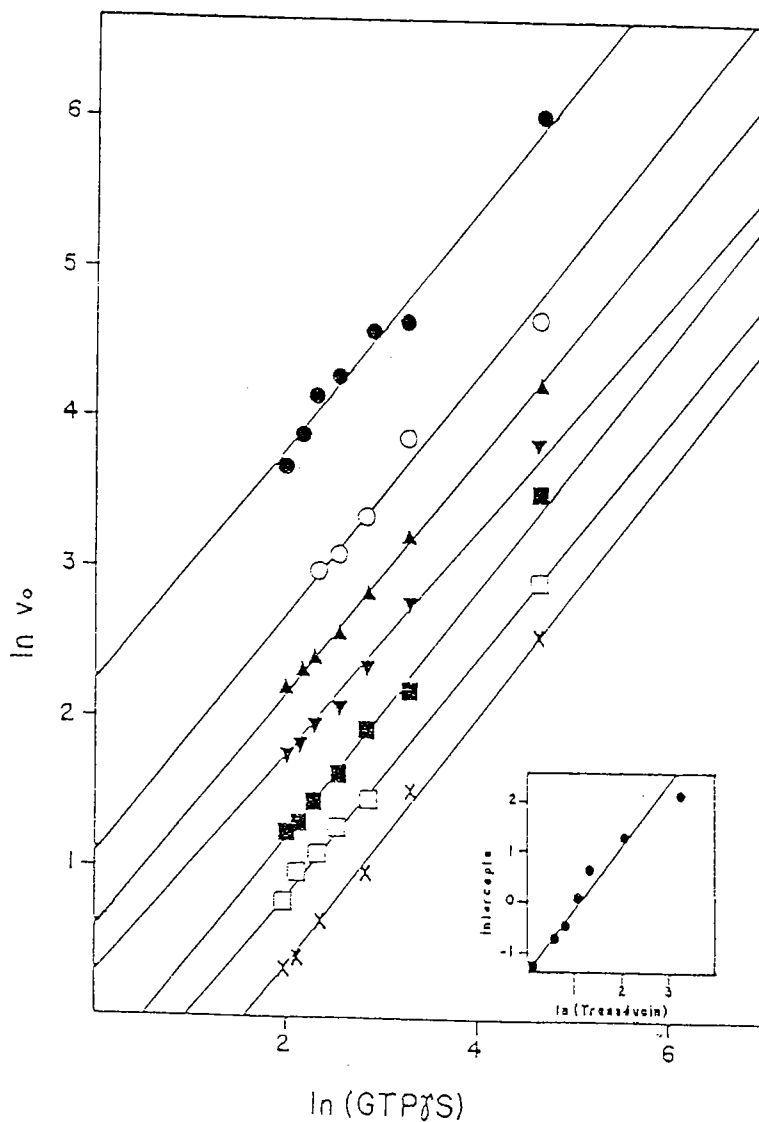


FIGURE 17 Plots of  $\ln v_0$  versus  $\ln [GTP\gamma S]$  as a function of  $[transducin]$ . Data from Figure 16 is presented in the converse plotting form of  $\ln v_0$  ( $10^{-2}$  pmol/min) versus  $\ln [GTP\gamma S]$  ( $10^{-2}$   $\mu M$ ) as measured using the following concentrations of transducin: 3  $\mu M$  ( $\bullet$ ), 0.75  $\mu M$  ( $\circ$ ), 0.34  $\mu M$  ( $\blacktriangle$ ), 0.30  $\mu M$  ( $\nabla$ ), 0.21  $\mu M$  ( $\blacksquare$ ), 0.19  $\mu M$  ( $\square$ ) and 0.10  $\mu M$  ( $\times$ ). Inset shows the intercepts of these lines as a function of  $\ln [transducin]$  ( $10^{-2}$   $\mu M$ ). The linear relationships demonstrated above, along with the data presented in Figure 16, indicate a dissociative type mechanism for transducin's guanine nucleotide exchange process.

The linear relationship determined for  $\ln v_0$  as a function of  $\ln$  [transducin] does not display any indication of similar behavior for the non-catalyzed reaction. This observation implies that the basis for the allosteric phenomenon resides in interactions between transducin and rhodopsin. The linear correlation demonstrated in Figures 16 and 17 is also indicative of the presence of a single population of binding sites for GTP $\gamma$ S. Under identical experimental conditions, purified  $T_\alpha$  exhibits much slower exchange rates. Since the presence of free  $T_\alpha$  subunit would be detected due to its altered kinetics, this result implies that over the experimental range of concentration transducin remains as a stable heterotrimer (in the absence of GTP $\gamma$ S) with minimal dissociation of  $T_\alpha$  from  $T_{\beta\gamma}$ . Finally, the linear correlation between  $\ln v_0$  and  $\ln$  [GTP $\gamma$ S] as well as  $\ln$  [transducin] is compatible with a dissociative type mechanism; this is consistent with the double displacement mechanism demonstrated for the rhodopsin-catalyzed guanine nucleotide exchange mechanism.

Although rigorous kinetic analysis has not been reported on the nucleotide exchange mechanism for all of the G proteins, the demonstration of a dissociative type mechanism for transducin is in good agreement with what is known. The second order rate constants for  $G_i$  ( $10^6 \text{ M}^{-1} \text{ sec}^{-1}$ ) and the  $\alpha$  subunit of  $G_o$  ( $10^7 \text{ M}^{-1} \text{ sec}^{-1}$ ) have been reported (101). These values are also comparable to what we observe for transducin ( $10^7 \text{ M}^{-1} \text{ sec}^{-1}$ ). The difference in the intrinsic rate constant between  $G_i$  and transducin may reflect contributions due to a  $\text{Mg}^{2+}$  effect, as discussed earlier. It is also possible, however, that this difference reflects alterations in the G proteins tertiary configuration which contribute to the exchange process.

It is with respect to the physical nature of transducin that the protein's hydrodynamic properties were characterized. Sucrose density gradient experiments were performed with transducin as well as isolated  $T\alpha$  and  $T\beta\gamma$  presented in Figure 18. Results tabulated in Table I show that holotransducin migrates at a greater rate relative to the individual subunits,  $T\alpha$  and the  $T\beta\gamma$  complex. The  $s_{20,w}$  values determined from three separate experiments were for transducin,  $4.23 \pm 0.25$ ,  $T\alpha$ ,  $3.42 \pm 0.37$ , and  $T\beta\gamma$ ,  $4.04 \pm 0.20$ . To complement this study, gel filtration experiments were performed as shown in Figure 19. Transducin was found to have a Stokes radius of  $37.5 \text{ \AA}$  and  $T\alpha$  migrated with a Stokes radius of  $24 \text{ \AA}$ .  $T\beta\gamma$  eluted in a position similar to that observed for  $T\alpha$ .

Table III summarizes the hydrodynamic data in comparison with results reported for other G proteins. The experimental data obtained for  $T\alpha$  and  $T\beta\gamma$  are in close agreement with the results of gel filtration on Bio-Gel P100 reported by Fung (71), which yielded molecular weight values of 41 and 43 kDa, respectively. The hydrodynamic parameters measured for holotransducin yield an  $M_r$  value of 68 kDa, well below the expected value of  $M_r \sim 80$  kDa. However, this value is in quite close agreement with the molecular mass estimation of 70 kDa from small angle neutron scattering measurements reported by Deterre *et al.* (91). Taken together, these results indicate that the heterotrimeric form of transducin has hydrodynamic characteristics suggestive of a compact shape relative to other globular proteins. By comparison, the information obtained for other G proteins is necessarily from detergent solutions, with a correction made for detergent binding. It is interesting to note that  $M_r$  values for G proteins which were determined in cholate solutions (see

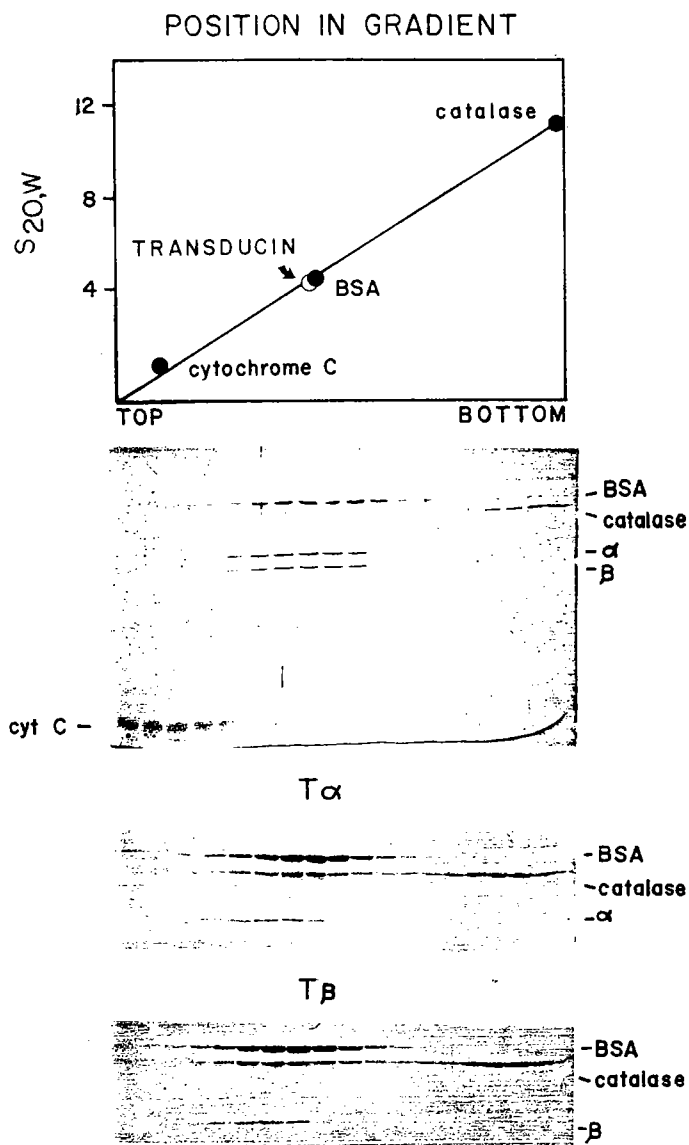


FIGURE 18 Sucrose density gradient ultracentrifugation of transducin. Linear 5-20% sucrose gradients (4.5 ml) were prepared and overlaid with 15  $\mu$ g of each protein indicated. Gradients were subjected to centrifugation for 13 hours at 40,000 rpm in a Beckman SW 50.1 rotor and fractionated into 250 ml aliquots, which were then analyzed by SDS-PAGE. Values for the marker proteins employed are: catalase, 11.2 S, BSA, 4.31 S and cytochrome C, 1.21 S. The  $s_{20,w}$  values for transducin, its  $\alpha$  subunit and the  $\beta\gamma$  subunit complex were determined from calibration curves as demonstrated at the top of the figure. Values of  $s_{20,w}$  obtained for transducin, T<sub>α</sub>, and T<sub>β</sub> were  $4.23 \pm 0.25$  S,  $3.42 \pm 0.37$  S and  $4.04 \pm 0.20$  S, respectively.

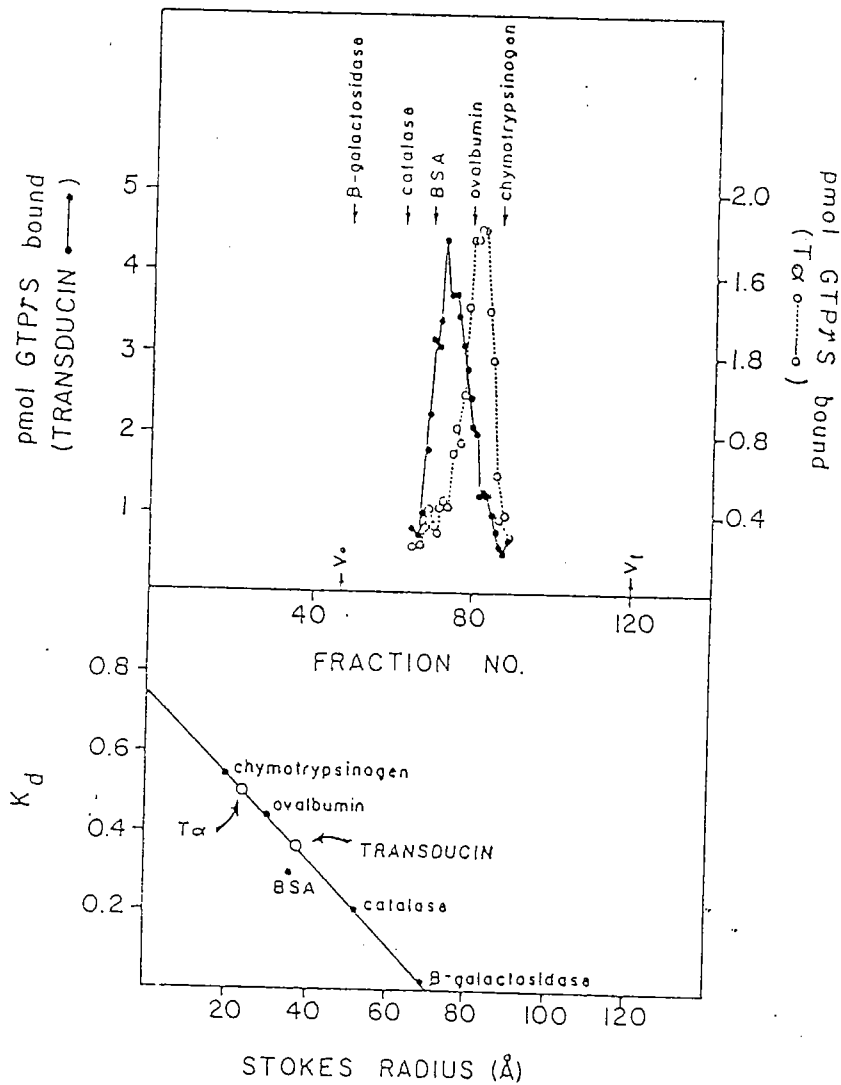


FIGURE 19 Determination of the Stokes radius for transducin. Gel filtration over Sephacryl S-300 was performed using the marker proteins indicated in order to calibrate the column as shown in the bottom panel ( $K_d = V_e - V_o / V_t - V_o - V_{gel}$ ). The elution profiles of transducin ( $\bullet$ ) and its  $\alpha$  subunit ( $\circ$ ) were obtained by assaying column fractions for GTPYS binding activity (top panel).

Table III) may actually be overestimated since no correction for detergent binding may be made. As transducin is the only soluble protein in the G protein family, the data might imply that complications arising from detergent binding may obscure similar anomalous behavior for  $G_i$ ,  $G_s$  and  $G_o$ .

Baehr et al. (66) have reported the results of non-denaturing gel electrophoresis and analytical ultracentrifugation experiments. These investigators concluded that, in solution, transducin consists of a population of  $T_\alpha$  dimers and  $T_\beta\gamma$  dimers and tetramers. However, based on the results presented here, it may be deduced that  $T_\alpha$  and  $T_\beta\gamma$  can be isolated in monomeric form, and that the heterotrimeric species exhibits unique hydrodynamic characteristics which are perhaps indicative of an unusual configuration other than that displayed by simple globular proteins. The conditions under which possible oligomeric assembly may be functionally relevant remain to be determined, but it should be emphasized that transducin's physiological activity occurs in a membrane environment. Although hydrodynamic studies of transducin in solution are vital to understanding the biophysical nature of the protein in relation to other G proteins, it will also be necessary to explore these relationships as they pertain to the cell surface.

### Conclusions

1. Transducin exchanges guanine nucleotides in the absence of rhodopsin.
2. The uncatalyzed exchange is independent of  $[Mg^{+2}]$ .
3. Unlike previous reports for other G proteins,  $Mg^{+2}$  does not promote dissociation of transducin's subunits.



4. The equilibrium constant for GTPYS binding to transducin is not altered by interactions with rhodopsin; a value of  $K_D = 0.05 \mu\text{M}$  is determined.
5. The initial rate kinetics of guanine nucleotide exchange of transducin suggests a dissociative type mechanism and a value for the forward rate constant for this reaction is found to be  $k_f = 2 \times 10^7 \text{ M}^{-1} \text{ sec}^{-1}$ .
6. The hydrodynamic parameters determined for transducin,  $S_{20,w} = 4.25$  and  $a = 37.5 \text{ \AA}$ , lead to a calculated  $M_r = 68,000$ , and do not support the presence of oligomeric forms of the G protein.

TABLE III Comparison of Hydrodynamic Parameters Reported for Purified G Proteins

|  | $S_{20,w}$ (S)** | Stokes Radius (Å) | $M_r^*$ | References                     |
|--|------------------|-------------------|---------|--------------------------------|
| Transducin, G <sub>T</sub> , bovine retina | 4.23             | 37.5              | 68,000  | present study                  |
| G <sub>S</sub> rabbit liver(a)             | 3.9              | 40                | 68,000  | Sternweis <u>et al.</u> (102)  |
| turkey erythrocyte(a)                      | 4.55             | 41.6              | 81,000  | Hanski <u>et al.</u> (103)     |
| human erythrocyte                          | 4.11             | 59                | 96,000  | Codina <u>et al.</u> (104-105) |
| G <sub>f</sub> rabbit liver(a)             | 4.31             | 44.3              | 82,000  | Bokoch <u>et al.</u> (106)     |
| human erythrocyte                          | 4.09             | 56                | 96,000  | Codina <u>et al.</u> (104-105) |
| G <sub>0</sub> bovine brain                | 4.2              | 47                | 80,000  | Huff <u>et al.</u> (96)        |

\* Molecular weight,  $M_r$ , was calculated according to the equation:

$$M_r = \frac{6 \cdot \pi \cdot N \cdot \eta_{20,w}}{1 - (\nu \cdot \rho_{20,w})} \cdot a \cdot s_{20,w}$$

where  $N$  is Avogadro's number,  $\eta_{20,w}$  is the viscosity of water at 20°C,  $\rho_{20,w}$  is the density of water of 20°C, and  $a$  is the Stokes radius. A value for partial specific volume,  $\nu = 0.735$ , was employed in this calculation for transducin.

\*\* Except for transducin,  $s_{20,w}$  values for other G proteins were obtained in Lubrol solutions unless otherwise indicated (a).  $M_r$  values for these other proteins are listed with the appropriate correction made for other detergent binding (refer to references cited).

(a) Measurements of  $s_{20,w}$  performed in cholate solutions; since cholate has a density similar to that of protein, no estimate of detergent binding may be made (refer to references cited).

## CHAPTER VI

## DISCUSSION: FUTURE DIRECTIONS

The results presented in the preceding chapters provide insight into the molecular mechanism of interactions between G proteins and receptors as well as raising further issues which remain to be clarified. What has been successfully accomplished is the development of a model for the interactions between rhodopsin and transducin as those of an enzyme and substrate. The kinetic investigation of the catalytic mechanism through which the receptor mediates the guanine nucleotide exchange process extends our current view of the nature of this signal transduction mechanism. These methods have not been previously applied and evidence is presented confirming the validity of the steady-state approach. The initial rate studies demonstrate that rhodopsin's catalytic activity proceeds via a double displacement mechanism. During the course of this investigation, remarkable allosteric behavior in the rhodopsin signal transduction system was observed. The results reveal positive cooperative behavior in the substrate-velocity curves of transducin with respect to  $v_0$ . Michaelis-Menten plots of GTP $\gamma$ S concentration versus initial velocity did not display this sigmoidal character. However, the cooperative effect was also observed in kinetic experiments performed with purified T $\alpha$ , implying that the molecular basis for the allosteric behavior is due to interactions between rhodopsin and transducin's  $\alpha$  subunit.

The positive cooperative behavior observed in the kinetic investigation was confirmed in studies of equilibrium binding between rhodopsin and transducin. These results represent the first direct analysis of binding

interactions between a receptor and G protein. The allosteric nature of these interactions is observed in the curvilinear Scatchard plots which verify that the molecular origins of this phenomenon arise from oligomeric assemblies between rhodopsin and transducin. A Hill coefficient,  $n_H = 2$ , was determined in both the kinetic and binding studies, indicating that at least two transducins are involved as oligomeric components of this system. However, the  $B_{max}$  values measured in the direct binding studies strongly suggest that multimers of rhodopsin may also contribute to the allosteric assembly.

Physical studies characterizing the kinetic and hydrodynamic properties of transducin presented in Chapter V do not support the presence of oligomers of the G protein in solution. However, it must be remembered that, physiologically, transducin functions in association with rhodopsin in a membrane environment. Thus, the oligomeric assemblies implied by the allosteric nature of the interactions between the G protein and receptor may be induced by their coupling. What the physical characterization of transducin presented in Chapter V does yield is the basis for comparison with other G proteins which have been studied. It is for this purpose that the entire investigation was initiated: to define structural and functional relationships between members of the family of G protein-coupled receptor systems described in Chapter I. The visual transduction system provides a paradigm within which a conceptual basis of the molecular events of these signal transduction mechanisms may be developed, and the results summarized above bear on several aspects of the relationships among these proteins.

### Receptors as Enzymes

Recent advances in the study of cell surface receptors had led to the identification of at least four functional classes into which these proteins may be categorized: receptors which display ligand-stimulated tyrosine kinase activity, receptors which serve as ligand-gated ion channels, receptors which mediate the internalization of ligands, and receptors which act upon ligand-binding to catalyze the exchange of guanine nucleotides of G proteins. The enormous task ahead is to define the structural characteristics which allow receptors the capacity to function in their appropriate roles in response to ligand binding in order to transmit this signal across the cell membrane. The difficulty of this task may be alleviated in part by developing conceptual models in order to investigate the molecular properties of receptor function. It is for this purpose that rhodopsin has been modelled as an enzyme by employing the kinetic methods which have provided a fundamental basis in mechanistic studies of soluble enzymes. The results presented in this thesis not only verify that this approach is valid, but also yield direct insight into the molecular mechanism of rhodopsin's activity.

The value of conceptual models lies in their ability to accurately fit the description projected by experimental data as well as in their capacity to provide a paradigm which permits the development of a testable hypothesis. Characterization of rhodopsin's behavior as an enzyme allows us to begin the analysis of the structure of the receptor protein in relationship to the wealth of knowledge regarding conformational changes associated with ligand binding to proteins. In examples where the three-dimensional structure of ligand-protein complexes have been determined,

several common features emerge. In general, the enzyme may be roughly divided into two domains joined by a hinge region. This configuration results in a cleft or pocket which contains the ligand-binding site. When the appropriate substrate occupies this site, it induces what has been referred to as a hinge-bending and cleft closure. This experimentally demonstrated structural change is similar to the induced fit hypothesis developed by Koshland (107). As reviewed by Scarborough (108), the general concept of the hinge-bending conformational change may be used to describe the catalytic mechanisms for integral membrane proteins involved in transport, as well as soluble enzymes.

The hypothesis may be made that similar conformational changes are promoted by the photolysis of rhodopsin: they would provide the opening of a cleft for transducin binding and the flexibility to undergo the hinge-bending associated with enzymatic activities. Thus, this consideration leads to a conceptual framework to test domains represented in G protein-coupled receptor systems that are involved in the activation process, relying on the well-characterized structural properties of enzymes. This concept may be globally envisioned to extend to other types of cell surface receptors as well: hinge-bending conformational changes resulting from ligand binding may be the means through which extracellular signals are transmitted through the membrane bilayer, allowing the receptor's appropriate functional response. Through combined approaches of enzyme kinetics, protein chemistry, and molecular biology, aspects of this model are both predictable and testable.

#### A General Class of Ligand-Exchange Enzymes

Several basic concepts also emerge by comparing the kinetic mechanism

of transducin's activation mediated by rhodopsin with information known for other enzymes. The initial rate studies delineate that rhodopsin performs its catalytic activity through a double displacement mechanism, described by the character of the double reciprocal plots. The rate equation developed from the experimental data requires that the first guanine nucleotide (GDP) exit from the reaction complex prior to the entry of the second guanine nucleotide (GTP $\gamma$ S), defining the double displacement or substituted enzyme type reaction mechanism. One of the distinguishing features of this mechanism is that it verifies the presence of a complex between rhodopsin and transducin which has been "unloaded" or devoid of guanine nucleotide. Alternative models might predict the presence of multiple guanine nucleotide binding sites operating in tandem (as in a ternary complex mechanism). The double-displacement mechanism is supported by the studies of guanine nucleotide exchange in the absence of rhodopsin which reveal a dissociative-type reaction scheme for transducin. Multiple guanine nucleotide binding sites have been suggested for transducin by labelling studies (109). However, our current knowledge of the primary structure for transducin's  $\alpha$  subunit shows the presence of a single binding site as defined by homologous domains known to compose GTP binding pockets in other proteins (110). Furthermore, guanine nucleotide binding studies are also in agreement with this description of transducin (65-71). All of this information is entirely consistent with the double displacement mechanism described for the interactions between rhodopsin and transducin.

Rhodopsin in this sense catalyzes the guanine nucleotide exchange of transducin analogous to the manner through which elongation factor Ts

serves as an exchange catalyst for elongation factor Tu (111). For example, both of these proteins mediate guanine nucleotide exchange by a double displacement mechanism. Proteins like rhodopsin and elongation factor Ts are unconventional in their activities as enzymes since they do not catalyze the formation or breakage of covalent bonds. In fact, in the International Union of Biochemists enzyme catalog, ferrochelatase is the only example of an enzyme which catalyzes ligand exchange. Hwang and Miller (111) have argued for the need to classify exchange catalysts as enzymes. Rhodopsin would indeed fall into this category, serving to catalyze the guanine nucleotide exchange of transducin. By analogy, other G protein-coupled receptors would also appear to fall into the class of exchange catalyst enzymes. Complete characterization of the molecular interactions between other receptors and G proteins in the process of signal transduction is lacking, primarily due to the relatively low abundance of these regulatory elements and the fact that these systems must be reconstituted into phospholipid vesicles. The double displacement model for catalytic interactions between rhodopsin, transducin and guanine nucleotides is consistent with what is known about the mechanism of molecular interactions for other members of the G protein-coupled receptor family. The fact that structural homologies are observed between members of this receptor class also suggests a common basis in their function (39-45). Future investigation should develop the concept of ligand-exchange catalysts as well as their precise nature and role in biological systems.

#### Allosteric Behavior

The unexpected finding revealed by the kinetic investigation of



rhodopsin and transducin was the observation of allosterism in their molecular interactions. This phenomenon was confirmed by equilibrium binding studies which verified that the basis for the positive cooperative behavior resides in oligomeric assemblies of these components of the visual transduction system. Considering the requirement for amplification in signal transduction systems, it is not surprising that transducin would display allosteric regulation in its interaction with rhodopsin.

Cooperative processes are widespread in nature, and it has been estimated that 90% of all proteins display some form of allosteric regulation (78).

What is necessary is a complete understanding of the role of the allosteric behavior in the biological process of visual transduction. Photolyzed rhodopsin serves to activate transducin, permitting the stimulation of cGMP phosphodiesterase (PDE) activity. It is not known whether or not similar cooperative interaction occurs between oligomeric  $T\alpha$  subunits in the interaction with the inhibitory subunit of PDE. Other enzymatic activities are also elevated in response to light, including that of phospholipase  $A_2$  (8). The latter studies suggest that not only can transducin stimulate phospholipase  $A_2$ , but that this enzyme's activity may also be under dual control by other G proteins. The fact that two forms of transducin have been identified in the rod outer segment (8,112) also raises interesting questions. Thus, little information is known about possible allosteric regulation at the level of effector systems, but it is becoming increasingly clear that transducin and possibly other G proteins may participate in the regulation of several activities which may be involved in the process of visual transduction. This is reminiscent of the pleotropic effects of G proteins recognized in other systems as

described in Chapter I.

Comparison of the processes involved in signal transduction by other receptors suggests a speculative role for the allosterism observed in visual transduction. It has been hypothesized that free  $\beta\gamma$  subunits may provide a communications network between G proteins through which the activity of  $\alpha$  subunits may be regulated (1). The positive cooperative interactions between multiple transducins acting at the receptor level would enhance the degree of this regulation, ensuring that the signal, represented by the activated G protein, would also be regulated by the critical concentration of free  $\alpha$  subunit. The latter concept is supported by experimental evidence which shows that while rhodopsin-catalyzed activation of  $T_\alpha$  exhibits reduced rates in the absence of  $T_{\beta\gamma}$ , the allosteric effect is still witnessed and therefore must arise from contact between  $\alpha$  subunits. The implication that transducin and possibly other G proteins can regulate several effector systems in the ROS may define the requirement for allosterism: the necessity to coordinate responses which participate in visual transduction. Thus, the observation of positive cooperativity in transducin activation does provide an interesting and exciting aspect to receptor regulation. It remains to be seen whether or not allosteric behavior observed in the molecular interactions between transducin and rhodopsin is another of the many analogies between G protein-coupled receptor systems.

#### Oligomeric Associations

The results of equilibrium binding studies show that the molecular basis of the allosteric behavior arises from interactions between at least two transducins with dimers, or possibly tetramers of rhodopsin. Such

interactions between multimeric assemblies of transducin and rhodopsin must be understood in terms of structural relationships. Hargrave and coworkers (62) have discussed the structural organization of the rhodopsin molecule in the rod outer disc membrane and conclude that the native protein is monomeric. There has been some controversy, however, about the possible existence of rhodopsin dimers (113). With the determination of structural information concerning transducin, it is hopeful that structure-function relationships will become evident to increase the current understanding of the G protein-coupled receptor system and provide insight into its allosteric behavior.

The possible existence of a transducin dimer has been suggested by light scattering measurements (69). Non-denaturing gel electrophoresis and ultracentrifugation experiments performed by Baehr et al. (66) have shown the presence of dimeric forms of  $\alpha$  subunits and the  $\beta\gamma$  complex. Indeed, oligomers of G proteins from other systems have been described by target size analysis (114). It is also interesting that elongation factor Tu, itself a GTP-binding protein, has been characterized as a dimer by neutron scattering (115). Another GTP-binding protein, the ADP-ribosylation factor ARF, interacts with the regulatory protein  $G_s$  in such a way as to enhance ribosylation by cholera toxin (116). Taken altogether, these phenomena indicate that GTP-binding proteins may associate with one another under certain conditions.

Hydrodynamic analysis of transducin, however, fails to support the presence of oligomeric forms of the protein (Chapter V). Such physical studies of transducin in solution would not reveal structural alterations which may occur at the membrane surface, though, and therefore provide only

speculative information. Alternative techniques must therefore be sought in order to attain a correct description of the physical nature of transducin. Preliminary results from electron microscopic rotary shadowing experiments provide micrographs of transducin revealing that approximately 10% of the protein population appears to exist in some oligomeric form.<sup>1</sup> These are toroid-shaped structures approximately 150 Å in diameter with some physical definition which resembles a "paw-print". The majority of the population are smaller particles with little shape definition. The larger species is not apparent in preparations of purified T $\alpha$  or T $\beta\gamma$  and is not apparent in preparations treated with GTPYS. The exact nature of these forms of transducin remains elusive, but it is hopeful that future cross-linking experiments will aid in defining these structures as well as characterizing possible oligomeric species of transducin.

It is possible that other investigators have failed to detect the interactions between oligomeric components of the visual transduction system due to the techniques they have employed which examine each protein species individually rather than focussing on the mechanism of coupling between rhodopsin and transducin. The kinetic and binding studies described here have the advantage of analyzing native interactions between both proteins at the membrane surface, and therefore reflect both environmental and structural interactions which most likely contribute to

<sup>1</sup>Wessling-Resnick, M., Johnson, G.L. and Craig, R.C., personal observations.

the allosteric phenomenon. This lends itself to the idea that interactions between the G protein and receptor may induce oligomeric assembly. Physical measurements of purified rhodopsin reconstituted at ratios of one to several molecules per liposome may begin to address the nature of the assemblies. Recent advances in obtaining two-dimensional crystalline arrays of membrane proteins (117) and the crystallization of membrane proteins out of detergent solutions (118) may also provide direction in ascertaining the physical nature of transducin and rhodopsin interactions. Future investigation towards this goal should provide insight into similar physical characteristics which may also exist for the family of G protein-coupled receptors.

#### Mg<sup>2+</sup> Effects and Transducin Structure

The results presented in Chapter V characterize the kinetic, physical and hydrodynamic properties of transducin. Previously, these parameters have not been described, and it is of interest, therefore, to compare this information with properties which have been reported for other members of the family of G proteins. The dissociative-type guanine nucleotide exchange mechanism demonstrated for transducin is analogous to the behavior of other G proteins. Transducin's kinetic parameters and equilibrium binding properties are also comparable to values reported for G<sub>s</sub>, G<sub>i</sub> and G<sub>o</sub>. It is not surprising that transducin displays kinetic behavior and guanine nucleotide binding characteristics similar to the other members of this class of proteins because of the remarkable sequence homology between their  $\alpha$  subunits. Alterations in the properties of the G proteins must therefore reflect variations in the amino acid sequence between these proteins which affect their tertiary structure and

characteristics of their regulation.

One of the most notable differences between transducin and the other G proteins ( $G_0$ ,  $G_i$  and  $G_s$ ) is the lack of any  $Mg^{2+}$  effect on the guanine nucleotide exchange reaction. The results presented in Chapter V indicate that  $Mg^{2+}$  is not required for GTPYS binding and subunit dissociation. The acidic side chains of aspartic or glutamic acid have been demonstrated to be the major sites for  $Mg^{2+}$  interaction with proteins. For example, asp<sup>80</sup> of EF-Tu has recently been shown to form a salt bridge with  $Mg^{2+}$  liganded to GDP situated in the guanine nucleotide binding site of the protein (119). A second regulatory  $Mg^{2+}$  binding site has been previously proposed for G proteins (102, 120-121). The data presented here indicate that this site is absent in transducin.

Examination of the  $\alpha$  subunit primary sequences offers one rather striking domain in which a substitution of a neutral for an acidic amino acid occurs in transducin relative to the other G proteins (Table IV). An alteration such as this could account for the specific loss of a  $Mg^{2+}$  binding site. In  $T\alpha$ , residue 162 is a glycine, whereas the corresponding residue is aspartic acid in  $G_{S\alpha}$  (189),  $G_{i\alpha}$  (167) and  $G_{O\alpha}$  (123, partial sequence). This residue is located within one of the most highly conserved domains recognized between the  $\alpha$  subunits of transducin (pro<sup>161</sup>-ser<sup>186</sup>),  $G_s$  (ala<sup>188</sup>-gln<sup>213</sup>),  $G_i$  (ser<sup>166</sup>-thr<sup>191</sup>) and  $G_0$  (ala<sup>122</sup>-thr<sup>147</sup>) as shown in Table IV. Although other sites in the  $\alpha$  subunit sequences must also be considered, this region is attractive since a structural basis for the different  $Mg^{2+}$  effects between the G proteins may be accommodated by the substitution of glycine for aspartic acid at this site in particular. This substitution occurs between consensus

domains involved in the formation of the GTP-binding site; for transducin, these include lys31-met49, phe195-arg20, ile217-ala225 and ser259-val269 (Table IV). Therefore, binding of  $Mg^{2+}$  to the aspartic acid in  $G_S$ ,  $G_i$  and  $G_O$  can easily be envisioned to induce conformational changes that would directly alter the properties of guanine nucleotide exchange. This effect would be lost in transducin because gly162 would be unable to form an ionic bond with  $Mg^{2+}$ .

Evidence for conformational alterations induced by  $Mg^{2+}$  has been provided by sucrose density gradient ultracentrifugation experiments performed by Codina et al. (105). These investigators have shown that  $Mg^{2+}$  promotes the formation of a species of  $G_S$  and  $G_i$  which displays unusual sedimentation behavior, referred to as a "pre-activated" form. The pre-activated forms of  $G_S$  and  $G_i$ , in the presence of  $Mg^{2+}$ , subsequently display subunit dissociation when incubated with guanine nucleotides as shown by sedimentation characteristics. In contrast, evidence for a "pre-activated" form associated with transducin is lacking, as suggested by the absence of an effect by  $Mg^{2+}$  on the kinetics of GTPYS binding. However, it is also observed that  $Mg^{2+}$  does not promote subunit dissociation; sucrose density gradient experiments with transducin show a shift in sedimentation only in the presence of GTPYS (Table I). Attention should be given to the physical properties associated with the preactivated forms of  $G_S$  and  $G_i$ , which migrate at a rate slower than expected for the heterotrimers, in comparison with the hydrodynamic analysis (Figures 18 and 19), which yields an  $M_r$  value below the expected 80 kDa for transducin. Thus, it appears that  $Mg^{2+}$  promotes a physical association between  $G_{S\alpha}$  and  $G_{i\alpha}$  and their  $\beta\gamma$  subunits which may be

TABLE IV Sequence Homologies Between GTP-Binding Regulatory Proteins

## A. Proposed Regulatory Region:

|                     |  |
|---------------------|--|
| G <sub>T</sub> 161: | P <sup>*</sup> G Y V P T E Q D V L R S R V K T T G I I E T Q F S |
| G <sub>S</sub> 188: | A D Y V P S D Q D L L R C R V L T S G I F E T K F Q              |
| G <sub>j</sub> 166: | S D Y I P T Q Q D V L R T R V K T T G I V E T H F T              |
| G <sub>O</sub> 122: | A D Y Q P T E Q D I L R T R V K T T G I V E T H F T              |

## B. Concensus Domains Forming Transducin's GTP-Binding Site:

Domain "A"G<sub>T</sub> 31: K L L L L G A G E S G K S T I V K Q MDomain "C"G<sub>T</sub> 195: F D V G G Q RDomain "E"G<sub>T</sub> 217: I I F I A A L S ADomain "G"G<sub>T</sub> 259: S I V L F L N K K D V

---

Sequence comparison from Itoh *et al.* (19). Single letter abbreviations are as follows: A, alanine; C, cysteine; D, aspartic acid; E, glutamic acid; F, phenylalanine; G, glycine; H, histidine; I, isoleucine; K, lysine; M, methionine; N, asparagine; P, proline; Q, glutamine; R, arginine; S, serine; T, threonine; V, valine; W, tryptophan; Y, tyrosine. For transducin (G<sub>T</sub>), gly<sup>162</sup> is marked with an asterisk.



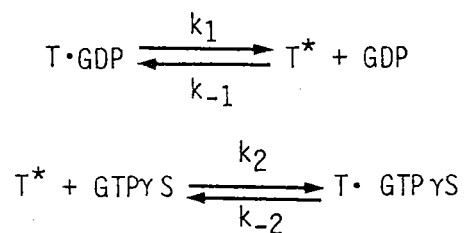
structurally analogous to heterotrimeric transducin; these forms are subsequently capable of exchanging guanine nucleotides.

Taken together, these results suggest that subtle structural differences between G proteins may produce profound alterations in the association of  $\alpha$  and  $\beta\gamma$  subunits, affecting regulation, physical characteristics and kinetic activities in response to  $Mg^{2+}$ . The comparison of the similarities and differences between members of this class of proteins provides a rationale for future research in site-directed mutagenesis and synthetic peptide studies, as well as providing further understanding of the physical properties of transducin in relation to its function.

#### Thermodynamic Considerations of Molecular Interactions

Having characterized the kinetic and binding properties of transducin-rhodopsin interactions and having analyzed the physical properties associated with the substrate G protein, attention should be focussed on the development of a model which incorporates this information in the context of structure-function relationships. For this purpose it is useful to consider these ideas in a thermodynamic background. Enzymes participate in catalyzing reactions by lowering activation barriers through specific complexes with substrates which favor the formation of a more reactive configuration. This activity can be accomplished through several consequences: entropy effects which result in the elimination of the need for collision events between two molecules, orbital steering which permits the alignment of substrates such that interaction between key reactive groups is favored, and propinquity effects which present binding domains stabilizing a reactive intermediate.

If the chemical kinetics of guanine nucleotide exchange of transducin are considered, this reaction may proceed via a dissociative type mechanism involving an "activated" species,  $T^*$  (Appendix II):



This reaction scheme presents two limiting cases depicted in the energy profiles of Figure 20. If it is considered that  $k_2 \gg k_{-1}$  (Panel A), then the rate-controlling step is the formation of  $T^*$ . Alternatively, for  $k_{-1} \gg k_2$  the rate-limiting step is considered to be the binding of  $\text{GTP}\gamma\text{S}$  to  $T^*$  (Panel B). The dashed lines depict the lowering of energy barriers which might occur during the rhodopsin catalyzed reaction.

Consideration of these two reaction coordinates leads to several conclusions about the manner through which rhodopsin may accomplish the catalysis of guanine nucleotide exchange. In order for the receptor to alleviate the activation energy involved in the binding of  $\text{GTP}\gamma\text{S}$  to  $T^*$  it could be envisioned that the receptor might bind the guanine nucleotide in order to eliminate the necessity for collision between the two substrates (entropy effects) or to bring the substrates into proper orientation (orbital steering). Remember that a catalyst cannot alter the intrinsic binding constants, as demonstrated by equilibrium binding studies between transducin and guanine nucleotides in the absence and presence of rhodopsin (Figure 15). There is, however, no evidence for such a guanine nucleotide binding domain represented either structurally or functionally for rhodopsin. Thus, if the formation of  $T^*$  is considered to be the rate-

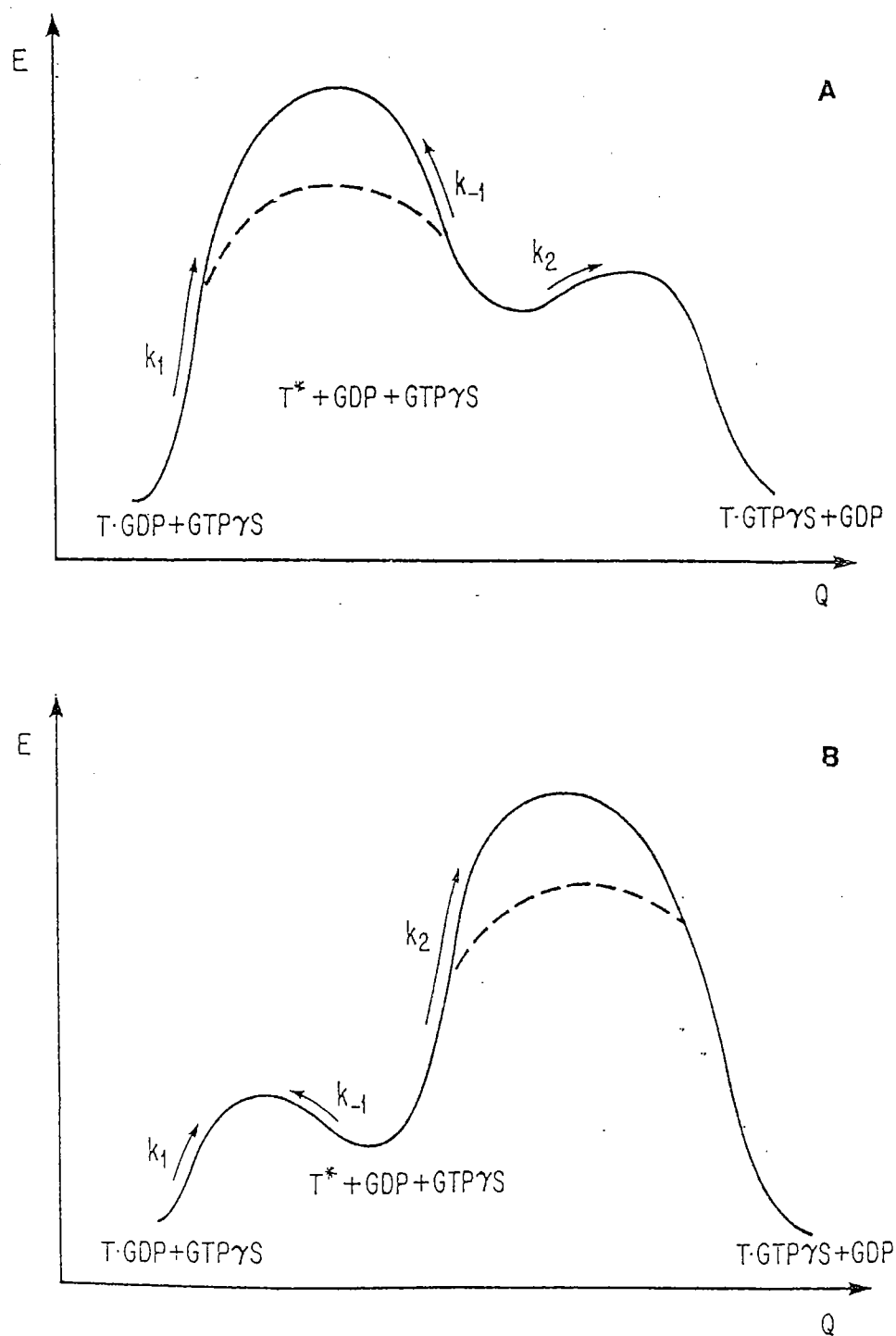


FIGURE 20 Energy profiles for a dissociative mechanism. Shown are the energy profiles along reaction coordinates corresponding to the two hypothetical limiting cases discussed in the text.  $T^*$  refers to an "activated" form of transducin. The dashed lines represents lowering of energy barriers by rhodopsin exerted through its catalytic activity.

limiting step (Figure 20, panel A), rhodopsin may serve to stabilize this reactive intermediate, lowering the activation barrier mainly through propinquity effects. This latter hypothesis is supported by the double displacement mechanism for the interactions between rhodopsin and transducin which verifies the existence of a complex between the receptor and G protein devoid of guanine nucleotide ( $T^*$ ) in the catalytic cycle.

What exactly are the molecular interactions which stabilize this reactive intermediate? The  $\beta\gamma$  subunit complex could participate in the exchange mechanism by providing a constraint against GDP release from the  $\alpha$  subunit. Rhodopsin might be considered to act as a lever, freeing the  $\alpha$  subunit from the restraints imposed by  $\beta\gamma$  and thereby promoting the release and exchange of guanine nucleotides. However, studies performed with purified  $T\alpha$  show that in the absence of  $T\beta\gamma$  the rate of guanine nucleotide exchange for both the catalyzed and non-catalyzed reactions is reduced, suggesting rather that the  $\beta\gamma$  complex plays a converse role by contributing to the stabilization of  $T^*$ .

Along similar lines, it may be envisioned that the positive cooperativity observed in interactions between  $\alpha$  subunits contributes in stabilizing the  $T^*$  reaction complex. Allosteric interactions between ligands can generate coupling free energies of up to 2.5 kcal/mole (122) and thus the presence of a second molecule of transducin may provide the necessary configurational orientation required for GDP release. Thus, oligomeric forms of rhodopsin can provide contact sites between the  $\alpha$  subunits which present domains aiding in the release of GDP and stabilizing the G protein devoid of guanine nucleotide in order for the binding of the second guanine nucleotide to occur. This may indeed be

what happens in analogy to the ADP-ribosylation factor, ARF, the GTP-binding protein involved in the ribosylation of  $G_s$  by cholera toxin (116). The site of this modification resides directly in the GTP-binding domains of  $\alpha_s$  and thus it would appear that a transitional complex of  $G_s$  without the presence of guanine nucleotides must be stabilized for cholera toxin recognition.

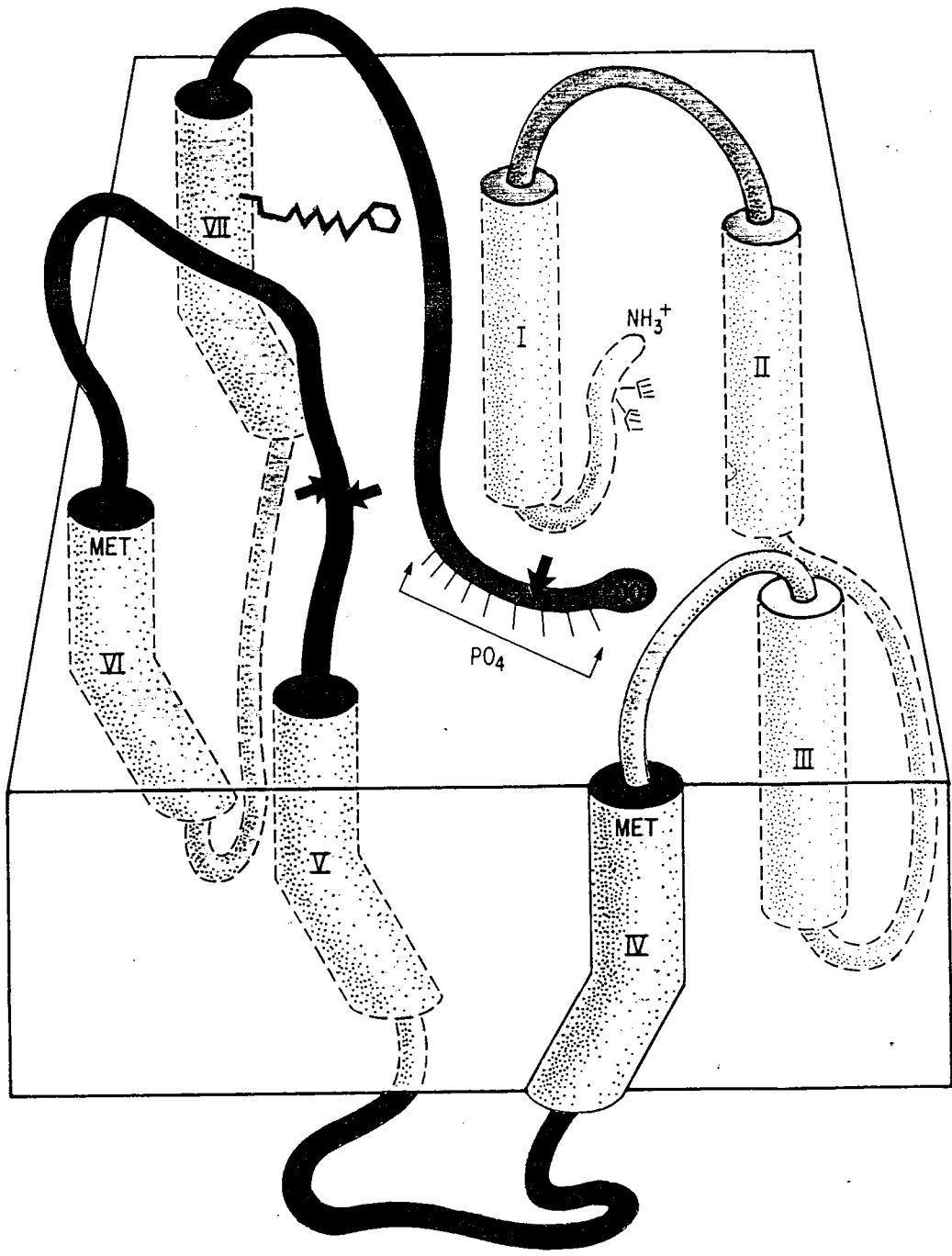
Subsequent to the binding of guanine nucleotide triphosphate, the apparent affinity of  $\beta\gamma$  for  $\alpha$  is diminished and the subunits are released from rhodopsin. This idea is supported by the fact that GTP $\gamma$ S-ligand  $\alpha$  does not migrate as a heterotrimeric complex with the  $\beta\gamma$  subunit complex on sucrose gradients (Figure 18). Thus,  $\beta\gamma$  may serve as anchor to stabilize binding interactions between  $\alpha$ •GDP and rhodopsin.






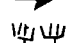
This hypothesis examines both the role of the  $\beta\gamma$  subunit complex and the influences exerted by the second molecule of transducin which interacts in an allosteric manner with the reaction complex. These issues must be addressed in order to develop a functional model. Product inhibition studies will provide a great deal of insight into the molecular involvement of these reaction components. Kinetic experiments defining the reaction profile for guanine nucleotide exchange by transducin will also aid in further defining this molecular mechanism of interactions between rhodopsin and transducin. It is interesting to consider that these ideas may represent a general motif through which the class of exchange enzymes may operate.

#### Structural Model for Rhodopsin

The predicted transmembrane structure of rhodopsin has been discussed in Chapter I. The accepted model proposes seven membrane-spanning helices

FIGURE 21 Structural model for rhodopsin. The molecular structure of rhodopsin is characterized as discussed in the text.



-  Flex Region
-  Regulatory Region
-  Binding Region
-  Chromophore
-  Protease Sites
-  Glycosylation

which provide three cytoplasmic loops along with the carboxy-terminal tail to be presented to transducin as potential binding domains (62-64). The absorption of a photon by 11-cis-retinal bound to lys<sup>296</sup> contained in the seventh and most C-terminal membrane-spanning helix must somehow induce conformational alterations in the protein which increase not only its binding affinity, but also its catalytic efficiency in interacting with transducin. Among the seven helices several contain proline residues causing distorted kinks in the  $\alpha$ -helical domains which most likely accommodate insertion of the chromophore in the midst of the membrane spanning region. The protonated Schiff's base linkage of retinal to lys<sup>296</sup> is thought to be neutralized by arg<sup>135</sup> in helix 3. The proximity of these charged groups is suggested by compact folding of rhodopsin in the bilayer, predicted to form a somewhat elongated "C", depicted in Figure 21. This structural model presents a framework of proposed functional domains of rhodopsin. Considering the receptor as an enzyme, a hinge-bending or flex region (blue) is conceptualized to breach two binding domains (yellow), one of which is also a regulatory region (orange) for the molecule. The following lines of evidence support this hypothetical model.

#### 1. Flex Region

Several conformational events are known to occur upon the photoisomerization of 11-cis-retinal. The carboxy terminus becomes more sensitive to thermolysin digestion following photobleaching (123). Also met<sup>155</sup> (helix 4) and met<sup>253</sup> (helix 6) display an increased susceptibility to CNBr cleavage in bleached rhodopsin compared to the unbleached molecule (124). In terms of identifying a hinge-bending domain for rhodopsin, this



area would present the most likely candidate for a region involved in conformational alterations which influence the protein's activity.

This hypothesis is supported by comparison of rhodopsin's primary sequence with those known for other members of the opsin family, particularly that of *Drosophila* (64). The intradiscal (or extracellular) loop connecting helices 4 and 5 displays the greatest conservation in primary structure. In particular, the invariant cysteine residues located on the latter loop region (cys187) and on the intradiscal loop connecting helices 2 and 3 (cys110) have been suggested to play a structural role (64). Thus, although occluded from contact with the G protein, the conservation of loop 4-5 suggests that it may play a critical role in rhodopsin's function in flex movements.

In contrast, the loop connecting helices 5 and 6 contains an insertion of 12 amino acids in *Drosophila* opsin, compared to mammalian opsin sequences (64). The dramatic divergence in loop 5-6, however, is compatible with its predicted major function to provide flexibility in the hinge mechanism to allow the conformational changes to occur. This is consistent with the observation that transducin does not block peptide-specific antibody binding to this loop.<sup>2</sup> Furthermore, thermolysin proteolytically clips loop 5-6 at ser<sup>140</sup>, an action which inhibits rhodopsin activation of transducin (125). Cleavage at this site would not

<sup>2</sup>E. Weiss and G.L. Johnson, personal communication.

allow signal transmission of the isomerization event across the loop structure to the appropriate membrane spanning helices, thereby preventing the proper conformational changes operating in the hinge-bending mechanism. It should be noted that loop 4-5 and loop 5-6 have the longest amino acid sequences predicted to connect the corresponding membrane helices and therefore, of all the loop structures, these are the most likely to have the greatest rotational flexibility which would be required for hinge domains.

A final consideration is that helix 7, containing the retinyl-lysine, would most likely be a primary element in the initiation of the hinge-bending movement. Argos et al. (126) have shown that this membrane-spanning domain is only minimally identified as a  $\alpha$  helix and thus, the possibility exists that an alternative conformation is adopted upon photolysis which may promote the hinge-bending motion.

## 2. Binding Domains

For this structural model, binding domains which interact with transducin are represented in the cytoplasmic loops connecting helices 1 and 2 as well as 3 and 4. Sequence comparison shows that the primary structures of these regions are remarkably conserved. Evidence that transducin may associate with these loop domains comes from the fact that while the G protein does not block peptide-specific antibody binding to loop 5-6, its interactions with the receptor does prevent antibody binding to loop 3-4. Recent experiments with V8 protease also show that

proteolysis of loop 5-6 is not inhibited by the presence of transducin,<sup>3</sup> suggesting that the latter loop is involved in functions of the receptor other than binding (see above). Thus, loop 5-6 does not appear to be involved in direct interactions with the G protein, strengthening the idea that other loop domains are strong candidates for this function, particularly loop 3-4.

### 3. Regulatory Domain

The final interesting comparison between opsins is at the carboxy-terminal tail. These proteins have a cys-cys sequence, followed a few amino acids away by either an asp-asp-glu or asp-asp sequence, and then a serine and threonine rich domain which contains the known sites of phosphorylation in mammalian opsins. This data indicates that the general hydropathy of the cytoplasmic tail has been conserved, and its probable regulatory role as well. Phosphorylation of rhodopsin at these sites has been shown to diminish the receptor's catalytic activity (53,60).

Recent evidence presented by Takemoto and coworkers (127) suggests that synthetic peptides corresponding to specific domains within the serine and threonine rich region of the carboxy-terminal tail could inhibit transducin activation. This finding indicates that this domain may be involved in transducin binding as well as the regulation of rhodopsin's catalytic activity by phosphorylation. Thus, the C-terminal

<sup>3</sup>M. Wessling-Resnick and G.L. Johnson, personal observations.

cytoplasmic tail provides the second functional domain which most likely contributes to forming a transducin binding site, connected by the hinge region through helix 7.

There is homology in the overall predicted structures of other G protein-coupled receptors and rhodopsin (39-45). These receptors are also predicted to have seven membrane-spanning helices, one of which only marginally fits the  $\alpha$ -helical configuration. These domains connect three analogous cytoplasmic loops and present the carboxy-terminus intracellularly. The carboxy tail for these receptors has been predicted to contain the sites of phosphorylation by regulatory kinases. The hypothetical hinge-bending model presented for rhodopsin may also be considered for these G protein-coupled receptors. What this model allows is some predictive level of addressing functional relationships between domains of receptors in order to conduct molecular studies, such as site-directed mutagenesis.

#### Summary

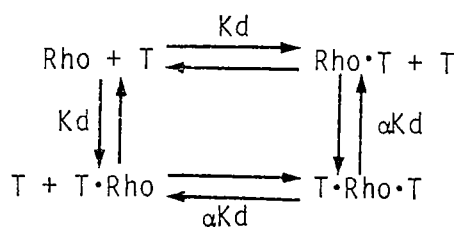
The ideas presented in this discussion provide a basis for future scientific direction in studies of the mechanism and regulation of receptor-GTP-binding protein interactions. The foundation for further molecular studies has been laid by characterizing the catalytic interactions between rhodopsin and transducin, the allosteric behavior witnessed in this system, and the structural parameters involved in G protein function. The results presented here permit a hypothetical framework within which the receptor, rhodopsin, may be modelled as an enzyme and predictions may be made as to functional domains for its activity. The hinge-bending model described provides the basis for

kinetic, physical and molecular studies. The concept of ligand-exchange catalysis allows the development of a paradigm for studies of other G protein-coupled receptor systems. It is hopeful that the molecular studies of rhodopsin and transducin will promote for their understanding of this mode of signal transduction, relevant to our understanding of structural relationships in the context of cellular function.

APPENDIX I

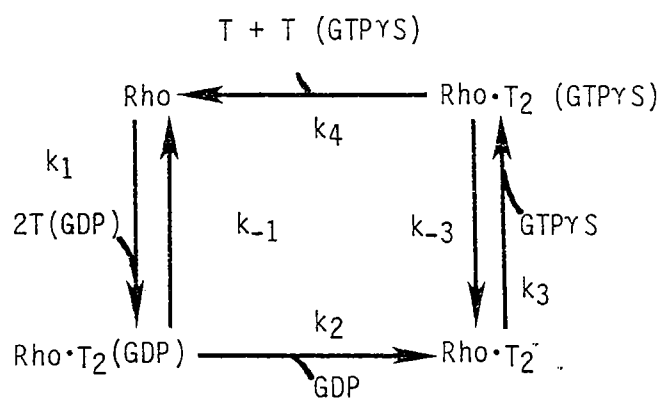
The most direct and obvious interpretation of the characteristics of the double reciprocal plots shown in Figures 6 and 7, is that rhodopsin catalyzes guanine nucleotide exchange by a double displacement mechanism and exhibits allosterism with respect to the GTP-binding protein, transducin. The formulation of an initial rate equation for the exchange reaction is required to incorporate both of these experimental criteria.

One interpretation of the sigmoidal substrate-velocity curves is that two transducins (or two  $T\alpha$  subunits) interact in a cooperative manner during exchange for a single GTPYS. This can be thought of as arising from dimerization of the GTP binding protein, or dimerization of rhodopsin, or the presence of two equivalent binding sites for transducin on a single rhodopsin. The latter idea may be represented by the scheme depicted below, considering that the binding of the first molecule of transducin to rhodopsin alters the intrinsic dissociation constant, by a factor of  $\alpha$ , towards a second molecule of transducin.



SCHEME I

If the allosteric behavior is due to strong cooperativity between two sites, that is, if the interaction factor  $\alpha$  is small, all complexes with rhodopsin containing a single occupied site will be negligible at  $[\text{transducin}] > K_d$ . In order to simplify our analysis, we will make this assumption, as suggested by Segel (78). The justification for this assumption is based on the goodness of fit to the Hill equation (demonstrated in the logarithmic plotting form shown in the inset of Figure 5) as well as the apparent Hill coefficient, determined to be close to an integer value. The catalytic mechanism can then be expressed in the scheme presented below, which depicts a double displacement mechanism for the exchange reaction.



SCHEME II

In terms of this model, the equation for initial velocity,  $v_0$ , may be written:

$$v_0 = k_2 [\text{Rho} \cdot \text{T}_2 \text{ (GDP)}] = k_4 [\text{Rho} \cdot \text{T}_2 \text{ (GTPYS)}]$$

The experimental conditions we imposed in this kinetic study are such that the concentrations of substrates, transducin and GTPYS, were much greater than rhodopsin concentration, and no products, GDP or T (GTPYS), were present at time = 0. This allows straightforward analysis along the

established description of steady-state enzyme kinetics (78). The following rate equations may be written in view of the steady-state:

$$d \frac{[\text{Rho}]}{dt} = d \frac{[\text{Rho} \cdot \text{T}_2 (\text{GDP})]}{dt} = d \frac{[\text{Rho} \cdot \text{T}_2]}{dt} = d \frac{[\text{Rho} \cdot \text{T}_2 (\text{GTPYS})]}{dt} = 0$$

$$d [\text{Rho} \cdot \text{T}_2 (\text{GDP})]/dt = k_1 [\text{T}(\text{GDP})]^2 [\text{Rho}] - k_{-1} [\text{Rho} \cdot \text{T}_2 (\text{GDP})] - k_2 [\text{Rho} \cdot \text{T}_2 (\text{GDP})]$$

$$d [\text{Rho} \cdot \text{T}_2]/dt = k_2 [\text{Rho} \cdot \text{T}_2 (\text{GDP})] - k_3 [\text{GTPYS}][\text{Rho} \cdot \text{T}_2] + k_{-3} [\text{Rho} \cdot \text{T}_2 (\text{GTPYS})]$$

$$d [\text{Rho} \cdot \text{T}_2 (\text{GTPYS})]/dt = k_3 [\text{Rho} \cdot \text{T}_2][\text{GTPYS}] - k_4 [\text{Rho} \cdot \text{T}_2 (\text{GTPYS})] - k_{-3} [\text{Rho} \cdot \text{T}_2 (\text{GTPYS})]$$

By rearrangement and substitution, the velocity equation may be rewritten:

$$v_0 = \frac{k_1 k_2 [\text{T} (\text{GDP})]^2 [\text{Rho}]_0}{(k_{-1} + k_2)}$$

Using the expression for the total concentration of rhodopsin,

$$[\text{Rho}]_0 = [\text{Rho}] + [\text{Rho} \cdot \text{T}_2 (\text{GDP})] + [\text{Rho} \cdot \text{T}_2] + [\text{Rho} \cdot \text{T}_2 (\text{GTPYS})]$$

the final form of the rate equation may be determined, which is expressed in double reciprocal form below

$$\frac{1}{v_0} = \left[ \frac{1}{[\text{Rho}]_0} \left( \frac{(k_{-1} + k_2)}{k_1 k_2} \right) \frac{1}{[\text{T} (\text{GDP})]^2} + \frac{(k_3 + k_4)}{k_3 k_4} \left( \frac{1}{[\text{GTPYS}]} \right) + \frac{(k_2 + k_4)}{k_2 k_4} \right]$$

We prefer to express this equation as follows:

$$\frac{1}{v_0} = \frac{1}{V_{\max}} \left[ \frac{K_m^{\text{GT}}}{[\text{GT}]^2} + \frac{K_m^{\text{GTPYS}}}{[\text{GTPYS}]} + 1 \right]$$

where

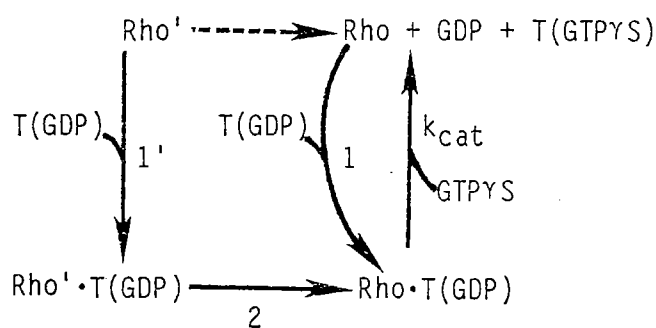
$$V_{\max} = \frac{(k_2 + k_4) [\text{Rho}]_0}{k_2 k_4}$$

$$K_m^{\text{GT}} = \frac{k_4 (k_{-1} + k_2)}{k_1 (k_2 + k_4)}$$

$$K_m^{\text{GTPYS}} = \frac{k_2 (k_{-3} + k_4)}{k_3 (k_2 + k_4)}$$



The rate equation developed is a 2/0 function, describing the sigmoidicity observed in the substrate-velocity plots. Alternative models which yield a similar function should also be considered. One consideration is that the allosteric behavior may be the result of hysteresis in the activity of rhodopsin. A distinguishing feature of a hysteric enzyme is the manifestation of an enzyme state which has a different physical form and kinetic properties; the availability of this additional state is altered by the presence of substrate (82). This idea is depicted in the following scheme:



SCHEME III

As this model suggests, two conformational isomers of rhodopsin exist, of which Rho' may be considered an inactive form. The interconversion process  $\text{Rho}' \rightarrow \text{Rho}$  is slow compared to all other steps. T(GDP) binds Rho' to produce Rho'·T(GDP) and to promote the conversion to Rho·T(GDP), which then participates in the exchange reaction, generating the products and the active form of Rho. Rabin (128) has discussed this kinetic model as an extension of Koshland's induced-fit hypothesis by

placing the restriction that  $k_2 \ll k_{-2}$ , such that  $k_{-1}/k_1 \ll k'_{-1}/k'_1$ . Thus, the  $K_d$  of  $\text{Rho}\cdot\text{T}(\text{GDP})$  is then smaller than that of  $\text{Rho}'\cdot\text{T}(\text{GDP})$  and the capacity of rhodopsin to bind transducin increases with the progress of the reaction; that is, the conversion of  $\text{Rho}'\cdot\text{T}(\text{GDP}) \longrightarrow \text{Rho}\cdot\text{T}(\text{GDP})$  causes an increase in the strength of interaction between rhodopsin and transducin. Since the conversion of  $\text{Rho}'$  into  $\text{Rho}$  is a function of transducin concentration, it is possible that the allosteric behavior witnessed experimentally could also be described by models incorporating this idea.

APPENDIX II

Schreier and Schimmel (129) have discussed the following method for interpreting binding data which reflect interacting site behavior (cooperativity). This phenomenon is clearly indicated by the asymptotic bell-shaped character observed in Scatchard plots (Figures 10 and 11, for example). These plots indicate that the ligand (transducin) binds to one class of interacting sites as well as at least one other class of independent sites (non-specific sites). For ease of manipulation, the fractional saturation parameter,  $v$  is used to represent  $B/B_{\max}$ . The variable  $L$  represents the concentration of free ligand. For the case of independent, non-interacting sites,  $v$  may be expressed as:

$$v = \sum_i \frac{n_i K_{a_i} L}{1 + K_{a_i} L}$$

or  $v/L = \sum_i \frac{n_i K_{a_i}}{1 + K_{a_i} L}$

The parameter  $i$  refers to the particular class having  $n$  sites;  $K_{a_i}$  is the intrinsic association constant of ligand binding to these sites.

Interacting sites arising from allosteric behavior display ligand binding characteristics which follow a dependence on ligand concentration given by  $\alpha$ , the interaction exponent:

$$v = \frac{n K_{a_i} L^{\alpha}}{1 + K_{a_i} L^{\alpha}}$$

$$v/L = \frac{n K_{a_i} L^{\alpha-1}}{1 + K_{a_i} L^{\alpha}}$$

For mixed interacting and non-interacting sites, contribution from each of these cases must be considered.

$$v = \frac{n K_a^\alpha L^\alpha}{1 + K_a^\alpha L^\alpha} + \sum_i \frac{n_i K_{a_i} L}{1 + K_{a_i} L}$$

$$v/L = \frac{n K_a^\alpha L^{\alpha-1}}{1 + K_a^\alpha L^\alpha} + \sum_i \frac{n_i K_{a_i}}{1 + K_{a_i} L}$$

Characteristics of this equation are reflected in the Scatchard plots of transducin binding to rhodopsin. These curves display a positive slope at small values of B, bound ligand, reflected in  $v$ , and a maximum reflecting the downward curvature predicted by the appearance of  $\alpha$  in the equation. The non-zero intercepts of these plots would be represented by the  $\sum n_i K_i$  term.

Schreier and Schimmel (129) propose the following method to decompose such complicated plots. If we assume only one class of non-denaturing sites (non-specific binding):

$$v/L = \frac{n K_a^\alpha L^{\alpha-1}}{1 + K_a^\alpha L^\alpha} + \frac{n' K_{a'}}{1 + K_{a'} L}$$

The intercepts given by this equation are:

$$(v/L) \quad v \rightarrow 0 = n K_{a'}$$

$$v \quad (v/L) \rightarrow 0 = n + n'$$

The tangent at  $v/L = 0$  may be determined:

$$v/L = \frac{(n + n')^2}{n} K_{a'} - \frac{(n + n')}{n} K_{a'}$$

The intercept of the tangent line is therefore:

$$(v/L) \quad v \rightarrow 0 = \frac{(n + n')^2}{n} \quad K_a'$$

By determining values for these intercepts, the relationships between  $n$ ,  $n'$ , and  $K_a'$  permit the calculation of these parameters. Accordingly, corrections may be made to the original data for contributions from non-specific binding. An iterative fit may be made in order to refine the binding parameters, resolving data to the form of the Scatchard equation describing interacting sites.

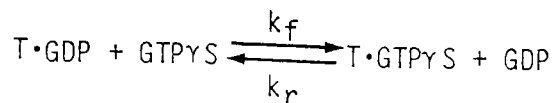
The Scatchard equation defining the positive cooperative behavior may be linearized by logarithmic transformation:

$$\log \left( \frac{v}{n-v} \right) = \alpha \log (L) - \log K_d$$

where  $K_d$  is employed to represent the apparent dissociation constant of the interacting sites. The parameter  $\alpha$  reflects the Hill coefficient,  $n_H$ . Binding data corrected as described above was employed to calculate these parameters. Values of  $n$ , the number of binding sites per receptor, were always found to be less than 1, indicating that assumed  $B_{max}$  values were greater than described by this analysis, or conversely, overestimated on the assumption the monomeric rhodopsin provides multiple binding sites for rhodopsin. Thus, oligomeric forms of the receptor must participate in creating the class of cooperative binding sites for transducin.

APPENDIX III

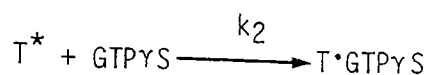
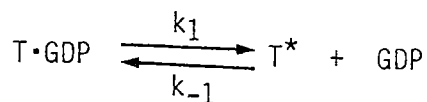
The non-catalyzed reaction of guanine nucleotide exchange by transducin must follow descriptions provided by classical kinetics:



The initial rate equation for the reaction may be written as follows:

$$v_0 = \frac{d[T \cdot GTPYS]}{dt} = k_f [T \cdot GDP] [GTPYS]$$

The independence of  $[T \cdot GDP]$  and  $[GTPYS]$  in linear logarithmic plotting forms shown in Figures 16 and 17 implies a dissociative type mechanism for this reaction. In such a model, the reaction may be envisioned as a two step process with an activated intermediate,  $T^*$ , combining with  $GTPYS$  in an essentially irreversible step.



Considering steady-state conditions,

$$\frac{d[T^*]}{dt} = 0 = k_1 [T \cdot GDP] - k_2 [T^*] [GTPYS]$$

$$[T^*] = \frac{k_1 [T \cdot GDP]}{k_{-1} [GDP] - k_{-2} [GTPYS]}$$

The overall velocity of the dissociation reaction may be described using the expression of  $[T^*]$ :

$$\frac{-d [T \cdot GDP]}{dt} = k_1 [T \cdot GDP] - k_{-1} [T^*] [GDP] = \frac{k_1 k_2 [GDP] [GTPyS]}{k_{-1} [GDP] + k_2 [GTPyS]}$$

By comparison with the equation for initial velocity,  $v_0$ , an expression for  $k_f$  may be obtained:

$$k_f = \frac{k_1 k_2}{k_{-1} [GDP] + k_2 [GTPyS]}$$

REFERENCES

1. Gilman, A.G. (1984) *Cell* 36, 577-579.
2. Evans, T., Brown, M.L., Fraser, E.D. and Northup, J.K. (1986) *J. Biol. Chem.* 261, 7052-7059.
3. Gomperts, B.D. (1983) *Nature* 306, 64-66.
4. Bokoch, G.M. and Gilman, A.G. (1984) *Cell* 39, 301-308.
5. Nakamura, T. and Ui, M. (1985) *J. Biol. Chem.* 260, 3584-3593.
6. Smith, C.D., Cox, C.C. and Snyderman, R. (1986) *Science* 232, 97-100.
7. Burch, R.M., Luini, A. and Axelrod, J. (1986) *Proc. Natl. Acad. Sci. USA* 83, 7201-7205.
8. Jelsema, C.L. (1987) *J. Biol. Chem.* 262, 163-168.
9. Yatani, A., Codina, J., Brown, A.M. and Birnbaumer, L. (1987) *Science* 235, 207-211.
10. Birnbaumer, L., Codina, J., Mattera, R., Cerione, K.A., Hildebrandt, J.P., Sunyer, T., Rojas, F.J., Caron, M.G., Lefkowitz, R.J. and Iyengar, R. (1985) *Rec. Prog. Hormone Res.* 41, 41-99.
11. Gill, D.M. (1977) *Adv. Cycl. Nucl. Res.* 6, 85-118.
12. Ui, M. (1984) *Trends Pharmacol. Sci.* 5, 277-279.
13. Medynski, D.C., Sullivan, K., Smith, D., Van Dop, C., Chang, F.-H., Fung, B.K.-K., Seeburg, P.H. and Bourne, H.R. (1985) *Proc. Natl. Acad. Sci. USA* 82, 4311-4315.
14. Yatsunami, K. and Khorana, H.G. (1985) *Proc. Natl. Acad. Sci. USA* 82, 4316-4320.
15. Tanabe, T., Nukada, T., Nishikawa, Y., Sugimoto, K., Suzuki, H., Takahashi, H., Noda, M., Haga, T., Ichiyama, A., Kangawa, K., Minamino, N., Matsuo, H. and Numa, S. (1985) *Nature* 315, 242-245.
16. Lochrie, M.A., Hurley, J.B. and Simon, M.I. (1985) *Science* 228, 96-99.
17. Robishaw, J.D., Russell, D.W., Harris, B.A., Smigel, M.D. and Gilman, A.G. (1986) *Proc. Natl. Acad. Sci. USA* 83, 1251-1255.
18. Nukada, T., Tanabe, T., Takahashi, H., Noda, M., Hirose, T., Inayama, S. and Numa, S. (1986) *FEBS Lett.* 195, 220-224.



19. Itoh, H., Kozasa, T., Nagata, S., Nakamura, S., Katada, T., Ui, M., Iwai, S., Ohtsuka, E., Kawasaki, H., Suzuki, K. and Kaziro, Y. (1986) Proc. Natl. Acad. Sci. USA 83, 3776-3780.
20. Sullivan, K.A., Liao, Y.-C., Alborzi, A., Beiderman, B., Chang, F.-H., Masters, S.B., Levinson, A.D. and Bourne, H.R. (1986) Proc. Natl. Acad. Sci. USA 83, 6687-6691.
21. Mattera, R., Codina, J., Crozat, A., Kidd, V., Woo, S.L.C. and Birnbaumer, L. (1986) FEBS Lett. 206, 36-42.
22. Manning, D.R. and Gilman, A.G. (1983) J. Biol. Chem. 258, 7059-7063.
23. Sugimoto, K., Nukada, T., Tanabe, T., Takahashi, H., Noda, M., Minamino, N., Kangawa, K., Matsuo, H., Hirose, T., Inayama, S. and Numa, S. (1985) FEBS Lett. 191, 235-240.
24. Fong, H.K.W., Hurley, J.B., Hopkins, R.S., Miake-Lye, R., Johnson, M.S., Doolittle, R.F. and Simon, M.I. (1986) Proc. Natl. Acad. Sci. USA 83, 2162-2166.
25. Codina, J., Stengel, D., Woo, S.L.C. and Birnbaumer, L. (1986) FEBS Lett. 207, 187-192.
26. Mumby, S.M., Kahn, R.A., Manning, D.R. and Gilman, A.G. (1986) Proc. Natl. Acad. Sci. USA 83, 265-269.
27. Hildebrandt, J.D., Codina, J., Rosenthal, W., Birnbaumer, L., Neer, E.J., Yamazaki, A. and Bitensky, M.W. (1985) J. Biol. Chem. 260, 14867-14872.
28. Gierschik, P., Codina, J., Simons, C., Birnbaumer, L. and Spiegel, A. (1985) Proc. Natl. Acad. Sci. USA 82, 721-727.
29. Yatsunami, K., Pandya, B.V., Oprian, D.D. and Khorana, H.G. (1985) Proc. Natl. Acad. Sci. USA 82, 1936-1940.
30. Van Dop, C., Medynski, D., Sullivan, K., Wu, A.M., Fung, B.K.-K. and Bourne, H.R. (1984) Biochem. Biophys. Res. Comm. 124, 250-255.
31. Hurley, J.B., Fong, H.K.W., Teplow, D.B., Dreyer, W.J. and Simon, M.I. (1984) Proc. Natl. Acad. Sci. USA 81, 6948-6952.
32. Northup, J.K., Smigel, M.D., Sternweis, P.C. and Gilman, A.G. (1983) J. Biol. Chem. 258, 11369-11376.
33. Katada, T., Bokoch, G.M., Northup, J.K., Ui, M. and Gilman, A.G. (1984) J. Biol. Chem. 259, 3568-3577.
34. Kanaho, Y., Tsai, S.C., Adamik, R., Hewlett, E.L., Moss, J. and Vaughn, M. (1984) J. Biol. Chem. 259, 7378-7381.

35. Sunyer, T., Codina, J. and Birnbaumer, L. (1984) *J. Biol. Chem.* 259, 15447-15451.
36. Cerione, R.A., Codina, J., Kilpatrick, B.F., Staniszewski, G., Gierschik, P., Somers, R.L., Spiegel, A.M., Birnbaumer, L. and Lefkowitz, R.J. (1985) *Biochemistry* 24, 4499-4503.
37. Cerione, R.A., Staniszewski, C., Benovic, J.L., Lefkowitz, R.J., Caron, M.G., Cierschik, P., Somers, R., Spiegel, A.M., Codina, J. and Birnbaumer, L. (1985) *J. Biol. Chem.* 260, 1493-1500.
38. Asano, T., Katada, T., Gilman, A.G. and Ross, E.M. (1984) *J. Biol. Chem.* 259, 9351-9354.
39. Hargrave, P.A., McDowell, J.H., Curtis, D.R., Wang, J.K., Juszczak, E., Fong, S.L., Mohana Rao, J.K. and Argos, P. (1983) *Biophys. Struct. Mech.* 9, 235-244.
40. Ovchinnikov, Y.A., Abdulaev, N.G., Feigina, M.Y., Artamonov, I.D., Zolotarev, A.S., Kostina, M.B., Bogachuk, A.S., Miroshnikov, A.I., Martinov, V.I. and Kudelin, A.B. (1982) *Bioorg. Khim.* 8, 1011-1014.
41. Nathans, J. and Hogness, D.S. (1983) *Cell* 34, 807-814.
42. Dixon, R.A.F., Kobilka, B.K., Strader, D.J., Benovic, J.L., Dohlman, H.G., Frielle, T., Bolanowski, M.A., Bennett, C.D., Rands, E., Diehl, R.E., Mumford, R.A., Slater, E.E., Sigal, I.S., Caron, M.G., Lefkowitz, R.J. and Strader, C.D. (1986) *Nature* 321, 75-79.
43. Yarden, Y., Rodriguez, H., Wong, S.K.-F., Brandt, D.R., May, D.C., Burnier, J., Harkins, R.N., Chen, E.Y., Ramachandran, J., Ullrich, A. and Ross, E.M. (1986) *Proc. Natl. Acad. Sci. USA* 83, 6795-6799.
44. Kobilka, B.K., Dixon, R.A.F., frielle, T., Dohlman, H.G., Bolanowski, M.A., Sigal, I.S., Yang-Feng, T.L., Francke, U., Caron, M.G. and Lefkowitz, R.J. (1987) *Proc. Natl. Acad. Sci. USA* 84, 46-50.
45. Kubo, T., Fukuda, K., Mikami, A., Maeda, A., Takahashi, H., Mishina, M., Haga, T., Haga, K., Ichiyama, A., Kangawa, K., Kojima, M., Matsuo, H., Hirose, T. and Numa, S. (1986) *Nature* 323, 411-416.
46. Weiss, E.R., Hadcock, J.R., Johnson, G.L. and Malbon, C.C. (1987) *J. Biol. Chem.* 262, 4319-4323.
47. Stryer, L., Hurley, J.B. and Fung, B.K.-K. (1981) *Curr. Topics Memb. Trans.* 15, 95-108.
48. Brown, J.E. and Lisman, J.E. (1975) *Nature* 258, 252-253.
49. Kuhn, H. (1974) *Nature* 250, 588-590.

50. Kuhn, H., McDowell, J.H., Leser, K.H. and Boder, S. (1977) *Biophys. Struct. Mech.* 3, 175-180.
51. Vandenberg, C.A. and Montal, M. (1984) *Biochemistry* 23, 2339-2347.
52. Sitaramayya, A. and Liebman, P.A. (1983) *J. Biol. Chem.* 258, 12106-12109.
53. Schichi, H., Yamamoto, K. and Somers, R.L. (1984) *Vis. Res.* 24, 1523-1531.
54. Fesenko, E.E., Kolesnikov, S.S. and Lyubarsky, A.L. (1985) *Nature* 313, 310-313.
55. Koch, K.-W. and Kaupp, U.B. (1985) *J. Biol. Chem.* 260, 6788-6800.
56. Fein, A., Payne, R., Wesley-Corson, P., Berridge, M.J. and Irvine, R.F. (1984) *Nature* 311, 157-160.
57. Kaupp, U.B., Schnethamp, P.M. and Jung, W. (1979) *Biochim. Biophys. Acta* 552, 390-403.
58. Brown, J.E., Rubin, L.J., Ghalazini, A.J., Tarver, A.P., Irvine, R.F., Berridge, M.J. and Anderson, R.E. (1984) *Nature* 311, 160-163.
59. Berridge, M.J. and Irvine, R.F. (1984) *Nature* 312, 315-321.
60. Kelleher, D.J. and Johnson, G.L. (1986) *J. Biol. Chem.* 261, 4749-4757.
61. Kapoor, C.L. and Chader, D.J. (1984) *Biochem. Biophys. Res. Comm.* 122, 1397-1403.
62. Dratz, E.A. and Hargrave, P.A. (1983) *Trends Biochem. Sci.* 8, 128-131.
63. Findlay, J.B.C. and Pappin, D.J.C. (1986) *Biochem. J.* 238, 625-642.
64. Applebury, M.L. and Hargrave, P.A. (1986) *Vision Res.* 26, 1881-1895.
65. Fung, B.K.-K., Hurley, J.B. and Stryer, L. (1981) *Proc. Natl. Acad. Sci. USA* 78, 152-156.
66. Baehr, W., Morita, E.A., Swanson, R.J. and Applebury, M.L. (1982) *J. Biol. Chem.* 257, 6452-6460.
67. Kuhn, H., Bennett, N., Michel-Villaz, M. and Chabre, M. (1981) *Proc. Natl. Acad. Sci. USA* 78, 6873-6877.
68. Bennett, N. (1982) *Eur. J. Biochem.* 123, 133-139.

69. Bennett, N. and Dupont, Y. (1985) *J. Biol. Chem.* 260, 4156-4168.
70. Fung, B.K.-K. and Stryer, L. (1980) *Proc. Natl. Acad. Sci. USA* 77, 2500-2504.
71. Fung, B.K.-K. (1983) *J. Biol. Chem.* 258, 10495-10502.
72. Yamazaki, A., Stein, P.J., Chernoff, N. and Bitensky, M.W. (1983) *J. Biol. Chem.* 258, 8188-8194.
73. Yamazaki, A., Bartucca, F., Ting, A. and Bitensky, M.W. (1982) *Proc. Natl. Acad. Sci. USA* 29, 3702-3706.
74. Watkins, P.A., Burns, D.L., Kanaho, Y., Liu, T.-Y., Hewlett, E.L. and Moss, J. (1985) *J. Biol. Chem.* 260, 13478-13482.
75. Hong, K. and Hubbell, W.L. (1973) *Biochemistry* 12, 4517-4523.
76. Litman, B.J. (1982) *Meth. Enzymol.* 81, 150-153.
77. Jackson, M.L. and Litman, B.J. (1982) *Biochemistry* 21, 5601-5608.
78. Segel, J.H. (1975) *Enzyme Kinetics*, John Wiley and Sons, New York.
79. Bradford, M. (1976) *Anal. Biochem.* 72, 248-254.
80. Laemmli, U.K. (1970) *Nature* 227, 680-685.
81. Plowman, K.M. (1972) *Enzyme Kinetics*, McGraw-Hill Publications, Minneapolis, MN.
82. Neet, K.E. (1980) *Methods Enzymol.* 64, 139-193.
83. Ainsworth, S. (1968) *J. Theor. Biol.* 19, 1-23.
84. Kuhn, H. (1980) *Nature* 283, 587-589.
85. Kuhn, H. (1981) *Curr. Topics Membr. Trans.* 15, 171-201.
86. Liebman, P.A., Sitaramayya, A. (1984) *Adv. Cyclic Nucl. Prot. Phos. Res.* 17, 215-255.
87. Findlay, J.B.C., Brett, M. and Pappin, D.J.C. (1981) *Nature* 293, 314-316.
88. Fung, B.K.-K. and Hubbell, W.L. (1982) *Meth. Enzymol.* 81, 269-275.
89. Asano, T., Pederson, S.E., Scott, C.W. and Ross, E.M. (1984) *Biochemistry* 23, 5460-5467.

90. Yamanaka, G., Eckstein, F. and Stryer, L. (1985) *Biochemistry* 24, 8094-8101.
91. Deterre, P., Bigay, J., Pfister, C. and Chabre, M. (1984) *FEBS Lett.* 178, 228-232.
92. Kelleher, D.J., Dudycz, L.W., Wright, G.E. and Johnson, G.L. (1986) *Mol. Pharmacol.* 30, 603-608.
93. Northup, J.K., Smigel, M.D. and Gilman, A.G. (1982) *J. Biol. Chem.* 257, 11416-11423.
94. Brandt, D.R. and Ross, E.M. (1985) *J. Biol. Chem.* 260, 266-272.
95. Bokoch, G.M., Katada, T., Northup, J.K., Ui, M. and Gilman, A.G. (1984) *J. Biol. Chem.* 259, 3560-3567.
96. Huff, R.M. and Neer, E.J. (1986) *J. Biol. Chem.* 261, 1105-1110.
97. Huff, R.M., Axton, J.M. and Neer, E.J. (1985) *J. Biol. Chem.* 260, 10864-10871.
98. Yamanaka, G., Eckstein, F. and Stryer, L. (1986) *Biochemistry* 25, 6149-6153.
99. Sunyer, T., Codina, J. and Birnbaumer, L. (1984) *J. Biol. Chem.* 259, 15447-15451.
100. Sternweis, P.C. and Robishaw, J.D. (1984) *J. Biol. Chem.* 259, 13806-13813.
101. Ferguson, K.M., Higashijima, T., Smigel, M.D. and Gilman, A.G. (1986) *J. Biol. Chem.* 261, 7393-7399.
102. Sternweis, P.C., Northup, J.K., Smigel, M.D. and Gilman, A.G. (1981) *J. Biol. Chem.* 256, 11517-11526.
103. Hanski, E., Sternweis, P.C., Northup, J.K., Dromerick, A.W. and Gilman, A.G. (1981) *J. Biol. Chem.* 256, 12911-12919.
104. Codina, J., Hildebrandt, J.D., Sekura, R.D., Birnbaumer, M., Bryan, J., Manclark, C.R., Iyengar, K. and Birnbaumer, L. (1984) *J. Biol. Chem.* 259, 5871-5886.
105. Codina, J., Hildebrandt, J.D., Birnbaumer, L. and Sekura, R.D. (1984) *J. Biol. Chem.* 259, 11408-11418.
106. Bokoch, G.M., Katada, T., Northup, J.K., Hewlett, E.L. and Gilman, A.G. (1983) *J. Biol. Chem.* 258, 2072-2075.

107. Koshland, E.E., Jr., (1970) in The Enzymes (P.D. Boyer, ed.) Academic Press, New York.
108. Scarborough, G.A. (1985) *Microbiol. Rev.* 49, 214-231.
109. Kohnken, R.E. and McConnell, D.G. (1985) *Biochemistry* 24, 3803-3809.
110. Halliday, K.R. (1984) *J. Cyclic Nucl. Prot. Phos. Res.* 9, 435-448.
111. Hwang, Y.W. and Miller, D.L. (1985) *J. Biol. Chem.* 260, 11498-11502.
112. Wensel, T.G. and Stryer, L. (1985) *J. Cell Biol.* 101, 221a.
113. Shaw, A., Crain, R., Marinetti, G.V., O'Brien, D. and Tyminski, P.N. (1980) *Biochim. Biophys. Acta* 603, 313-321.
114. Rodbell, M. (1980) *Nature* 284, 17-21.
115. Antonsson, B., Leberman, R., Jacrot, B. and Zacchai, G. (1986) *Biochemistry* 25, 3655-3659.
116. Kahn, R.A. and Gilman, A.G. (1986) *J. Biol. Chem.* 261, 7906-7911.
117. Ludwig, D.S., Ribí, H.O., Schoolnik, G.K. and Kornberg, R.D. (1980) *Proc. Natl. Acad. Sci. USA* 83, 8585-8588.
118. Michel, H., Oesterhelt, D. and Henderson, R. (1980) *Proc. Natl. Acad. Sci. USA* 77, 338-342.
119. Jurnak, F. (1985) *Science* 230, 32-36.
120. Brandt, D.R. and Ross, E.M. (1986) *J. Biol. Chem.* 261, 1656-1664.
121. Iyengar, R. and Birnbaumer, L. (1982) *Proc. Natl. Acad. Sci. USA* 79, 5179-5183.
122. Cantor, C.R. and Schimmel, P.R. (1980) Biophysical Chemistry, W.H. Freeman and Co., San Francisco.
123. Kuhn, H., Mommertz, O. and Hargrave, P.A. (1982) *Biochim. Biophys. Acta* 679, 95-100.
124. Pellicone, C., Nullans, G. and Virmaux, N. (1985) *FEBS Lett.* 181, 179-183.
125. Kuhn, H. (1984) *Prog. Retinal. Res.* 3, 123-156.
126. Argos, P., Mohanna Rao, J.K. and Hargrave, P.A. (1982) *Eur. J. Biochem.* 128, 565-575.

127. Takemoto, D.J., Takemoto, L.J., Hansen, J. and Morrison, D. (1985) Biochem. J. 232, 669-672.
128. Rabin, B.R. (1967) Biochem. J. 102, 226-230.
129. Schreier, A.A. and Schimmel, P.R. (1974) J. Mol. Biol. 86, 601-620.